# INDUCTION AND TRANSPLANTATION OF CORNEAL EPITHELIAL CELLS DERIVED FROM HUMAN WHARTON'S JELLY MESENCHYMAL STEM CELLS INTO THE LIMBAL STEM CELL DEFICIENCY RABBIT MODEL

NGUYEN THI HONG



A Thesis Submitted in Partial Fulfillment of the Requirements for the
Degree of Doctor of Philosophy Program in Biotechnology
Suranaree University of Technology
Academic Year 2021

# การเหนี่ยวนำและการปลูกถ่ายเซลล์เยื่อบุผิวกระจกตาที่เปลี่ยนแปลงมาจากเซลล์ต้นกำเนิดมีเซ็นไคม์จากวาร์ตันเจลลี่มนุษย์ในกระต่ายโมเดลโรคพร่องเซลล์ต้นกำเนิดลิมบัส

เหงียน ถิ ฮง



วิทยานิพนธ์นี้เป็นส่วนหนึ่งของการศึกษาตามหลักสูตรปริญญาวิทยาศาสตรดุษฎีบัณฑิต
สาขาวิชาเทคโนโลยีชีวภาพ
มหาวิทยาลัยเทคโนโลยีสุรนารี
ปีการศึกษา 2564

INDUCTION AND TRANSPLANTATION OF CORNEAL EPITHELIAL CELLS DERIVED FROM HUMAN WHARTON'S JELLY MESENCHYMAL STEM CELLS INTO THE LIMBAL STEM CELL DEFICIENCY RABBIT MODEL

Suranaree University of Technology has approved this thesis submitted in partial fulfillment of the requirements for the Degree of Doctor of Philosophy.

Thesis Examining Committee

(Dr. Tatsanee Phermthai)
Chairperson

(Assoc. Prof. Dr. Rangsun Parnpai)
Member (Thesis Advisor)

(Dr. Ruttachuk Rungsiwiwut)
Member

(Dr. Juthaporn Assawachananont)
Member

(Dr. Pishyaporn Sritangos)
Member

(Assoc. Prof. Dr. Chatchai Jothityangkoon)
Vice Rector for Academic Affairs and Quality Assurance

(Prof. Dr. Neung Teaumroong)
Dean of Institute of Agricultural Technology

เหงียน ถิ ฮง : การเหนี่ยวนำและการปลูกถ่ายเซลล์เยื่อบุผิวกระจกตาที่เปลี่ยนแปลงมาจากเซลล์ต้นกำเนิดมีเซ็นไคม์จากวาร์ตันเจลลี่มนุษย์ในกระต่ายโมเดลโรคพร่องเซลล์ต้นกำเนิดลิมบัส (INDUCTION AND TRANSPLANTATION OF CORNEAL EPITHELIAL CELLS DERIVED FROM HUMAN WHARTON'S JELLY MESENCHYMAL STEM CELLS INTO THE LIMBAL STEM CELL DEFICIENCY RABBIT MODEL) อาจารย์ที่ปรึกษา : รองศาสตราจารย์ ดร.รังสรรค์ พาลพ่าย, 111 หน้า.

คำสำคัญ: เซลล์ต้นกำเนิดมีเซ็นไคม์/เซลล์เยื่อบุผิวกระจกตา/การเปลี่ยนแปลงเซล์/การปลูกถ่าย/กระต่าย

เยื่อบุผิวกระจกตาประกอบด้วยเซลล์เยื่อบุผิวกระจกตา (corneal epithelial cells: CECs) ซึ่งถูกสร้างใหม่อย่างต่อเนื่องโดย limbal epithelial stem cells (LESCs) เมื่อ LESCs สูญเสียไปหรือมีการทำงานที่ผิดปกติจะทำให้เกิดโรคพร่องเซลล์ต้นกำเนิดลิมบัส (limbal stem cell deficiency: LSCD) ซึ่งทำให้เสียเยื่อบุผิวกระจกตาและการมองเห็นบกพร่อง การสร้างเยื่อบุผิวกระจกตาขึ้นมาใหม่จำเป็นต้องได้รับการปลูกถ่ายเซลล์ต้นกำเนิดของเซลล์เยื่อบุผิวกระจกตา การทดลองที่ 1 ของงานวิจัยนี้เป็นการศึกษาผลของสารทดสอบต่อ signaling pathway 3 กระบวนการที่เกี่ยวข้องกับการเปลี่ยนแปลงไปเป็นเซลล์เยื่อบุผิวกระจกตา รวมทั้งหาสภาวะที่เหมาะสมในการเหนี่ยวนำเซลล์ต้นกำเนิดมีเซ็นไคม์จากวาร์ตันเจลลี่ของมนุษย์ไปเป็นเซลล์เยื่อบุผิวกระจกตา พบว่า All-trans retinoic acid (RA) ยับยั้ง Wnt signaling pathway โดยยับยั้งการเคลื่อนย้าย β-catenin จากไซโทพลาสซึมเข้าสู่นิวเคลียส SB505124 ยับยั้ง TGF-β signaling pathway โดยลดการเกิด phosphorylation ที่ Smad2 ส่วน BMP4 ไม่ทำให้ phosphorylation ของ Smad1/5/8 ใน BMP signaling pathway เพิ่มขึ้น การใช้สารผสมของ RA, SB505124, BMP4 และ EGF ใน 3 วันแรกของการเหนี่ยวนำ แล้วเปลี่ยนมาใช้ supplemented hormonal epidermal medium ในการเหนี่ยวนำต่ออีก 6 วัน ทำให้เกิดเซลล์เยื่อบุผิวกระจกตาที่ปรากฏ CK12 ซึ่งเป็นโมเลกุลบ่งชี้ความเป็นเซลล์กระจกตา การทดลองที่ 2 ได้สร้าง cell sheet จากเซลล์เยื่อบุผิวกระจกตาที่ได้จากเซลล์ต้นกำเนิดมีเซ็นไคม์จากวาร์ตันเจลลี่ของมนุษย์โดยใช้สภาวะที่เหมาะสมในการเหนี่ยวนำจากการทดลองที่ 1 และประเมินประสิทธิภาพของการปลูกถ่าย cell sheet ในการรักษาโรคพร่องเซลล์ต้นกำเนิดลิมบัสในกระต่าย เยื่อถุงน้ำคร่ำของมนุษย์ถูกนำมาลอกเยื่อบุผิวออกโดยใช้สารละลายโซเดียมไฮดรอกไซด์เข้มข้ม 0.5 N เป็นเวลา 30 วินาที ทำให้ได้ de-epithelialized amniotic membrane (dAM) จากนั้นจึงสร้าง cell sheet โดยการเพาะเลี้ยงเซลล์เยื่อบุผิวกระจกตาลงบน dAM ทำให้ได้ cell

sheet ที่ประกอบด้วยชั้นของเซลล์ 1 – 4 ชั้น ซึ่งเซลล์ยังคงปรากฏ CK12 อยู่ กระต่ายจำนวน 9 ตัว ถูกทำให้ตาข้างขวาเป็นโรคพร่องเซลล์ต้นกำเนิดลิมบัส โดยใช้สารละลายโซเดียมไฮดรอกไซด์เข้มข้ม 1 N เป็นเวลา 30 วินาที หลังจากนั้น 28 วัน จึงแบ่งกระต่ายออกเป็น 3 กลุ่มเท่าๆกัน กลุ่มที่ 1 ไม่ได้รับการรักษา กลุ่มที่ 2 ได้รับการปลูกถ่าย dAM และ กลุ่มที่ 3 ได้รับการปลูกถ่าย cell sheet ผลการทดลองพบว่าวิธี alkali burn treatment ในกลุ่มที่ 1 ไม่สามารถกำจัด LESCs ได้หมด ทำให้ LESCs ที่เหลืออยู่สร้างเซลล์เยื่อบุผิวกระจกตาขึ้นมาใหม่บริเวณขอบกระจกตาและยับยั้งการงอกของเนื้อเยื่อ conjunctiva และ หลอดเลือดเข้าสู่กลางกระจกตา กลุ่มที่ 2 วิธี alkali burn treatment และกระบวนการผ่าตัดสามารถกำจัด LESCs ออกได้ทั้งหมด ทำให้เนื้อเยื่อ conjunctiva และ หลอดเลือดงอกเข้ามาในกระจกตาอย่างรวดเร็วและไม่พบเซลล์เยื่อบุผิวกระจกตาเกิดขึ้น ในกลุ่มที่ 3 เซลล์เยื่อบุผิวกระจกตาที่ปลูกถ่ายยังคงมีชีวิตรอดและเจริญเติบโตบนกระจกตาของกระต่าย ทำให้เกิดเยื่อบุผิวกระจกตาขึ้นมาใหม่และทำให้กระตาใสขึ้น สรุปได้ว่าเซลล์ต้นกำเนิดมีเซ็นไคม์จากวาร์ตันเจลลี่ของมนุษย์เป็นตัวเลือกที่ดีในการสร้างเซลล์เยื่อบุผิวกระจกตาซึ่งเมื่อนำไปปลูกถ่ายในกระต่ายที่เป็นโรคพร่องเซลล์ต้นกำเนิดลิมบัส สามารถทำให้เกิดเยื่อบุผิวกระจกตาขึ้นมาใหม่ได้



สาขาวิชาเทคโนโลยีชีวภาพ
ปีการศึกษา 2564

ลายมือชื่อนักศึกษา_____
ลายมือชื่ออาจารย์ที่ปรึกษา_____
ลายมือชื่ออาจารย์ที่ปรึกษาร่วม_____
ลายมือชื่ออาจารย์ที่ปรึกษาร่วม_____

NGUYEN THI HONG : INDUCTION AND TRANSPLANTATION OF CORNEAL EPITHELIAL CELLS DERIVED FROM HUMAN WHARTON'S JELLY MESENCHYMAL STEM CELLS INTO THE LIMBAL STEM CELL DEFICIENCY RABBIT MODEL. THESIS ADVISOR : ASSOC. PROF. RANGSUN PARNPAI, Ph.D., 111 PP.

Keywords: Mesenchymal stem cells/Corneal epithelial cells/Differentiation/ transplantation/Rabbit

Corneal epithelium comprises of corneal epithelial cells ( CECs) that are continuously renewed by limbal epithelial stem cells ( LESCs). Loss or dysfunction of LESCs causes limbal stem cell deficiency ( LSCD) which results in loss of corneal epithelial integrity and visual impairment. To regenerate the ocular surface, transplantation of stem cells-derived CECs is necessary. The first experiment of this study aimed to test the effects of treatments on three signaling pathways involved in CEC differentiation as well as examined the optimal protocol for inducing CECs derived from human WJ-MSCs. All-trans retinoic acid (RA) inhibited Wnt signaling pathway via suppressing the translocation of β- catenin from the cytoplasm into the nucleus. SB505124 downregulated TGF-β signaling pathway via reducing the phosphorylation of Smad2. BMP4 did not increase the phosphorylation of Smad1/5/8 that involved in BMP signaling. The combination of RA, SB505124, BMP4, and EGF for the first 3 days of differentiation followed by the supplemented hormonal epidermal medium for additional 6 days could generate CECs that expressed CK12 which is a specific marker of CECs. The second experiment of this study aimed to generate cell sheet from the induced CECs derived from human WJ-MSCs and evaluate the efficiency of cell sheet transplantation on recovery of LSCD in rabbit model. CECs were induced from human WJ- MSCs following the optimal method of the first experiment. Human amniotic membrane (hAM) was de-epithelialized by 0.5N NaOH treatment for 30s then rubbing with cotton-tipped applicator. The cell sheet was generated by seeding induced CECs on human de-epithelialized AM (dhAM). The cell sheet consisted of 1- to 4-layers of

cells and these cells retained the expression of CK12. LSCD rabbit model was created by treatment with 1N NaOH for 30s in 9 right eyes of rabbits. After 28 days, rabbit right eyes were divided into 3 group: G1 (no transplantation), G2 (dhAM transplantation) and G3 (cell sheet transplantation). The results indicated that only alkali burn treatment (G1) could not destroy all LESCs so remained LESCs regenerated CECs (expressed CK12) in peripheral cornea and inhibited growing into central cornea of conjunctiva and blood vessels. In G2, alkali burn, and surgery process removed all LESCs that were functioned in both barrier and generation CECs, so conjunctiva and blood vessels grew faster, and CECs were not observed. In G3, induced CECs could survive, grow in rabbit cornea and they could support recovery of cornea epithelium, improving cornea opacity. Overall, human WJ-MSCs could be a good candidate for induced CECs that further supported reconstruction of corneal epithelium after transplantation into rabbit LSCD model.



School of Biotechnology
Academic Year 2021

Student's Signature _____
Advisor's Signature _____
Co-advisor's Signature _____
Co-advisor's Signature _____

# ACKNOWLEDGEMENTS

This study was supported by the Office of National Higher Education Science Research and Innovation Policy Council (NXPO), Thailand (Grant Number: B05F630042) and One Research One Graduate fellowships (Suranarree University of Technology, SUT).

First of all, I would like to express my sincere gratitude to my advisor, Assoc. Prof. Dr. Rangsun Parnpai, who made this work possible. He gave me the opportunity to study in his laboratory at SUT. His guidance, support and encouragement carried me throughout my study and research. I would also like to give a special thanks to my both co-advisors, Dr. Ruttachuk Rungsiwiwut and Dr. Juthaporn Assawachananont, for their valuable advice and kind help. I wish to express my sincere thanks to Dr. Tatsanee Phermthai, a chair of committee and Dr. Pishyaporn Sritangos, a committee member for their valuable comments and suggestion. Moreover, I am also grateful to Dr. Pishyaporn Sritangos for her guidance in Western Blot technique.

I would like to express my gratitude for all the lecturers at School of Biotechnology who taught me not only the biotechnology knowledges but also self-learning, communication and writing skills. I am deeply thankful to Assoc. Prof. Dr. Mariena Ketudat-Cairns for her guidance and kind help from beginning of my PhD study. Besides, I would like to extend my special thanks to all Embryo Technology and Stem Cell Research Center members (especially, Dr. Kasem Theerakittayakorn, Sirilak Somrednган, Natchanok Puangjit, Dr. Jidapa Musika, Thanya Pranomphon, Sumate Chomphutawach, Dr. Kanokwan Srirattana, Dr. Sujittra Khampang) who supported me during three years of study.

I would like to thank Dr. Thanate Anusaksathien, an ophthalmologist veterinarian, for his kind help in transplantation onto rabbit eyes. The immunohistochemistry

analysis couldn't have been done without the kind help of Assist. Prof. Dr. Apichart Ngernsoungnern and Assist. Prof. Dr. Piyada Ngernsoungnern. Moreover, I wish to acknowledge Dr. Rangsirat Wongsan, a veterinarian in SUT, for her support during experiment with rabbits.

I wish to express my appreciation to Dr. Nguyen Bui Xuan and Assoc. Prof. Dr. Quyen Dong Van for their recommendations to SUT One Research One Graduate fellowships. Without Dr. Nguyen's guidance and encouragement, my study journey in SUT could not begin. I would like to thank my colleagues in Laboratory of Embryo Technology, Institute of Biotechnology (Vietnam) for their support.

I would like to express my biggest thanks to my family for all their love, support, and encouragement. I am deeply indebted to my parents and my brother and sister who taking care of my children when I went abroad to study. For my kids, I am sorry that I stayed far from them for long time, and thank them for being such a good, understanding and healthy kids. Furthermore, I also thank my husband for his love and appreciation.

NGUYEN THI HONG

# TABLE OF CONTENTS

Page

Page

# LIST OF TABLES

# LIST OF FIGURES

# LIST OF FIGURES (Continued)

# LIST OF ABBREVIATIONS

| | | |
|---|---|---|
| CECs | = | Corneal epithelial cells |
| LESCs | = | Limbal epithelial stem cells |
| LSCD | = | Limbal stem cell deficiency |
| CLET | = | Cultivated limbal epithelial transplantation |
| COMET | = | Cultivated oral mucosal epithelial transplantation |
| CK | = | Cytokeratin |
| ESCs | = | Embryonic stem cells |
| iPSCs | = | Induced pluripotent stem cells |
| PSCs | = | Pluripotent stem cells |
| MSCs | = | Mesenchymal stem cells |
| WJ | = | Wharton's Jelly |
| AM | = | Amniotic membrane |
| hAM | = | Human amniotic membrane |
| dhAM | = | De-epithelialized human amniotic membrane |
| EGFR | = | Epithelial growth factor receptor |
| ZO-1 | = | Zonula occludens-1 |
| Cx43 | = | Conexin 43 |
| ABCG2 | = | ATP-binding cassette transporter G2 |
| C/EBPδ | = | CCAAT enhancer binding protein δ |
| CM | = | Conditioned medium |

# LIST OF ABBREVIATIONS (Continued)

| | | |
|---|---|---|
| SUT | = | Suranaree University of Technology |
| bFGF | = | Basic fibroblast growth factor |
| BMP | = | Bone morphogenetic protein |
| DKSFM | = | Defined keratinocyte serum-free medium |
| SHEM | = | Supplemented hormonal epidermal medium |
| CFU-F | = | Colony Forming Unit-Fibroblast |
| TACs | = | Transit-amplifying cells |
| USA | = | United States of America |
| MA | = | Massachusetts |
| NJ | = | New Jersey |
| NY | = | New York |
| CA | = | California |
| DE | = | Delaware |
| NC | = | North Carolina |
| BM-MSCs | = | Bone marrow stem cells |
| EGF | = | Epidermal growth factor |
| KGF | = | Keratinocyte growth factor |
| HGF | = | Hepatocyte growth factor |
| SF | = | Silk fibroin |
| CF | = | Chitosan |
| PNIPAM | = | poly(N-isopropyl acrylamide) |

# LIST OF ABBREVIATIONS (Continued)

| | | |
|---|---|---|
| H&E | = | Heamatoxylin and eosin |
| MNRH IRB | = | Maharat Nakhon Ratchasima Hospital Institution Review Board |
| CMC-DA | = | Carboxymethyl cellulose and dopamine |
| PDT | = | Population doubling time |
| P | = | passage |
| NaOH | = | Sodium hydroxide |
| BM | = | Basic medium |
| PAS | = | Periodic acid-Schiff |
| IF | = | Immunofluorescent |
| PVDF | = | Poly(vinylidene fluoride) |
| DMSO | = | Dimethyl sulfoxide |
| PBS | = | Phosphate buffer saline |
| RT | = | Room temperature |
| ITS-X | = | Insulin-transferrin-selenium-ethanolamine |
| ITS-H | = | Insulin-transferrin—sodium selenite |
| DEX | = | Dexamethasone |
| IBMX | = | Isobutylmethylxanthine |
| A2P | = | Ascorbate-2-phosphate |
| MTT | = | 3-(4,5-Dimethylthiazol-2-yl)-2,5-Diphenultetrazolium Bromide |

# LIST OF ABBREVIATIONS (Continued)

| | | |
|---|---|---|
| hUCMS | = | Human umbilical cord matrix stem cells |
| BSA | = | Bovine serum albumin |
| FBS | = | Fetal bovine serum |
| HRP | = | Horseradish peroxidase |
| F | = | Forward |
| R | = | Reverse |
| SEM | = | Standard error of the mean |
| PAX6 | = | Paired Box 6 |
| BCRP1 | = | Breast cancer resistance protein 1 |
| G | = | Group |
| FL | = | Fluorescein |
| 3D | = | Three-dimensional |
| µg | = | microgram |
| ng | = | nanogram |
| mg | = | milligram |
| µl | = | microliter |
| ml | = | milliliter |
| % | = | percentage |
| °C | = | Degree Celsius |
| M | = | molar |
| mM | = | millimolar |

# LIST OF ABBREVIATIONS (Continued)

| | | |
|---|---|---|
| TGF | = | Transforming growth factor |
| μM | = | micromolar |
| U | = | unit |
| mm | = | millimeter |
| RA | = | All-trans retinoic acid |
| p-Smad | = | Phosphorylated Smad |
| μm | = | micrometer |
| rpm | = | Round per minute |

# CHAPTER 1
# INTRODUCTION

## 1.1 Background and significance

Cornea is the transparent region that allows light to enter the eye and the photoreceptor cells in the retina. Corneal epithelium, the outmost layer of the cornea, protects the eye from the outside environment. Corneal epithelium comprises 5-6 layers of non-keratinized, stratified squamous epithelial cells (Deng et al., 2012; Mort et al., 2012) or corneal epithelial cells (CECs). Due to exposure to the environment, the corneal epithelium undergoes continuous renewal throughout life (Yoon et al., 2014). Limbal epithelial stem cells (LESCs) reside at the basal layer of the limbus, can divide asymmetrically to produce both LESC daughters and the transit-amplifying cells (TACs). While LESCs remain in the limbus, TACs migrate into the central cornea and move upward to the superficial layer of the cornea to differentiate into CECs (Liu and Kao, 2015; Yoon et al., 2014). Function of LESCs is not only to keep a constant number of CECs but also be a barrier between the conjunctiva and the cornea. Several reasons, such as chemical or thermal injury, chronic or genetic conditions, can cause loss or disfunction of LESCs, resulting in limbal stem cell deficiency (LSCD) (Norata et al., 2010; Puangsricharern and Tseng, 1995). LSCD makes a loss of corneal integrity and function, resulting in visual impairment and corneal blindness (Ahmad, 2012).

To treat LSCD, cultivated limbal epithelial transplantation (CLET) and cultivated oral mucosal epithelial transplantation (COMET) are two popular applied therapies. Both techniques give promising results for the stabilization of the ocular surface. However, autologous CLET is impossible in the case of bilateral LSCD, and allogenic CLET requires the long-term use of systemic immunosuppression (Baylis et al., 2011). The transplanted oral cells in COMET do not fully transdifferentiate into CECs (not express cytokeratin 12 (CK12), a specific marker of corneal epithelium)

(Utheim et al., 2016). Moreover, both techniques give variation in success rate, use animal-derived material, and cause peripheral corneal neovascularization (Chen et al., 2004; Satake et al., 2011; Sotozono et al., 2013).

To solve these problems, researchers are trying to find new cell sources that are better candidates for transplantation to treat LSCD, such as embryonic stem cells (ESCs), induced pluripotent stem cells (iPSCs), mesenchymal stem cells (MSCs) from Wharton's Jelly (WJ) or dental pulp, etc. Transplantation of ESCs from animals and humans successfully reconstructed the ocular surface of host species (He et al., 2020; Homma et al., 2004; Kumagai et al., 2010; Norata et al., 2012; Ueno et al., 2007). Although ESCs are pluripotent, research on human ESCs is ethically and politically controversial because isolation of human ESCs involves the destruction of human embryos (Lo and Parham, 2009). Human iPSCs could generate cornea organoids that expressed markers of adult corneal tissue (Susaimanickam et al., 2017) or showed similar features of the developing cornea (Foster et al., 2017). Human iPSCs have the same differentiation capacity as human ESCs and even avoid post-transplantation rejection by using the patient's somatic cells. However, the factors associated with iPSCs generation have been linked to oncogenic transformation, a form of *in vitro* produced tumor cells (Riggs et al., 2013). Although MSCs have lower differentiation potential, they are safer. Human MSCs from bone marrow were transplanted in rats (Ma et al., 2006) or rabbits (Guo et al., 2006) after culture on the amniotic membrane (AM). Cell sheets from human immature dental pulps-derived MSCs also were transplanted in rabbits (Gomes et al., 2010; Monteiro et al., 2009). Besides, human MSCs from adipose tissues were directly transplanted on wounded cornea of rats (Zeppieri et al., 2013), mice (Lin et al., 2013), or expanded on AM before transplantation in rabbits (Galindo et al., 2017). Transplantation of MSCs successfully reconstructed ocular surface, improved corneal transparency but terminal differentiation in some experiments was very low (Lin et al., 2013) or cannot be obtained (Ma et al., 2006). The therapeutic effectiveness of MSC transplantation may be caused by their suppression of inflammation and angiogenesis rather than the epithelial

transdifferentiation (Galindo et al., 2017; Ma et al., 2006). These results indicated that the transdifferentiation potential of transplanted MSCs *in vivo* model was uncertain. Therefore, finding an efficient method of generating CECs derived MSCs *in vitro* for generating cell sheets before transplantation is necessary. WJ-MSCs are good candidates for cellular therapies in allogenic transplantation due to their capacity for immune suppression and immune avoidance (Marino et al., 2019). However, the optimal protocol for generation of CECs from WJ-MSCs has not been reported yet. Moreover, the method for the generation of CECs is based on several signaling pathways, but there are few studies that evaluated the effects of treatment factors on these signaling pathways, especially in WJ-MSCs. Therefore, this study aimed to determine the effects of treatment factors related to main signaling pathways, investigate the optimal protocol for induction CECs from human WJ-MSCs, then use induced CECs to generate cell sheets and evaluate effectiveness of induced CEC sheet transplantation onto LSCD eyes of the rabbit model.

## 1.2 Research Objectives

1.2.1 Test effect of treatment factors (all-trans retinoic acid (RA), SB505124, BMP4) on three signaling pathways involved in CEC differentiation.

1.2.2 Find the optimal method to differentiate human WJ-MSCs into CECs by using several combinations of treatment factors

1.2.3 Generate induced CEC sheet by seeding induced CECs derived from human WJ-MSCs onto de-epithelialized human amniotic membrane (dhAM)

1.2.4 Evaluate efficiency of induced CEC sheet transplantation on recovery of rabbit LSCD eyes

## 1.3 References

Ahmad, S. (2012). Concise review: Limbal stem cell deficiency, dysfunction, and distress. **Stem Cells Transl. Med.** 1(2): 110-115.

Baylis, O., Figueiredo, F., Henein, C., Lako, M., and Ahmad, S. (2011). 13 years of cultured limbal epithelial cell therapy: A review of the outcomes. **J. Cell Biochem.** 112(4): 993: 1002.

Chen, Z., de Paiva, C. S., Luo, L., Kretzer, F. L., Pflugfelder, S. C., and Li, D. Q. (2004). Characterization of putative stem cell phenotype in human limbal epithelia. **Stem Cells** 22(3): 355-366.

Deng, S. X., Sejpal, K. D., Tang, Q., Aldave, A. J., Lee, O. L., and Yu, F. (2012). Characterization of limbal stem cell deficiency by *in vivo* laser scanning confocal microscopy: A microstructural approach. **Arch. Ophthalmol.** 130(4): 440-445.

Foster, J. W., Wahlin, K., Adams, S. M., Birk, D. E., Zack, D. J., and Chakravarti, S. (2017). Cornea organoids from human induced pluripotent stem cells. **Sci. Rep.** 7(1): 41286.

Galindo, S., Herreras, J. M., López-Paniagua, M., Rey, E., de la Mata, A., Plata-Cordero, M., Calonge, M., Nieto-Miguel, T. (2017). Therapeutic effect of human adipose tissue-derived mesenchymal stem cells in experimental corneal failure due to limbal stem cell niche damage. **Stem Cells** 35(10): 2160-2174.

Gomes, J. A., Geraldes Monteiro, B., Melo, G. B., Smith, R. L., Cavenaghi Pereira da Silva, M., Lizier, N. F., Kerkis, A., Cerruti, H., and Kerkis, I. (2010). Corneal reconstruction with tissue-engineered cell sheets composed of human immature dental pulp stem cells. **Invest. Ophthalmol. Vis. Sci.** 51(3): 1408-1414.

Guo, T., Wang, W., Zhang, J., Chen, X., Li, B. Z., and Li, L. S. (2006). Experimental study on repairing damage of corneal surface by mesenchymal stem cells transplantation. **Zhonghua Yan Ke Za Zhi** 42(3): 246-250.

He, J., Ou, S., Ren, J., Sun, H., He, X., Zhao, Z., Wu, H., Qu, Y., Liu, T., Jeyalatha, V., Zhang, L., Li, Q., Reinach, P. S., Quantock, A., Hao, J., Liu, Z., and Li, W. (2020). Tissue engineered corneal epithelium derived from clinical-grade human embryonic stem cells. **Ocul. Surf.** 18(4): 672-680.

Homma, R., Yoshikawa, H., Takeno, M., Kurokawa, M. S., Masuda, C., Takada, E., Tsubota, K., Ueno, S., and Suzuki, N. (2004). Induction of epithelial progenitors *in vitro* from mouse embryonic stem cells and application for reconstruction of damaged cornea in mice. **Invest. Ophthalmol. Vis. Sci.** 45(12): 4320-4326.

Kumagai, Y., Kurokawa, M. S., Ueno, H., Kayama, M., Tsubota, K., Nakatsuji, N., Kondo, Y., Ueno, S., and Suzuki, N. (2010). Induction of corneal epithelium–like cells from cynomolgus monkey embryonic stem cells and their experimental transplantation to damaged cornea. **Cornea** 29(4): 432-438.

Lin, K.-J., Loi, M.-X., Lien, G.-S., Cheng, C.-F., Pao, H.-Y., Chang, Y.-C., Ji, A. T.-Q., and Ho, J. H.-C. (2013). Topical administration of orbital fat-derived stem cells promotes corneal tissue regeneration. **Stem Cell Res. Ther.** 4(3): 72.

Liu, C.-Y., and Kao, W. W.-Y. (2015). Chapter five - Corneal epithelial wound healing. In J. F. Hejtmancik and J. M. Nickerson (Eds.), **Progress in Molecular Biology and Translational Science** 134: 61-71.

Lo, B., and Parham, L. (2009). Ethical issues in stem cell research. **Endocrine reviews** 30(3): 204-213.

Ma, Y., Xu, Y., Xiao, Z., Yang, W., Zhang, C., Song, E., Du, Y., and Li, L. (2006). Reconstruction of chemically burned rat corneal surface by bone marrow–derived human mesenchymal stem cells. **Stem Cells** 24(2): 315-321.

Marino, L., Castaldi, M. A., Rosamilio, R., Ragni, E., Vitolo, R., Fulgione, C., Castaldi, S. G., Serio, B., Bianco, R., Guida, M., and Selleri, C. (2019). Mesenchymal stem cells from the wharton's jelly of the human umbilical cord: Biological properties and therapeutic potential. **Int. J. Stem Cells**, 12(2): 218-226.

Monteiro, B. G., Serafim, R. C., Melo, G. B., Silva, M. C. P., Lizier, N. F., Maranduba, C. M. C., Smith, R. L., Kerkis, A., Cerruti, H., Gomes, J. A. P., and Kerkis, I. (2009). Human immature dental pulp stem cells share key characteristic features with limbal stem cells. **Cell Prolif.** 42(5): 587-594.

Mort, R. L., Douvaras, P., Morley, S. D., Dorà, N., Hill, R. E., Collinson, J. M., and West, J. D. (2012). Stem cells and corneal epithelial maintenance: insights from the mouse and other animal models. **Results. Probl. Cell. Differ.** 55: 357-394.

Notara, M., Alatza, A., Gilfillan, J., Harris, A. R., Levis, H. J., Schrader, S., .Vernon, A., and Daniels, J. T. (2010). In sickness and in health: Corneal epithelial stem cell biology, pathology and therapy. **Exp. Eye Res.** 90(2): 188-195.

Notara, M., Hernandez, D., Mason, C., and Daniels, J. T. (2012). Characterization of the phenotype and functionality of corneal epithelial cells derived from mouse embryonic stem cells. **Regen. Med.** 7(2):167-178.

Puangsricharern, V., and Tseng, S. C. G. (1995). Cytologlogic evidence of corneal diseases with limbal stem cell deficiency. **Ophthalmology** 102(10): 1476-1485.

Riggs, J. W., Barrilleaux, B. L., Varlakhanova, N., Bush, K. M., Chan, V., and Knoepfler, P. S. (2013). Induced pluripotency and oncogenic transformation are related processes. **Stem Cells Dev.** 22(1): 37-50.

Satake, Y., Higa, K., Tsubota, K., and Shimazaki, J. (2011). Long-term outcome of cultivated oral mucosal epithelial sheet transplantation in treatment of total limbal stem cell deficiency. **Ophthalmology** 118(8): 1524-1530.

Sotozono, C., Inatomi, T., Nakamura, T., Koizumi, N., Yokoi, N., Ueta, M., Matsuyama, K., Miyakoda, K., Kaneda, H., Fukushima, M., and Kinoshita, S. (2013). Visual improvement after cultivated oral mucosal epithelial transplantation. **Ophthalmology** 120(1): 193-200.

Susaimanickam, P. J., Maddileti, S., Pulimamidi, V. K., Boyinpally, S. R., Naik, R. R., Naik, M. N., Reddy, G. B., Sangwan, V. S., and Mariappan, I. (2017). Generating minicorneal organoids from human induced pluripotent stem cells. **Development** 144(13): 2338-2351.

Ueno, H., Kurokawa, M. S., Kayama, M., Homma, R., Kumagai, Y., Masuda, C., Takada, E., Tsubota, K., Ueno, S., and Suzuki, N. (2007). Experimental transplantation of

corneal epithelium-like cells induced by pax6 gene transfection of mouse embryonic stem cells. **Cornea** 26(10): 1220-1227.

Utheim, T. P., Utheim, Ø. A., Khan, Q.-E. S., and Sehic, A. (2016). Culture of oral mucosal epithelial cells for the purpose of treating limbal stem cell deficiency. **J. Funct. Biomater.** 7(1): 5.

Yoon, J. J., Ismail, S., and Sherwin, T. (2014). Limbal stem cells: Central concepts of corneal epithelial homeostasis. **World J. Stem Cells** 6(4): 391-403.

Zeppieri, M., Salvetat, M. L., Beltrami, A. P., Cesselli, D., Bergamin, N., Russo, R., Cavaliere, F., Varano, G. P., Alcalde, I., Merayo, J., Brusini, P., Beltrami, C. A., and Parodi, P. C. (2013). Human adipose-derived stem cells for the treatment of chemically burned rat cornea: preliminary results. **Curr. Eye Res.** 38(4): 451-463.

# CHAPTER 2
# LITERATURE REVIEW

## 2.1 Characterization of corneal epithelial cells

Cornea is the transparent region that allows light to enter the eye and come to the photoreceptor cells in the retina. Moreover, it also is the protective, impermeable barrier (Mort et al., 2012) that protects the eye from the external environment. The cornea comprises five layers. However, there are only three cellular layers (epithelium, stroma, and endothelium). The other two layers are the matrix layers (Bowman's layer and Descemet's membrane). The corneal epithelium is the outermost layer which consists of 5-6 layers of CECs (Deng et al., 2012; Mort et al., 2012). These cells are connected by tight junctions. There are three types of CECs: basal cells, wing cells, and superficial cells (Wijnholds, 2019). Basal cells are the epithelial columnar cells that form a single layer attached to Bowman's layer. These basal cells can divide and migrate to the center of the cornea (Wijnholds, 2019). Wing cells are polyhedral cells that stratifies two to three layers covering the basal cell layer. Lastly, the superficial cells are squamous cells, with flattened nuclei, which age and slough off into the tear film.

Maintaining the structure of the cornea is necessary for the high-quality vision (Lobo et al., 2016). Like skin that exposes to the external environment, CECs are continuously renewal throughout life (Yoon et al., 2014). The regeneration of new CECs is attributed to the LESCs located in limbus (Kim et al., 2004). These LESCs can divide asymmetrically to produce TACs which migrate centripetally from periphery to the central cornea to form the basal cells that migrate vertically to the cornea surface to form superficial cells (Yoon et al., 2014). As the mention of the central dogma of corneal homeostasis, the mass of the corneal epithelium remains constant, so the rate of cellular proliferation must equal to the rate of cell desquamation (Sharma and Coles, 1989).

The phenotype of CECs varies from basal cells to superficial differentiated cells (Kim et al., 2004). Both epithelial growth factor receptor (EGFR) and integrin β1, a putative stem cell marker for epidermal keratinocytes, express higher in the cell membrane of basal cells than suprabasal cells (Chen et al., 2004). However, other putative stem cell markers of epidermal keratinocytes, integrin α6 expresses in the cell membrane of suprabasal cells (Chen et al., 2004). In contrast, involucrin, a differentiated marker, is stained in the superficial layer while PAX6 expresses in all layers of the corneal epithelium (Lin et al., 2012; Kitazawa et al., 2017). Moreover, the resistance barrier function of the corneal epithelium is created by the tight junction proteins, such as zonula occludens-1 (ZO-1), occludin, and claudin. ZO-1 is presented between the superficial cells (Sosnová-Netuková et al., 2007; Surgue and Zieske, 1997; Wang et al., 1993) while claudin and occluding express in most layers of the cornea epithelium (Sosnová-Netuková et al., 2007). E-cadherin, an intercellular junction protein, also is showed in all layers of corneal epithelium while Connexin 43 (Cx43), a gap junction protein, mostly expresses in the basal layer of corneal epithelium (Bardag-Gorce et al., 2016). Especially, two specific markers of CECs are CK3 and CK12, express in all layers of corneal epithelium (Gouveia et al., 2019; Kitazawa et al., 2017). CECs do not express CK10 (Kitazawa et al., 2017) and show very low expression of CK15, ΔNp63, α9, Lamγ3, and nuclear β-catenin (Gouveia et al., 2019).

## 2.2 Characterization of LESCs

LESCs are the stem cell population located at the basal layer of the limbus (Norata et al., 2018) which is the border between the cornea and sclera. LESCs can divide asymmetrically to produce both limbal stem cell daughters which remained in limbus and TAC daughters (Liu and Kao, 2015; Yoon et al., 2014). LESCs are mitotically quiescent or slow-cycling cells that express CCAAT enhancer-binding protein δ (C/EBPδ), Bmi1, and ΔNp63α and can generate holoclones in culture (Barbaro et al., 2007). When the cornea is damaged, LESCs switch off C/EBPδ and Bmi1, highly proliferate, and differentiate into mature CECs (Barbaro et al., 2007). Unlike basal cells of the corneal epithelium, LESCs are smaller and have a high nucleus/cytoplasm ratio (Chen et al., 2004).

LESCs expressed EGFR, integrin β1, integrin α9, CK19, CD71, and Enolase (Chen et al., 2004). Moreover, LESCs showed expression of ATP-binding cassette transporter G2 (ABCG2), CK15 (Gouveia et al., 2019), ABCB5 (Ksander et al., 2014), frizzled 7, CK14, N-cadherin (Mei et al., 2014), CK109 (Bojic et al., 2018). However, LESCs were negative with Cx43, E-cadherin, Involucrin, CK3, and CK12 (Chen et al., 2004). Murine LESCs highly expressed CD200 while human LESCs showed few expression of this marker (Bojic et al., 2018). Although many markers expressed in LESCs, specific markers of LESCs remain unknown (Notara et al., 2018). Unlike CECs, LESCs expressed high level of β-catenin in the nucleus (Gouveia et al., 2019).

## 2.3 LSCD: cause, symptom, and treatments

The function of LESCs is not only to remain a constant number of CECs but also be a barrier between the conjunctiva and cornea. So loss or dysfunction of LESCs causes LSCD that further makes corneal epithelium to lose its integrity and function, leading to persistent pain and severe visual defect (Dua et al., 2000). Moreover, limbal barrier failure results in process of corneal conjunctivalization that makes a loss of corneal clarity and visual impairment (Ahmad, 2012). LSCD can be caused by internal and external reasons. The internal reasons are genetic mutations that happened in some diseases, such as aniridia, congenital epidermal dysplasia, dyskeratosis, Turner syndrome, etc. The external reasons result from external factors that damage LESCs, the stem cell niche that is necessary for maintaining LESCs, or both LESCs and the stem cell niche (Le et al., 2018). The external factors that cause LSCD are chemical or thermal burns, inflammation directed from the limbal microenvironment, etc. (Cabral et al., 2020).

LSCD can be diagnosed by slit-lamp bio-microscopy under white light without fluorescein staining (FL) and cobalt blue light using FL (Deng et al., 2012). The affected area of the cornea contains an abnormal conjunctival/metaplastic epithelium layer. This layer is thin and lacks cell-cell tight junctions so fluorescein can go through and stain in an alkaline environment of Bowman's membrane under the affected corneal area. The stages of LSCD are graded as mild, moderate, several stages (Le et al., 2018).

In the mild stage, the corneal surface is dull/irregular and loss of light reflex, corneal epithelial opacity, and limbus was lost of palisades of Vogt (Le et al., 2018). Stippling FL is present in the area covered by both hazed or neovascularized corneal epithelium which are less than half of the sector (Deng et al., 2012; Sacchetti et al., 2005). Stromal scarring is also involved in less than half of the sector (Sacchetti et al., 2005). In the moderate stage, late FL, and epithelial thinning are shown in a vortex pattern (Deng et al., 2012). Epithelial deficiency, superficial neovascularization, and stromal scarring are included in more than half of the sector (Sacchetti et al., 2005). Iris details are invisible, and pupil can be difficultly seen (Shortt et al., 2014). Finally, in the several stages, same vortex patterns of FL pooled at abnormal corneal epithelial area that is persistent epithelial defect, with or without vascularization of cornea (Deng et al., 2012). Moreover, stromal scarring is involved in the entire sector (Sacchetti et al., 2005). Both iris details and pupil cannot be seen (Shortt et al., 2014). Recently, a clinical scoring system for classification of LSCD using clinical and confocal grading is developed (Aravena et al., 2019).

There are two common techniques that were used for treatment LSCD. The first technique is COMET which was first described in the rabbit model (Nakamura et al., 2003). This technique uses autologous cells, so it gives promising results for stabilization of the ocular surface. The second technique is CLET which can be done with both autologous and allogeneic transplantation. However, autologous CLET is impossible when both eyes are impaired and allogenic CLET requires the use of long-term systemic immunosuppression (Baylis et al., 2011). Moreover, cell sources of CLET from limbal tissues are limited. Both techniques give variation in success rate, use animal-derived materials in culture protocols, and cause peripheral corneal neovascularization (Chen et al., 2004; Satake et al., 2011; Sotozono et al., 2013).

To overcome these disadvantages, researchers are trying to find new cell sources that are better candidates for treatment LSCD, such as iPSCs, ESCs, MSCs derived from WJ, dental pulp, etc.

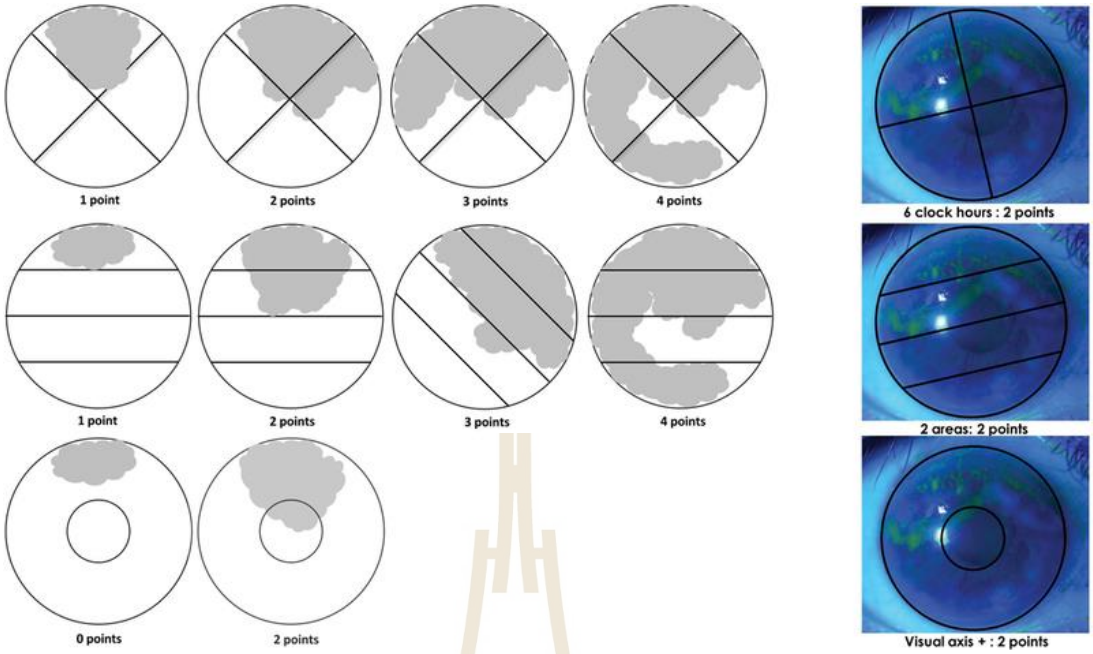


**Figure 2.1** Classification of LSCD (Aravena et al., 2019).

Transplantation of corneal epithelial-like cells derived from mouse ESCs (Notara et al., 2012; Ueno et al., 2007), and monkey ESCs (Kumagai et al., 2010) could repair the ocular surface of host species. After transplantation of mouse induced corneal epithelial-like cells that expressed CK12 and p63α, the damaged cornea of porcine was healed with several layers of corneal epithelium, and the transplanted cells retained expression of corneal marker (Norata et al., 2012). In mouse model, transplanted corneal epithelial-like cells that were induced by transfection of Pax6 cDNA into mouse ESCs could develop to generate three epithelial cell layers on mouse wounded cornea (Ueno et al., 2007). Moreover, the damaged cornea of mouse was recovered with the formation of multiple cell layers after transplantation of induced corneal epithelial-like cells from monkey ESCs (Kumagai et al., 2010). Besides, induced epithelial progenitor cells from mouse ESCs, and induced epithelial cells from human ESCs were also used for transplantation into animal models (He et al., 2020; Homma et al., 2004). Transplantation of induced epithelial progenitor cells derived from mouse ESCs successfully repaired mouse corneal surface (Homma et al., 2004). LSCD treatment on rabbit model successfully repaired the corneal epithelium by transplantation of induced epithelial

cell sheet derived from human ESCs (He et al., 2020).

Treatment LSCD by iPSCs transplantation has not yet been reported but iPSCs promise a valuable opportunity for visual treatments. These cells have similar differentiation potentiality to ESCs. Moreover, iPSC transplantation can avoid immune rejection because they can be generated from patients' somatic cells. Human iPSCs could form minicorneal organoids that showed markers of adult corneal tissue (Susaimanickam et al., 2017) or presented similar characteristics of the developing cornea (Foster et al., 2017). The induced cell sheets that were generated by explant cultures of minicorneas on dhAM for 10 days showed expression of CEC markers (PAX6 and CK12) (Susaimanickam et al., 2017). Human iPSC-organoids consisted of three cell types that stained with corneal epithelial markers (CK3, p63), stromal markers (collagen type I and V), and endothelial markers (Collagen type VIII) (Foster et al., 2017).

Transplantations of MSCs in animal models were also studied for treatment of LSCD. Human MSCs from bone marrow were transplanted in rats (Ma et al., 2006) or rabbits (Guo et al., 2006) after culture on AM. Cell sheets from human immature dental pulps-derived MSCs also were transplanted in rabbits (Gomes et al., 2010; Monteiro et al., 2009). Besides, human MSCs from adipose tissues were directly transplanted on wounded cornea of rat (Zeppieri et al., 2013), mice (Lin et al., 2013) or expanded on AM before transplantation in rabbits (Galindo et al., 2017). Transplantation of MSCs successfully reconstructed ocular surface, improved corneal transparency. However, in some experiments, terminal differentiation into CECs *in vivo* was very low (Lin et al., 2013) or cannot be obtained (Ma et al., 2006).

## 2.4 Human pluripotent stem cells (PSCs): definition, capacity to differentiate into CECs

Human PSCs have two types: human ESCs and iPSCs. Human ESCs were first successfully isolated from the inner cell mass of a blastocyst (Thomson et al., 1998). Human ESCs express high levels of telomerase activity, specific cell surface markers (SSEA-3, SSEA-4, TRA-1-60, TRA-1-81, and alkaline phosphatase), and have capacity to

differentiate into all three embryonic germ layers (endoderm, mesoderm, and ectoderm) (Thomson et al., 1998). Human iPSCs, firstly generated from human adult fibroblasts in 2007, have similar characterization with human ESCs that are unlimited self-renewal and have the differentiation potentialities to generate any cell type of the adult organism (Takahashi et al., 2007).

Two differentiation methods to generate CECs from PSCs are transgenic and non-transgenic method. While the transgenic method was only conducted in mouse ESCs (Ueno et al., 2007), non-transgenic method was performed in human PSCs. Non-transgenic method comprises the defined induction medium and conditioned medium (CM). CM was collected from human limbal fibroblasts (Ahmad et al., 2007; Brzeszczynska et al., 2014) or human limbal stromal cells (Cieślar-Pobuda et al., 2016). After isolating and expanding by subculture up to 10 – 15 passages, limbal fibroblasts or stromal cells were treated with mitomycin C and re-plated on tissue culture flasks with epithelium medium. CM was collected daily for 7 days (Ahmad et al., 2007; Brzeszczynska et al., 2014) or 10 days (Cieślar-Pobuda et al., 2016). After culturing on collagen IV with CM, human ESCs were differentiated into corneal epithelial-like cells (Ahmad et al., 2007). Brzeszczynska et al. (2014) followed the protocol of Ahmad et al. (2007) by using CM for generate CECs with some modifications, such as human ESCs (H9 and RCM1) were culture on Matrigel without feeder cells. Because of culture with CM from other cell types and other species, there are risks of contamination or disease transmission.

To overcome the disadvantage of CM, researchers focused on investigating the defined medium supplement with serum-free and xeno-free to differentiated human ESCs or iPSCs into CECs. Differentiation into CECs from human iPSCs or ESCs often follows two main steps (Kamarudin et al., 2018; Lian et al., 2013; Mikhailova et al., 2014). In the first step, human ESCs/human iPSCs were treated with small molecules and/or growth factors to differentiate to ectodermal cells or keratinocytes. The second step, corneal epithelium medium (Cnt-30 or CnT prime + 10% FBS) or defined

keratinocyte serum-free medium (DKSFM) were used to further differentiated to CECs (key markers: CK3 and CK12). Lian et al. (2013) used DMEM/F12 supplemented with RA alone or combination of RA with β-mercaptoethanol, basic fibroblast growth factor (bFGF), and bone morphogenetic protein 4 (BMP4) for the first step and DKSFM in the second step to differentiate human iPSCs into corneal epithelial-like cells. However, that method could induce CECs with low efficiency (only 5% positive with CK3) (Lian et al., 2013). Mikhailova et al. (2014) used RegES medium supplemented with two small molecules (SB505124, IWP2) and bFGF for the first step and move to Cnt-30 medium in the second step could differentiate human iPSC into CECs with higher efficiency (about 70% expression CK12 and 30% expression CK3 in average). Comparison of several combinations of small molecules and BMP4, RA was evaluated by Kamarudin et al. (2018). The finding of their research suggests that DMEM/F12 supplement with BMP4, RA, EGF for the first step was the best choice for the first step (Kamarudin et al., 2018). However, the efficiency of differentiation depended on the cell lines with a variety level of BMP signaling activity (Kamarudin et al., 2018).

## 2.5 MSCs: definition, capacity to differentiate into CECs

MSCs are often isolated from many sources including bone-marrow, adipose tissue, dental pulp, WJ of the umbilical cord, or placenta, etc. The Mesenchymal and Tissue Stem Cell Committee of the International Society for Cellular Therapy (ISCT) proposes the minimal criteria to define human MSCs as follows: 1) MSCs must be plastic-adherent when maintained in standard culture conditions; 2) MSCs must express CD105, CD73, CD90, and lack the expression of CD45, CD34, CD14 or CD11b, CD79 alpha or CD19 and HLA-DR surface molecules; 3) MSCs must differentiate to osteoblasts, adipocytes, and chondroblasts *in vitro* (Dominici et al., 2006). Besides, MSCs are referred to as a population of fibroblast-like cells that can formed clonal colonies (Colony Forming Unit-Fibroblast, CFU-F) *in vitro* at low density of seeding (Friedenstein et al., 1974). MSCs are among the most commonly used cell type for regenerative medicine (Hmadcha et al., 2020) because of these numerous advantages, such as availability and ease of isolation, ability to differentiate into multiple cell lineages and cause immunosuppression, safety

without any possibility of malignant transformation after infusion of allogeneic cells, and the lack of ethical issues (Kim and Park, 2017).

MSCs can differentiate into CECs using CM from limbal stem cells or co-culture with limbal stem cells (Gu et al., 2009). CECs can be generated from both methods in a short time, 2 days, but with very low efficiency (7-9% in average positive with CK3) (Gu et al., 2009). The further study also used the limbal CM for differentiation of human bone marrow stem cells (BM-MSCs) into CECs (Rohaina et al., 2014). Rohaina et al. (2014) generated CECs in 10 days with higher efficiency (54% positive with CK3) than Gu et al. (2009), however, expression of CK3 in induced CECs from BM-MSCs was not clear compared with that in CECs (Rohaina et al., 2014). Comparison of the CM derived from different cell sources was reported (Nieto-Miguel et al., 2013). Using the CM from human CECs was better than from limbal fibroblasts for differentiated human adipose stem cells to CECs (Nieto-Miguel et al., 2013).

Another method for differentiation of MSCs into CECs using the defined medium. The epidermal growth factor (EGF), keratinocyte growth factor (KGF) and hepatocyte growth factor (HGF) are believed to play an important role in the maintenance of CECs and wound healing (Saichanma et al., 2012). The effects of these factors and RA on epithelial differentiation of rabbit adipose-derived stem cells were evaluated (Li et al., 2012). The optimal concentration of RA, KGF, HGF, EGF were determined (2.5 mM, 10 ng/ml, 10 ng/ml, 20 ng/ml, respectively) (Li et al., 2012). By using a combination of these agents, rabbit adipose-derived stem cells could be differentiated to be epithelial cells expressed epithelial marker (22% express CK13, 63% express CK19) (Li et al., 2012). Without using RA, a combination of KGF, EGF, and HGF (20 ng/ml, 10ng/ml, 20 ng/ml, respectively) could generate corneal epithelial-like cells from human skin-derived precursor cells (Saichanma et al., 2012). However, the cells expressed only CK3 mRNA after 14 days and did not express CK12 mRNA and the protein expression results showed that the cells were positive with CK3/12 (Saichanma et al., 2012). These results suggested that the induced cells might express only CK3.

To research the function of gene-related capacity of differentiation into CECs, researchers separated human BM-MSCs into two groups (positive and negative with SSEA4 marker) and using 3-step method to differentiate to CECs (Katikireddy et al., 2014). The SSEA4+ cells could differentiate into CECs (expressed corneal markers: CK3, CK12, CK15, and E-cadherin) but these cells were only 4.9% in BM-MSC population (Katikireddy et al., 2014). These results indicated that MSCs have a low capacity to differentiate into CECs by using the above method.

## 2.6 Signaling pathways related to corneal epithelial differentiation

During embryogenesis, corneal epithelium originated from the ocular surface ectoderm (Wolosin et al., 2004). Arkell and Tam (2012) reported that the initial events in the formation of the murine head depend on the signaling activity of the Wnt/β-catenin, Nodal/activin and BMP pathways (Arkell and Tam, 2012).

Down regulating or blocking the canonical Wnt signaling is necessary for generating CECs. Suppression Wnt signaling by small-molecule inhibitor of the Src family kinases (SU6656) or RA was shown to promote simple epithelial differentiation of human PSCs (Lian et al., 2013). Both of them downregulated Wnt signaling pathway via inhibiting the translocation of β-catenin, a key component in the Wnt signaling pathway, from the cytoplasm into the nucleus (Lian et al., 2013). FSU6656 treatment with β-mercaptoethanol and without bFGF can differentiate human PSCs into simple epithelial cells (expressed CK18), then RA combined with β-mercaptoethanol, bFGF and BMP4 could further differentiate these simple epithelial cells into both keratinocytes and CECs (Lian et al., 2013). A combination of RA, BMP4, EGF could generate corneal epithelial-like cells from human iPSCs and ESCs (Kamarudin et al., 2018). Treatment cells with BMPs induce activation of ALK3, ALK6, leading to phosphorylation of Smad1/5/8, resulting in increasing BMP signaling pathway (Mayeur et al., 2014). The results of Kamarudin et al. (2018) revealed that the activity of the endogenous BMP signaling pathway effected on the differential capacity of human iPSC lines toward CECs. Blocking the Wnt pathway by knockout β-catenin or co-receptor

LRP5/6 could drive corneal stroma keratinocytes into corneal epithelium via interaction with BMP4 (Zhang et al., 2015). The model of the interaction between Wnt signaling and BMP4 is shown in Figure 2.2. Wnt signaling activation increased β-catenin content in the cell nucleus so that BMP4 transcription was blocked before stratification. In contrast, the deletion of β-catenin or LPR5/6 resulted in no β-catenin in cell nucleus that increased BMP4 transcription, leading to enhance p63, pERK1/2, pSmad1/5 expression before eyelid opening.

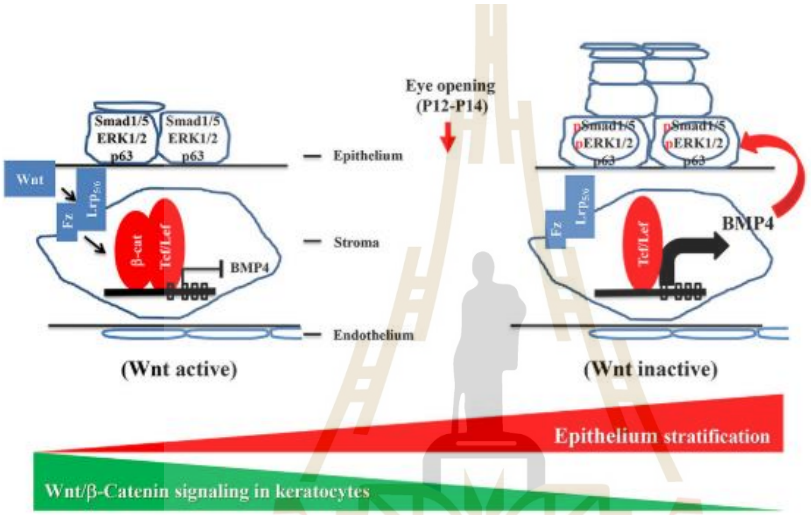


**Figure 2.2** Model of the interaction between corneal stroma (canonical Wnt signaling) and epithelium (BMP4 signaling) during mouse corneal development (Zhang et al., 2015).

Blocking the transforming growth factor-beta (TGF-β), Wnt signaling pathway and activating FGF signaling generated pure populations of CECs from human iPSCs (Mikhailova et al., 2014). Mikhailova et al. (2014) reported that combination treatment of two small molecules (SB505124, an inhibitor of TGF-β and activin signaling, and IWP2, an inhibitor of Wnt signaling pathway) and bFGF (an activator of FGF signaling) downregulated the expression of pluripotency markers and differentiated human iPSCs toward CECs. SB505124 selectively and concentration-dependently inhibits cytoplasmic signal transducers (Smad2 and Smad3) via inhibition of TGF-β receptor type I receptors (ALK4, ALK5, and ALK7) (Byfield et al., 2004). SB505124 inhibits TGF-

β/activin signaling more efficiently than its analog SB-431542 (Byfield et al., 2004). Moreover, SB505124 does not inhibit ALK1, ALK2, ALK3, ALK6-induced Smad1/5/8 which are cytoplasmic signal transducers of BMP signaling pathway (Byfield et al., 2004; Heldin et al., 1997). Lee et al. (2017) investigated the effect of IWP2 on the proliferation and differentiated capacity of the limbal epithelial progenitor cells which were isolated from explant culture or enzymatic digestion (Lee et al., 2017). Their results showed that IWP2 decreased total β-catenin content, the main component of the Wnt signaling pathway. However, IWP2 increased stem/progenitor cell marker (p63α and ABCG2) and colony formation capacity in the explants but decreased these markers on isolated cells. Summary of main signaling pathways (Wnt, FGF, BMP4, and TGF-β) related differentiation of human PSCs into CECs is shown in Figure 2.3.

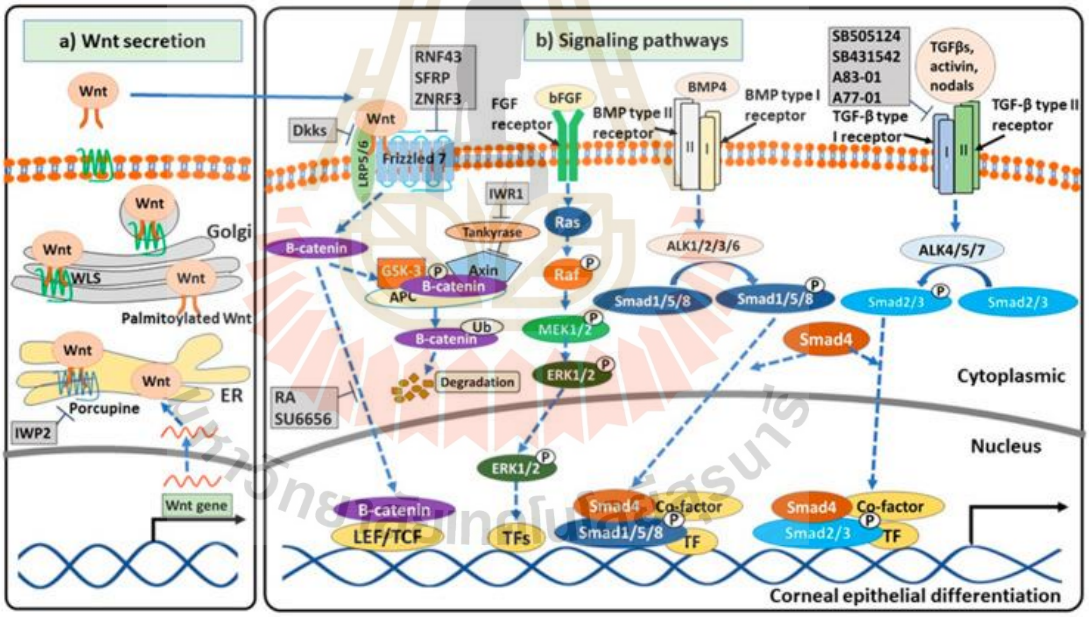


**Figure 2.3** Summary of signaling pathways involved in the differentiation of PSCs into CECs (Theerakittayakorn et al., 2020).

## 2.7 Cell carriers/carrier-free transplantation

Many materials were examined for the generation of the cell sheet for ocular surface reconstruction by transplantation. Silk fibroin (SF), isolated from the silkworm,

can be a candidate for a transparent membrane (Haagdorens et al., 2016) because SF is non-immunogenic, degradable, mechanically strong, and transparent. SF combined with chitosan (CS) was used in constructed scaffolds (Guan et al., 2013a; Guan et al., 2013b). Primary rabbit CECs and corneal stroma cells were seeded on corneal lamellar scaffolds (SF-CS). The reconstructed lamellar cornea expressed a high level of K3/12 than native tissue (Guan et al., 2013a). Moreover, SF-CS films have been seen in rabbit corneas for up to six months (Guan et al., 2013b). SF film from non-mulberry silkworm *Antheraea mylitta* is suggested as a valuable candidate for generate the corneal scaffold (Hazra et al., 2016) because SF film supported the growth of CECs and keratocytes from rat corneal explants and generated cell sheets expressed CK3 and vimentin respectively. Furthermore, implanted SF film remains transparent, stable, easy to handle and the corneal surface integrity is maintained (Hazra et al., 2016). Transparent SF film from mulberry silkworm *Bombyx mori* supported the generation of artificial endothelial grafts with the characteristic of endothelial cells and SF artificial endothelial graft restored the corneal transparency and thickness (Vázquez et al., 2017).

Cell sheets with carrier-free was also used for the ocular therapy. A temperature-responsive polymer (poly(N-isopropyl acrylamide) or PNIPAM) can generate intact, transplantable epithelial sheets that retain stem cells and epithelial cells (Nishida et al., 2004). Human or rabbit limbal stem cells were co-cultured with mitomycin C-treated 3T3 feeder layer on dished coated with PNIPAM and cell sheets were then harvested by decreasing temperature to 20°C. Harvested sheets were easily manipulated, transplantable without any carriers, and corneal surface reconstruction in rabbits was highly successful. Nowadays, commercial dishes coated with PNIPAM are sold from many companies. However, the dishes for temperature-sensitive cell sheet generation are very expensive and difficult to apply to numerous experiments for clinical application (Patel and Zhang, 2013). Coating dish with PNIPAM at the laboratory also required expensive equipment and temperature decrease for cell detachment may affect gene expression of cells (Sonna et al., 2002). A new method for cell sheet generation could overcome the disadvantage of PNIPAM coated dish by using cheap materials (carboxymethyl

cellulose and dopamine (CMC-DA)) (Hong et al., 2018). Human MSCs or corneal limbal epithelial cells were seeded on the cell culture inserts coated with CMC-DA, cultured until reaching the confluent point and the cell sheets were then detached using cellulase (Hong et al., 2018). Human CEC sheets were generated with a well-preserved morphology and transparency after detachment (Hong et al., 2018). Their results suggested that the strategy of coating dish with CMC-DA and harvesting cell sheets by cellulase is an effective option for the generation cell sheet.

Although many materials were evaluated for generating cell sheet to transplant onto cornea, hAM is the most popular cell carrier used for ophthalmology (Schwab et al., 2000; Tananuvat et al., 2017) because it is anti-bacterial, anti-angiogenic, poorly immunogenic, contains important growth factor, supports wound healing ophthalmology (Ramuta and Kreft, 2018). hAM, the innermost layer of the placenta sac, is usually 0.02 to 0.5mm thick (Bourne, 1960) and consists of three layers: epithelium (monolayer of amniotic epithelial cells), basal lamina, and avascular stroma which composed of three layers: the compact layer, amniotic mesenchymal stroma cell layer, and spongy layer (Ramuta and Kreft, 2018). hAM can be used as intact or de-epithelialized. Although both hAM and de-epithelialized amniotic membrane (dhAM) support the growth of LESCs and remain the expression of putative LESC markers, dhAM promotes to better migration of LESCs than hAM (Shortt et al., 2009). Several methods have been used to de-epithelialization of hAM, such as treatment with trypsin-EDTA, EDTA, thermolysin, Dispase, urea, etc. (Zhang et al., 2013; Hopkinson et al., 2008) . However, these treatments take long time that may damage the hAM or remove its components and even they fail to remove all epithelial cells. Recently, a simple method using sodium hydroxide for decellularization of hAM is reported (Saghizadeh et al., 2013). The procedure of using sodium hydroxide is fast and efficient in totally removing epithelium of hAM.

## 2.8 References

Ahmad, S. (2012). Concise review: Limbal stem cell deficiency, dysfunction, and distress. **Stem Cells Transl. Med.** 1(2): 110-115.

Ahmad, S., Stewart, R., Yung, S., Kolli, S., Armstrong, L., Stojkovic, M., Figueiredo, F., and Lako, M. (2007). Differentiation of human embryonic stem cells into corneal epithelial-like cells by *in vitro* replication of the corneal epithelial stem cell niche. **Stem Cells** 25(5): 1145-1155.

Aravena, C., Bozkurt, K., Chuephanich, P., Supiyaphun, C., Yu, F., and Deng, S. X. (2019). Classification of limbal stem cell deficiency using clinical and confocal grading. **Cornea** 38(1): 1-7.

Arkell, R. M., and Tam, P. P. L. (2012). Initiating head development in mouse embryos: Integrating signalling and transcriptional activity. **Open Biol.** 2(3): 120030.

Barbaro, V., Testa, A., Di Iorio, E., Mavilio, F., Pellegrini, G., and De Luca, M. (2007). C/EBPdelta regulates cell cycle and self-renewal of human limbal stem cells. **J. Cell Biol.** 177(6): 1037-1049.

Bardag-Gorce, F., Hoft, R. H., Wood, A., Oliva, J., Niihara, H., Makalinao, A., Thropay, J., Pan, D., Meepe, I., Tiger, K., Garcia, J., Laporte, A., French, S. W., and Niihara, Y. (2016). The role of E-cadherin in maintaining the barrier function of corneal epithelium after treatment with cultured autologous oral mucosa epithelial cell sheet grafts for limbal stem deficiency. **J. Ophthalmol.** 4805986-4805986.

Baylis, O., Figueiredo, F., Henein, C., Lako, M., and Ahmad, S. (2011). 13 years of cultured limbal epithelial cell therapy: A review of the outcomes. **J. Cell Biochem.** 112(4): 993: 1002.

Bojic, S., Hallam, D., Alcada, N., Ghareeb, A., Queen, R., Pervinder, S., Buck, H., Amitai Lange, A., Figueiredo, G., Rooney, P., Stojkovic, M., Shortt, A., Figueiredo, F. C., and Lako, M. (2018). CD200 expression marks a population of quiescent limbal epithelial stem cells with holoclone forming ability. **Stem Cells** 36(11): 1723-1735.

Bourne, G. L. (1960). The microscopic anatomy of the human amnion and chorion. **Am. J. Obstet. Gynecol.** 79(6): 1070-1073.

Brzeszczynska, J., Samuel, K., Greenhough, S., Ramaesh, K., Dhillon, B., Hay, D. C., and Ross, J. A. (2014). Differentiation and molecular profiling of human embryonic stem cell-derived corneal epithelial cells. **Int. J. Mol. Med.** 33(6): 1597-1606.

Byfield, S. D., Major, C., Laping, N. J., and Roberts, A. B. (2004). SB-505124 is a selective inhibitor of transforming growth factor-beta type I receptors ALK4, ALK5, and ALK7. **Mol. Pharmacol.** 65(3), 744-752.

Chen, Z., de Paiva, C. S., Luo, L., Kretzer, F. L., Pflugfelder, S. C., and Li, D.-Q. (2004). Characterization of putative stem cell phenotype in human limbal epithelia. **Stem Cells** 22(3): 355-366.

Cieślar-Pobuda, A., Rafat, M., Knoflach, V., Skonieczna, M., Hudecki, A., Małecki, A., Urasińska, E., Ghavami, S., and Łos, M. J. (2016). Human induced pluripotent stem cell differentiation and direct transdifferentiation into corneal epithelial-like cells. **Oncotarget** 7(27): 42314.

Deng, S. X., Sejpal, K. D., Tang, Q., Aldave, A. J., Lee, O. L., and Yu, F. (2012). Characterization of limbal stem cell deficiency by *in vivo* laser scanning confocal microscopy: A microstructural approach. **Arch. Ophthalmol.** 130(4): 440-445.

Dominici, M., Le Blanc, K., Mueller, I., Slaper-Cortenbach, I., Marini, F., Krause, D., Deans, R., Keating, A., Prockop, D., and Horwitz, E. (2006). Minimal criteria for defining multipotent mesenchymal stromal cells. The International Society for Cellular Therapy position statement. **Cytotherapy** 8(4): 315-317.

Dua, H. S., Saini, J. S., Azuara-Blanco, A., and Gupta, P. (2000). Limbal stem cell deficiency: Concept, aetiology, clinical presentation, diagnosis and management. **Indian J. Ophthalmol.** 48(2): 83-92.

Foster, J. W., Wahlin, K., Adams, S. M., Birk, D. E., Zack, D. J., and Chakravarti, S. (2017). Cornea organoids from human induced pluripotent stem cells. **Sci. Rep.** 7(1): 41286.

Friedenstein, A. J., Chailakhyan, R. K., Latsinik, N. V., Panasyuk, A. F., and Keiliss-Borok, I. V. (1974). Stromal cells responsible for transferring the microenvironment of the hemopoietic tissues: Cloning *in vitro* and retransplantation *in vivo*. **Transplantation** 17(4): 331-340.

Galindo, S., Herreras, J. M., López-Paniagua, M., Rey, E., de la Mata, A., Plata-Cordero, M., Calonge, M., Nieto-Miguel, T. (2017). Therapeutic effect of human adipose tissue-derived mesenchymal stem cells in experimental corneal failure due to limbal stem cell niche damage. **Stem Cells** 35(10): 2160-2174.

Gomes, J. A., Geraldes Monteiro, B., Melo, G. B., Smith, R. L., Cavenaghi Pereira da Silva, M., Lizier, N. F., Kerkis, A., Cerruti, H., and Kerkis, I. (2010). Corneal reconstruction with tissue-engineered cell sheets composed of human immature dental pulp stem cells. **Invest. Ophthalmol. Vis. Sci.** 51(3): 1408-1414.

Gouveia, R. M., Lepert, G., Gupta, S., Mohan, R. R., Paterson, C., and Connon, C. J. (2019). Assessment of corneal substrate biomechanics and its effect on epithelial stem cell maintenance and differentiation. **Nat. Commun.** 10(1): 1496.

Gu, S., Xing, C., Han, J., Tso, M. O. M., and Hong, J. (2009). Differentiation of rabbit bone marrow mesenchymal stem cells into corneal epithelial cells *in vivo* and *ex vivo*. **Mol. Vis.** 15: 99-107.

Guan, L., Ge, H., Tang, X., Su, S., Tian, P., Xiao, N., Zhang, H., Zhang, L., and Liu, P. (2013). Use of a silk fibroin-chitosan scaffold to construct a tissue-engineered corneal stroma. **Cells Tissues Organs** 198(3): 190-197.

Guan, L., Tian, P., Ge, H., Tang, X., Zhang, H., Du, L., and Liu, P. (2013). Chitosan-functionalized silk fibroin 3D scaffold for keratocyte culture. **J. Mol. Histol.** 44(5): 609-618.

Guo, T., Wang, W., Zhang, J., Chen, X., Li, B. Z., and Li, L. S. (2006). Experimental study on repairing damage of corneal surface by mesenchymal stem cells transplantation. **Zhonghua Yan Ke Za Zhi** 42(3): 246-250.

Haagdorens, M., Van Acker, S. I., Van Gerwen, V., Ni Dhubhghaill, S., Koppen, C., Tassignon, M. J., and Zakaria, N. (2016). Limbal stem cell deficiency: Current treatment options and emerging therapies. **Stem Cells Int.** 2016: 9798374.

Hazra, S., Nandi, S., Naskar, D., Guha, R., Chowdhury, S., Pradhan, N., Kundu, S. C., and Konar, A. (2016). Non-mulberry silk fibroin biomaterial for corneal regeneration. **Sci. Rep.** 6(1): 21840.

He, J., Ou, S., Ren, J., Sun, H., He, X., Zhao, Z., Wu, H., Qu, Y., Liu, T., Jeyalatha, V., Zhang, L., Li, Q., Reinach, P. S., Quantock, A., Hao, J., Liu, Z., and Li, W. (2020). Tissue engineered corneal epithelium derived from clinical-grade human embryonic stem cells. **Ocul. Surf.** 18(4): 672-680.

Heldin, C. H., Miyazono, K., and ten Dijke, P. (1997). TGF-beta signalling from cell membrane to nucleus through SMAD proteins. **Nature** 390(6659): 465-471.

Hmadcha, A., Martin-Montalvo, A., Gauthier, B. R., Soria, B., and Capilla-Gonzalez, V. (2020). Therapeutic potential of mesenchymal stem cells for cancer therapy. **Front. bioeng. biotechnol.** 8: 43.

Homma, R., Yoshikawa, H., Takeno, M., Kurokawa, M. S., Masuda, C., Takada, E., Tsubota, K., Ueno, S., and Suzuki, N. (2004). Induction of epithelial progenitors *in vitro* from mouse embryonic stem cells and application for reconstruction of damaged cornea in mice. **Invest. Ophthalmol. Vis. Sci.** 45(12): 4320-4326.

Hong, S., Sunwoo, J. H., Kim, J. S., Tchah, H., and Hwang, C. (2018). Conjugation of carboxymethyl cellulose and dopamine for cell sheet harvesting. **Biomater. Sci.** 7(1): 139-148.

Hopkinson, A., Shanmuganathan, V. A., Gray, T., Yeung, A. M., Lowe, J., James, D. K., and Dua, H. S. (2008). Optimization of amniotic membrane (AM) denuding for tissue engineering. **Tissue Eng. Part C Methods** 14(4): 371-381.

Kamarudin, T. A., Bojic, S., Collin, J., Yu, M., Alharthi, S., Buck, H., Shortt, A., Armstrong, L., Figueiredo, F. C., and Lako, M. (2018). Differences in the activity of endogenous bone morphogenetic protein signaling impact on the ability of induced pluripotent stem cells to differentiate to corneal epithelial-like cells. **Stem Cells** 36(3): 337-348.

Katikireddy, K. R., Dana, R., and Jurkunas, U. V. (2014). Differentiation potential of limbal fibroblasts and bone marrow mesenchymal stem cells to corneal epithelial cells. **Stem Cells** 32(3): 717-729.

Kim, H.-S., Jun Song, X., de Paiva, C. S., Chen, Z., Pflugfelder, S. C., and Li, D.-Q. (2004). Phenotypic characterization of human corneal epithelial cells expanded *ex vivo* from limbal explant and single cell cultures. **Exp. Eye Res.** 79(1): 41-49.

Kim, H. J., and Park, J.-S. (2017). Usage of human mesenchymal stem cells in cell-based therapy: advantages and disadvantages. **Dev. Reprod.** 21(1): 1-10.

Kitazawa, K., Hikichi, T., Nakamura, T., Sotozono, C., Kinoshita, S., and Masui, S. (2017). PAX6 regulates human corneal epithelium cell identity. **Exp. Eye Res.** 154: 30-38.

Ksander, B. R., Kolovou, P. E., Wilson, B. J., Saab, K. R., Guo, Q., Ma, J., McGuire, S. P., Gregory, M. S., Vincent, W. J. B., Perez, V. L., Cruz-Guilloty, F., Kao, W. W. Y., Call, M. K., Tucker, B. A., Zhan, Q., Murphy, G. F., Lathrop, K. L., Alt, C., Mortensen, L. J., Lin, C. P., Zieske, J. D., Frank, M. H., and Frank, N. Y. (2014). ABCB5 is a limbal stem cell gene required for corneal development and repair. **Nature** 511(7509): 353-357.

Kumagai, Y., Kurokawa, M. S., Ueno, H., Kayama, M., Tsubota, K., Nakatsuji, N., Kondo, Y., Ueno, S., and Suzuki, N. (2010). Induction of corneal epithelium–like cells from cynomolgus monkey embryonic stem cells and their experimental transplantation to damaged cornea. **Cornea** 29(4): 432-438.

Le, Q., Xu, J., and Deng, S. X. (2018). The diagnosis of limbal stem cell deficiency. **Ocul. Surf.** 16(1): 58-69.

Lee, H. J., Wolosin, J. M., and Chung, S.-H. (2017). Divergent effects of Wnt/β-catenin signaling modifiers on the preservation of human limbal epithelial progenitors according to culture condition. **Sci. Rep.** 7(1): 15241.

Li, H., Xu, Y., Fu, Q., and Li, C. (2012). Effects of multiple agents on epithelial differentiation of rabbit adipose-derived stem cells in 3D culture. **Tissue Eng. Part A** 18(17-18): 1760-1770.

Lian, X., Selekman, J., Bao, X., Hsiao, C., Zhu, K., and Palecek, S. P. (2013). A small molecule inhibitor of Src family kinases promotes simple epithelial differentiation of human pluripotent stem cells. **PLoS One** 8(3): e60016.

Lin, J., Yoon, K. C., Zhang, L., Su, Z., Lu, R., Ma, P., De Paiva, C., Pflugfelder, S., and Liu, W. (2012). A native-like corneal construct using donor corneal stroma for tissue engineering. **PLoS One** 7: e49571.

Lin, K.-J., Loi, M.-X., Lien, G.-S., Cheng, C.-F., Pao, H.-Y., Chang, Y.-C., Ji, A. T.-Q., and Ho, J. H.-C. (2013). Topical administration of orbital fat-derived stem cells promotes corneal tissue regeneration. **Stem Cell Res. Ther.** 4(3): 72.

Liu, C.-Y., and Kao, W. W.-Y. (2015). Chapter five - Corneal epithelial wound healing. In J. F. Hejtmancik and J. M. Nickerson (Eds.), **Progress in Molecular Biology and Translational Science** 134: 61-71.

Lobo, E. P., Delic, N. C., Richardson, A., Raviraj, V., Halliday, G. M., Di Girolamo, N., Myerscough, M. R., Lyons, J. G. (2016). Self-organized centripetal movement of corneal epithelium in the absence of external cues. **Nat. Commun.** 7(1): 12388.

Ma, Y., Xu, Y., Xiao, Z., Yang, W., Zhang, C., Song, E., Du, Y., and Li, L. (2006). Reconstruction of chemically burned rat corneal surface by bone marrow–derived human mesenchymal stem cells. **Stem Cells** 24(2): 315-321.

Mayeur, C., Lohmeyer, L. K., Leyton, P., Kao, S. M., Pappas, A. E., Kolodziej, S. A., Spagnolli, E., Yu, B., Galdos, R. L., Yu, P. B., Peterson, R. T., Bloch, D. B., Bloch, K. D., andSteinbicker, A. U. (2014). The type I BMP receptor Alk3 is required

for the induction of hepatic hepcidin gene expression by interleukin-6. **Blood** 123(14): 2261-2268.

Mei, H., Nakatsu, M. N., Baclagon, E. R., and Deng, S. X. (2014). Frizzled 7 maintains the undifferentiated state of human limbal stem/progenitor cells. **Stem Cells** 32(4): 938-945.

Mikhailova, A., Ilmarinen, T., Uusitalo, H., and Skottman, H. (2014). Small-molecule induction promotes corneal epithelial cell differentiation from human induced pluripotent stem cells. **Stem Cell Rep.** 2(2): 219-231.

Monteiro, B. G., Serafim, R. C., Melo, G. B., Silva, M. C. P., Lizier, N. F., Maranduba, C. M. C., Smith, R. L., Kerkis, A., Cerruti, H., Gomes, J. A. P., and Kerkis, I. (2009). Human immature dental pulp stem cells share key characteristic features with limbal stem cells. **Cell Prolif.** 42(5): 587-594.

Mort, R. L., Douvaras, P., Morley, S. D., Dorà, N., Hill, R. E., Collinson, J. M., and West, J. D. (2012). Stem cells and corneal epithelial maintenance: insights from the mouse and other animal models. Results. **Probl. Cell. Differ.** 55: 357-394.

Nakamura, T., Endo, K., Cooper, L. J., Fullwood, N. J., Tanifuji, N., Tsuzuki, M., Koizumi, N., Inatomi, T., Sano, Y., and Kinoshita, S. (2003). The successful culture and autologous transplantation of rabbit oral mucosal epithelial cells on amniotic membrane. **Invest. Ophthalmol. Vis. Sci.** 44(1): 106-116.

Nieto-Miguel, T., Galindo, S., Reinoso, R., Corell, A., Martino, M., Pérez-Simón, J. A., and Calonge, M. (2013). *In vitro* simulation of corneal epithelium microenvironment induces a corneal epithelial-like cell phenotype from human adipose tissue mesenchymal stem cells. **Curr. Eye Res.** 38(9): 933-944.

Nishida, K., Yamato, M., Hayashida, Y., Watanabe, K., Maeda, N., Watanabe, H., Yamamoto, K., Nagai, S., Kikuchi, A., Tano, Y., and Okano, T. (2004). Functional bioengineered corneal epithelial sheet grafts from corneal stem cells expanded *ex vivo* on a temperature-responsive cell culture surface. **Transplantation** 77(3): 379-385.

Notara, M., Hernandez, D., Mason, C., and Daniels, J. T. (2012). Characterization of the phenotype and functionality of corneal epithelial cells derived from mouse embryonic stem cells. **Regen. Med.** 7(2): 167-178.

Notara, M., Lentzsch, A., Coroneo, M., and Cursiefen, C. (2018). The role of limbal epithelial stem cells in regulating corneal (lymph)angiogenic privilege and the micromilieu of the limbal niche following UV exposure. **Stem Cells Int.** 2018: 8620172-8620172.

Patel, N. G., and Zhang, G. (2013). Responsive systems for cell sheet detachment. **Organogenesis** 9(2): 93-100.

Ramuta, T. Ž., and Kreft, M. E. (2018). Human amniotic membrane and amniotic membrane-derived cells: How far are we from their use in regenerative and reconstructive urology? **Cell Transplant.** 27(1): 77-92.

Rohaina, C. M., Then, K. Y., Ng, A. M. H., Halim, W. H. W. A., Zahidin, A. Z. M., Saim, A., and Idrus, R. B. (2014). Reconstruction of limbal stem cell deficient corneal surface with induced human bone marrow mesenchymal stem cells on amniotic membrane. **Transl. Res.** 163(3): 200-210.

Sacchetti, M., Lambiase, A., Cortes, M., Sgrulletta, R., Bonini, S., Merlo, D., and Bonini, S. (2005). Clinical and cytological findings in limbal stem cell deficiency. **Graefes. Arch. Clin. Exp. Ophthalmol.** 243(9): 870-876.

Saghizadeh, M., Winkler, M. A., Kramerov, A. A., Hemmati, D. M., Ghiam, C. A., Dimitrijevich, S. D., Sareen, D., Ornelas, L., Ghiasi, H., Brunken, W. J., Maguen, E., Rabinowitz, Y. S., Svendsen, C. N., Jirsova, K., and Ljubimov, A. V. (2013). A simple alkaline method for decellularizing human amniotic membrane for cell culture. **PLoS One** 8(11): e79632.

Saichanma, S., Bunyaratvej, A., and Sila-Asna, M. (2012). *In vitro* transdifferentiation of corneal epithelial-like cells from human skin-derived precursor cells. **Int. J. Ophthalmol.** 5(2): 158-163.

Satake, Y., Higa, K., Tsubota, K., and Shimazaki, J. (2011). Long-term outcome of cultivated oral mucosal epithelial sheet transplantation in treatment of total limbal stem cell deficiency. **Ophthalmology** 118(8): 1524-1530.

Schwab, I. R., Reyes, M., and Isseroff, R. R. (2000). Successful transplantation of bioengineered tissue replacements in patients with ocular surface disease. **Cornea** 19(4): 421-426.

Sharma, A., and Coles, W. H. (1989). Kinetics of corneal epithelial maintenance and graft loss. A population balance model. **Invest. Ophthalmol. Vis. Sci.** 30(9): 1962-1971.

Shortt, A. J., Bunce, C., Levis, H. J., Blows, P., Doré, C. J., Vernon, A., Secker, G. A., Tuft, S. J., and Daniels, J. T. (2014). Three-year outcomes of cultured limbal epithelial allografts in aniridia and stevens-johnson syndrome evaluated using the clinical outcome assessment in surgical trials assessment tool. **Stem Cells Transl. Med.** 3(2): 265-275.

Shortt, A. J., Secker, G. A., Lomas, R. J., Wilshaw, S. P., Kearney, J. N., Tuft, S. J., and Daniels, J. T. (2009). The effect of amniotic membrane preparation method on its ability to serve as a substrate for the *ex-vivo* expansion of limbal epithelial cells. **Biomaterials** 30(6): 1056-1065.

Sonna, L. A., Fujita, J., Gaffin, S. L., and Lilly, C. M. (2002). Invited review: Effects of heat and cold stress on mammalian gene expression. **J. Appl. Physiol. (1985)** 92(4): 1725-1742.

Sosnová-Netuková, M., Kuchynka, P., and Forrester, J. V. (2007). The suprabasal layer of corneal epithelial cells represents the major barrier site to the passive movement of small molecules and trafficking leukocytes. **Br. J. Ophthalmol.** 91(3): 372-378.

Sotozono, C., Inatomi, T., Nakamura, T., Koizumi, N., Yokoi, N., Ueta, M., Matsuyama, K., Miyakoda, K., Kaneda, H., Fukushima, M., and Kinoshita, S. (2013). Visual improvement after cultivated oral mucosal epithelial transplantation. **Ophthalmology** 120(1): 193-200.

Sugrue, S. P., and Zieske, J. D. (1997). ZO1 in corneal epithelium: Association to the zonula occludens and adherens junctions. **Exp. Eye Res.** 64(1): 11-20.

Susaimanickam, P. J., Maddileti, S., Pulimamidi, V. K., Boyinpally, S. R., Naik, R. R., Naik, M. N., Reddy, G. B., Sangwan, V. S., and Mariappan, I. (2017). Generating minicorneal organoids from human induced pluripotent stem cells. **Development** 144(13): 2338-2351.

Takahashi, K., Tanabe, K., Ohnuki, M., Narita, M., Ichisaka, T., Tomoda, K., and Yamanaka, S. (2007). Induction of pluripotent stem cells from adult human fibroblasts by defined factors. **Cell** 131(5): 861-872.

Tananuvat, N., Bumroongkit, K., Tocharusa, C., Mevatee, U., Kongkaew, A., and Ausayakhun, S. (2017). Limbal stem cell and oral mucosal epithelial transplantation from *ex vivo* cultivation in LSCD-induced rabbits: histology and immunologic study of the transplant epithelial sheet. **Int. Ophthalmol.** 37(6): 1289-1298.

Theerakittayakorn, K., Thi Nguyen, H., Musika, J., Kunkanjanawan, H., Imsoonthornruksa, S., Somrednga n, S., Ketudat-Cairns, M., and Parnpai, R. (2020). Differentiation induction of human stem cells for corneal epithelial regeneration. **Int. J. Mol. Sci.** 21(21): 7834.

Thomson, J. A., Itskovitz-Eldor, J., Shapiro, S. S., Waknitz, M. A., Swiergiel, J. J., Marshall, V. S., and Jones, J. M. (1998). Embryonic stem cell lines derived from human blastocysts. **Science** *282*(5391): 1145-1147.

Ueno, H., Kurokawa, M. S., Kayama, M., Homma, R., Kumagai, Y., Masuda, C., Takada, E., Tsubota, K., Ueno, S., and Suzuki, N. (2007). Experimental transplantation of corneal epithelium-like cells induced by pax6 gene transfection of mouse embryonic stem cells. **Cornea** 26(10): 1220-1227.

Vázquez, N., Rodríguez-Barrientos, C. A., Aznar-Cervantes, S. D., Chacón, M., Cenis, J. L., Riestra, A. C., Sánchez-Avila, R. M., Persinal, M., Brea-Pastor, A., Fernández-Vega Cueto, L., Meana, Á., and Merayo-Lloves, J. (2017). Silk fibroin films for

corneal endothelial regeneration: transplant in a rabbit descemet membrane endothelial keratoplasty. **Investig. Ophthalmol. Vis. Sci.** 58(9): 3357-3365.

Wang, Y., Chen, M., and Wolosin, J. M. (1993). ZO-1 in corneal epithelium; stratal distribution and synthesis induction by outer cell removal. **Exp. Eye Res.** 57(3): 283-292.

Wijnholds, J. (2019). "Basal cell migration" in regeneration of the corneal wound-bed. **Stem Cell Rep.** 12(1): 3-5.

Wolosin, J. M., Budak, M. T., and Akinci, M. A. M. (2004). Ocular surface epithelial and stem cell development. **Int. J. Dev. Biol.** 48(8-9): 981-91

Yoon, J. J., Ismail, S., and Sherwin, T. (2014). Limbal stem cells: Central concepts of corneal epithelial homeostasis. **World J. Stem Cells** 6(4), 391-403.

Zeppieri, M., Salvetat, M. L., Beltrami, A. P., Cesselli, D., Bergamin, N., Russo, R., Cavaliere, F., Varano, G. P., Alcalde, I., Merayo, J., Brusini, P., Beltrami, C. A., and Parodi, P. C. (2013). Human adipose-derived stem cells for the treatment of chemically burned rat cornea: preliminary results. **Curr. Eye Res.** 38(4): 451-463.

Zhang, T., Yam, G. H., Riau, A. K., Poh, R., Allen, J. C., Peh, G. S., Beuerman, R. W., Tan, D. T., and Mehta, J. S. (2013). The effect of amniotic membrane de-epithelialization method on its biological properties and ability to promote limbal epithelial cell culture. **Invest. Ophthalmol. Vis. Sci.** 54(4): 3072-3081.

Zhang, Y., Yeh, L.-K., Zhang, S., Call, M., Yuan, Y., Yasunaga, M., Kao, W. W. Y., and Liu, C.-Y. (2015). Wnt/β-catenin signaling modulates corneal epithelium stratification via inhibition of Bmp4 during mouse development. **Development** 142(19): 3383-3393.

# CHAPTER 3
# SIGNALING PATHWAYS IMPACT ON INDUCTION OF CORNEAL EPITHELIAL-LIKE CELLS DERIVED FROM HUMAN WJ-MSCs

## 3.1 Abstract

Corneal epithelium, the outmost layer of the cornea, comprises CECs that are continuously renewed by LESCs. Loss or dysfunction of LESCs causes LSCD which results in corneal epithelial integrity loss and visual impairment. To regenerate the ocular surface, transplantation of stem cells-derived CECs is necessary. Human WJ-MSCs are a good candidate for cellular therapies in allogenic transplantation. This study aimed to test the effects of treatments on three signaling pathways involved in CEC differentiation as well as examined the optimal protocol for inducing corneal epithelial differentiation of human WJ-MSCs. RA (5 or 10 μM) inhibited Wnt signaling pathway via suppressing the translocation of β-catenin from the cytoplasm into the nucleus. SB505124 downregulated TGF-β signaling pathway via reducing phosphorylation of Smad2. BMP4 did not increase phosphorylation of Smad1/5/8 that involved in BMP signaling. The combination of RA, SB505124, BMP4, and EGF for the first 3 days of differentiation followed by supplementing hormonal epidermal medium for additional 6 days could generate corneal epithelial-like cells that expressed CEC specific marker CK12. This study reveals that WJ-MSCs has the potential to transdifferentiate into CECs which would be beneficial for further applications in LSCD treatment therapy.

## 3.2 Introduction

Cornea, the anterior transparent part of the eye, permits light transmission to photoreceptor cells in the retina and protects the eye from the external environment. The cornea consists of three cell layers: corneal epithelium, stroma, and endothelium. The corneal epithelium, the outmost layer of the cornea, CECs that are continuously

renewed by LESCs. LESCs are located at the basal layer of the limbus (Notara et al., 2018) which is the border between the cornea and the sclera. LESCs can divide asymmetrically to produce both LESC daughters and TACs. While LESCs remain in limbus, TACs migrate into the central cornea and move upward to the superficial layer of cornea to differentiate into CECs (Liu and Kao, 2015; Yoon et al., 2014). Loss or dysfunction of LESCs due to several types of damages (chemical or thermal burns), microbial infections, diseases such as Stevens-Johnson syndrome can result in LSCD (Nakamura et al., 2003; Notara et al., 2010; Puangsricharern and Tseng, 1995). LSCD leads to loss of corneal epithelial integrity and function, resulting in vision loss or corneal blindness (Dua et al., 2000; Ahmad, 2012).

Common therapeutic treatments of LSCD include cultivated limbal epithelial transplantation (CLET) and cultivated oral mucosal epithelial transplantation (COMET). However, autologous CLET is impossible in the case of bilateral LSCD, and allogenic CLET requires the long-term use of systemic immunosuppression (Baylis et al., 2011). COMET gives promising results for the stabilization of the ocular surface (Mikhailova et al., 2014), but the transplanted oral cells did not fully transdifferentiate into CECs (not express CK12, a specific marker of CECs) (Utheim et al., 2016). Both techniques give variation in success rate, use animal feeder cells in culture protocols that has risks of contamination or disease transmission from other species, and cause peripheral corneal neovascularization (Chen et al., 2004; Satake et al., 2011; Sotozono et al., 2013).

To solve these problems, researchers are trying to find new cell sources that are better candidates for transplantation to treat LSCD, such as ESCs, iPSCs, MSCs from WJ or dental pulp, etc. ESCs are PSCs but research on human ESCs is ethically and politically controversial because of its involvement in the destruction of human embryos (Lo and Parham, 2009). Human iPSCs have the same differentiation capacity as human ESCs and even avoid post-transplantation rejection by using the patient's own somatic cells. However, the factors associated with iPSCs generation have been linked to oncogenic transformation, a form of *in vitro* produced tumor cells (Riggs et al., 2013). MSCs have lower differentiation potential but they are safer than iPSCs.

Especially, WJ-MSCs are good candidates for cellular therapies in allogenic transplantation due to their capacity for immune suppression and immune avoidance (Marino et al., 2019). However, the optimal protocols for generating corneal epithelial cells (CECs) from WJ-MSCs *in vitro* have not been reported yet.

Both CM and defined induction medium were used to differentiate PSCs into CECs ((Theerakittayakorn et al., 2020). In methods using defined induction medium, several combinations of treatment factors that functioned in inhibiting Wnt signaling pathway (retinoic acid, IWP2, IWR1), upregulating TGF-β signaling pathway (SB505124, A83-01) with/without increasing BMP signaling pathway (BMP4) had succeeded generating CECs from iPSCs and ESCs (Yang et al., 2018; Kamarudin et al., 2018; Mikhailova et al., 2014). However, there are few studies evaluating the effects of treatment factors on these signaling pathways, especially with WJ-MSCs. Therefore, this study aimed to determine effects of treatment factors (all-trans retinoic acid (RA), SB505124, and BMP4) on Wnt, BMP and TGF-β signaling pathways and investigate the optimal protocol for generating CECs from human WJ-MSCs.

## 3.3 Materials and Methods

### 3.3.1 Ethics Statement

The study was conducted in accordance with the Declaration of Helsinki and approved by Maharat Nakhon Ratchasima Hospital Institution Review Board (MNRH IRB), Approval Number: 066/2019.

### 3.3.2 Reagents

All chemical compounds and cell culture reagents were purchased from Sigma-Aldrich Corporation (St. Louis, Missouri, USA) and Thermo Fisher Scientific (Waltham, MA, USA), respectively. The cell culture ware was obtained from SPL Life Science (Gyeonggi-do, South Korea), unless stated otherwise.

### 3.3.3 Isolation and expansion of human WJ-MSCs

The human umbilical cord was collected from Maharat Nakhon Ratchasima

Hospital (Nakhon Ratchasima, Thailand) after the mother's informed consent was obtained. Human WJ-MSCs were isolated from the umbilical cord and cultured as previously described (Petsa et al., 2009; Tanthaisong et al., 2017). Briefly, the umbilical cord was put into 75% ethanol for 30 sec, 10% betadine, and washed in sterilized PBS. Then the umbilical cord was cut lengthwise, the arteries and vein were removed. The gelatinous WJ tissue was excised and cut into small fragments (3 x 3 mm). WJ fragments were plated into 60 mm dishes and covered with 4 ml of αMEM supplemented with 10% fetal bovine serum (FBS), 100 U/ml penicillin, 100 µg/ml streptomycin. WJ fragments were incubated at 37°C in a humidified atmosphere of 5% $CO_2$ for 10-13 days. The culture medium was replaced every 3 days. When the visible colonies were observed, cells were sub-cultured into T75 flasks at the density of $10^4$ cells/$cm^2$. The cells were expanded until passage 3 (P3), then the cells were either directly used for experiments (sub-culture to P4) or cryopreserved in culture media supplemented with 10% dimethyl sulfoxide (DMSO, Calbiochem, San Diego, CA, USA) and stored in liquid nitrogen.

3.3.4 Flow cytometry

Human WJ-MSCs were harvested and washed with PBS. Afterwards, approximately $2x10^5$ cells were suspended in a final volume of 100 µL PBS and incubated with primary antibodies (CD73-APC, CD90-APC/Cy7, CD105/PE, CD34-PE, and CD45/FITC) for 20 min at room temperature, in the dark. As negative controls, isotype control antibodies were used. The cells were washed and resuspended in a final volume of 500 µl PBS. At least $10^4$ cells were determined with flow cytometer (Attune™ NxT , Thermo Fisher Scientific). Finally, the data obtained were analyzed using FlowJo™ v10.8 Software (BD Life Sciences). The details of primary antibodies are shown in Table 3.1.

3.3.5 Trilineage differentiation capacity

Trilineage differentiation capacity of human WJ-MSCs was evaluated as previously described (Tanthaisong et al., 2017). Briefly, cells were cultured in 35 mm at the density of $2x10^3$ cells/$cm^2$ for 2-3 days. Cells treated with adipogenic medium were stained with Oil Red O after 21 days. And chondrogenic media treated cells were stained

with Alcian Blue on day 21. Besides, cells treated with osteogenic medium for 21 days were stained with Alizarin Red. Adipogenic medium comprised αMEM supplemented with 5% FBS, 10 µg/ml insulin, 10 µM indomethacin, 1 µM dexamethasone (DEX), 0.5 mM isobutylmethylxanthine (IBMX). Chondrogenic medium contained of αMEM supplemented with 2% FBS, 1% Insulin-Transferrin-Selenium-Ethanolamine (ITS-X), 50 µg/ml ascorbate-2-phosphate (A2P), 40 µl L-proline, 100 µg/ml sodium pyruvate, 100 nM DEX and 10 ng/ml of TGF-β3 (Prospec, East Brunswick, NJ, USA). Osteogenic medium consisted of αMEM supplemented with 5% FBS, 100 nM DEX, 0.2 mM A2P and 10 mM β-glycerophosphate. Medium was changed every three days.

3.3.6 Population doubling time (PDT)

Cells at passage 3-10 were plated in triplicate onto the 12-well plate at a density of 5000 cells/$cm^2$ and cultured in αMEM supplemented with 10% FBS. After 3 days, the numbers of viable cells were counted using Trypan blue staining. PDT was calculated using the following formula: PDT = (CT x ln2)/ln(Nf/Ni), where CT is the cell culture time (hours), Ni and Nf are the initial and the final numbers of cells, respectively (Redaelli et al., 2012).

3.3.7 Cytotoxicity test

Cells were seeded at a density of 3000 cells/well in 96-well culture plates in the culture medium for 24 h. Then the cells were treated with culture medium supplemented with several concentrations of SB505124 (0, 5, 10, and 20 µM) or DMSO (0, 0.1, 0.25, 0.5, 1%) or RA (0, 2.5, 5, 10 and 20 µM) at 37°C for 72 h in a humidified atmosphere of 5% $CO_2$ in air. After treatment, cell viability was quantified by MTT assay as previously described (Tanthaisong et al., 2017). Briefly, cells were incubated with culture medium supplemented with 0.5 mg/ml 3-(4,5-Dimethylthiazol-2-yl)-2,5-Diphenyltetrazolium Bromide (MTT, Invitrogen) for 3 h at 37°C. Then 0.01 M DMSO was added, and the cells were incubated for 10 min at 37°C. The absorbance at 540 nm was measured by microplate spectrophotometer (Thermo Scientific™ Multiskan™ GO, Thermo Fisher Scientific, Waltham, MA, USA). Each treatment condition was performed in 4 replicates.

3.3.8 Effect of RA on localization and expression of β-catenin

Cells were seeded at a density of $10^3$ cells/$cm^2$ and incubated for 48 h. They were then treated with basic medium (BM: DMEM low glucose supplemented with 2% FBS, 1% NEAA, 100 U/ml penicillin, 100 µg/ml streptomycin) supplemented with RA (0, 2.5, 5, 10 µM) for 3 additional days at 37°C and 5% $CO_2$. The expression of β-catenin was analyzed by immunofluorescent staining, Western Blot, and qPCR.

3.3.9 Effect of SB505124 on inhibition of p-Smad2/3

Cells were seeded at a density of $10^3$ cells/$cm^2$ and cultured in the cultured medium for 3 days. Then cells were cultured in DMEM/F12 medium without FBS for 24 h. Afterwards, cells were treated with SB505124 (0, 5, 10, and 20 µM) in DMEM/F12 for 1 h. The expressions of total Smad2/3, pSmad2/3, β-actin were evaluated by Western Blot.

3.3.10 Effect of BMP4 for increasing p-Smad1/5/8

Cells were seeded at a density of $10^3$ cells/$cm^2$ and cultured in the culture medium for 3 days. Then they were cultured in DMEM/F12 medium without FBS for 24 h. Afterwards, they were treated with BMP4 (0, 25, and 50 ng/ml) in BM for 1 or 2 h. The expression of total Smad1/5/8/9, pSmad1/5/8, and β-actin were evaluated by Western Blot.

3.3.11 Isolation and characterization of human CECs

Human cadaveric limbal tissue consisting of peripheral cornea and limbus was obtained from Eye Bank of Thailand (The Thai Red Cross Society, Bangkok, Thailand) and stored in Optisol GS (Bausch & Lomb, Rochester, NY, USA) at 4°C. The endothelial layer and iris remnants were removed, and the cornea was then cut into small fragments (2x2 mm). These fragments were used for mRNA isolation or cultured in supplemented hormonal epidermal medium (SHEM) containing mixture of DMEM low glucose and DMEM/F12 medium (1:1 v/v) supplemented with 5% FBS, 10 ng/ml EGF, 1% of insulin-transferrin-sodium selenite (ITS-H, Capricorn Scientific GmbH, Ebsdorfergrund, Germany), 0.5 µg/ml hydrocortisone, 0.05% DMSO, 200 nM adenine, 100 U/ml penicillin, 100 µg/ml streptomycin in 37°C and 5% $CO_2$. After cell

proliferation, the fragments were removed, and the cells were cultured for an additional week. The culture medium was changed every 3 days. When the cells reached 70-80% confluence, cells were sub-cultured and seeded at density 3 x $10^4$ cells/$cm^2$. Cells were then characterized by immunofluorescent staining for CK12, E-cadherin (an intercellular junction protein), zonula occludens-1 (ZO-1, a tight junction protein), Involucrin.

3.3.12 Optimization of human WJ-MSC differentiation into CECs

Human WJ-MSCs were seeded at a density of $10^3$ cells/$cm^2$ and cultured in αMEM supplemented with 10% FBS for 2 days. Then these cells were treated with BM supplemented with or without combinations of treatment factors (G1: RA + SB505124 + BMP4 + bFGF + EGF; G2: RA + SB505124 + BMP4 + EGF; G3: RA + BMP4 +bFGF + EGF) for 3 days. Concentrations of these factors were 10 μM RA, 10 μM SB505124, 25 ng/ml BMP4, 50 ng/ml bFGF, 10 ng/ml EGF. Afterwards, these cells were cultured in SHEM medium for additional 6 or 9 days. These cells at day 0, 3, 9, 12 were evaluated by immunofluorescent staining, Western Blot, and qPCR. Schematic outline of CEC differentiation process is shown in Figure 3.1.

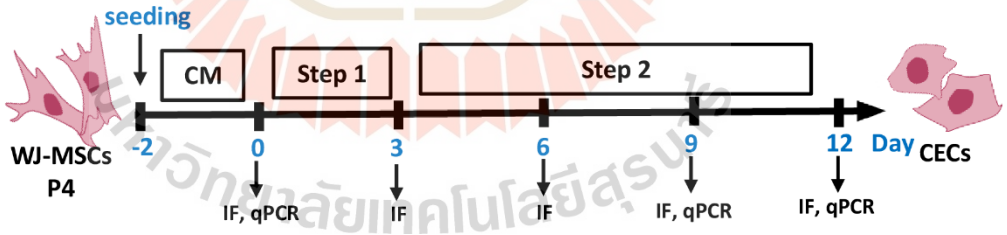


| Group | CM | Step 1 | Step 2 |
|---|---|---|---|
| BM | αMEM medium + 10% FBS | BM medium | SHEM medium |
| G1 | | BM + RA + SB505124 + BMP4 + bFGF + EGF | |
| G2 | | BM + RA + SB505124 + BMP4 + EGF | |
| G3 | | BM + RA + BMP4 +bFGF + EGF | |

**Figure 3.1** Schematic outline of CEC differentiation from human WJ-MSCs. IF: immunofluorescent.

3.3.13 Immunofluorescent staining

Expression of β-catenin, CK12, CK19, ABCG2 was qualitatively evaluated with immunofluorescent staining. Cells were fixed in cold absolute methanol for 20 min and washed three times with PBS. Cell membranes were permeabilized for 30 min in 0.2% Triton X-100. Nonspecific binding sites were blocked with 1% BSA in PBS for 1 h. Cells were then stained with primary antibodies diluted with 1% BSA/PBS for 1 h at room temperature (RT) or overnight in 4°C. Afterwards, cells were stained with secondary antibodies diluted in PBS for 1 h at RT. Nuclei were stained with 1 μg/ml 4, 6-diamino-2-phenylindole (DAPI, Millipore) for 5 min. Then the cells were mounted with Vectashield® antifade mounting medium (H-1000, Vector Laboratories, Burlingame, CA, USA). Cell images were captured with a fluorescent microscope equipped with a DS-Ri1 camera (Eclipse Ti-S, Nikon Instruments Inc., Tokyo, Japan). Intensity of β-catenin in nucleus and cytoplasm was measured using CellProfiler software (*www.cellprofiler.org*).

3.3.14 Western Blotting analysis

Cell samples were lysed in lysate buffer (10 mM Tris-HCl, 150 mM NaCl, 0.5% Triton X-100, 1 mM EDTA, pH 7.2) supplemented with protease inhibitor cocktail (cOmplete™) and phosphatase inhibitor cocktail (PhosSTOP™). The cell lysates were separated by centrifugation at 14,000 rpm for 20 min at 4°C, then the total protein concentration was determined by Bradford assay (Coomassie protein assay reagent). Equal amount of total protein (10-20 μg) from each sample was mixed with 5x Laemmli buffer prior to denature at 95°C for 5 min and separate on 7.5% or 10% Acrylamide/Bis gels. Afterwards, separated proteins were transferred onto PVDF membranes (Immu-Blot PVDF membrane, Bio-Rad, Hercules, CA, USA). Nonspecific binding sites were blocked by blocking buffer (5% skim milk in Tris-buffered saline supplemented with 0.1% Tween-20 (TBST)) for 1 h at RT. The membranes were then incubated with primary antibodies diluted in 1% BSA in PBS at 4°C overnight. After washing in TBST, membranes were incubated with secondary antibody conjugated to horseradish peroxidase (HRP) diluted 1:5000 in 5% skim milk in TBST at RT for 1 h and then developed by using ECL substrate kit (Ultra high sensitivity, Abcam). Protein bands were imaged by ImageQuant LAS 500 (GE Healthcare Life Sciences, Piscataway, NJ,

USA) and then quantified using Image J. Details of primary and secondary antibodies are listed in Table 3.1. β-actin was used as a protein loading control.

3.3.15 Real-time quantitative PCR (qPCR)

Total mRNA was extracted from samples by using FavorPrep™ Tissue total RNA mini kit (Favorgen Biotech corp., Taiwan). RNA concentration of each sample was measured using NanoDrop Spectrophotometer (NanoDrop Technologies, Wilmington, DE, USA). From each RNA sample, 500 ng was used to synthesize first-strand cDNA using cDNA synthesis kit (Biotech rabbit, Berlin, Germany). Then qPCR reactions were carried out with cDNA, KAPA SYBR®FAST qPCR kit (KAPA Biosystems, Woburn, MA, USA), primers showed in Table 3.2 and the amplifications were performed in QuantStudio™ 5 real-time PCR system (Thermo Fisher Scientific). Results were analyzed with QuanStudio™ Design & Analysis and Microsoft Excel software. Melting curve analysis was used to confirm the specificity of the primers. The relative quantification of each gene was calculated by applying the $-2^{\Delta\Delta Ct}$ method (Livak and Schmittgen, 2001). Results were normalized to GAPDH with undifferentiated WJ-MSCs as the calibrator to determine the relative quantities of gene expression in each sample. All samples and controls were run as triplicate reactions.

3.3.16 Statistical Analysis

All experiments were repeated three times. All data were presented as mean ± standard error of the mean (SEM) from three separate experiments. All statistical analyses were carried out in SAS® Studio (SAS Institute, Cary, NC, USA), using one-way ANOVA, and Duncan's multiple range test was used as a post hoc test. $p < 0.05$, $p < 0.001$ were considered statistically significant.

**Table 3.1** Antibodies used for IF, flow cytometry and Western blot.

| Antibodies | Companies | Cat # |
|---|---|---|
| PE mouse anti-CD105 | BioLegend | 323206 |
| APC/Cy7 mouse anti-CD90 | BioLegend | 328132 |

**Table 3.1** Antibodies used for IF, flow cytometry and Western blot. (continue)

| Antibodies | Companies | Cat # |
|---|---|---|
| APC mouse anti-CD73 | BioLegend | 344006 |
| FITC mouse anti-CD45 | BioLegend | 368508 |
| FITC mouse IgG, isotype Ctrl | BioLegend | 400109 |
| APC mouse IgG, isotype Ctrl | BioLegend | 400120 |
| PE mouse IgG, isotype Ctrl | BioLegend | 400113 |
| PE mouse anti-CD34 | Beckman Coulter | A07776 |
| Rabbit anti-ZO-1 | Thermo Fisher Scientific | 61-7300 |
| Mouse anti-E-cadherin | Abcam | ab231303 |
| Rabbit anti-β-catenin | Sigma-Aldrich | 06-734/NA |
| Mouse anti-β-actin | Affinity Biosciences | T0022 |
| Rabbit anti-Smad1/5/8/9 | Abcam | ab13723 |
| Rabbit anti-phospho-Smad1/5/8 | Sigma-Aldrich | AB3848-I |
| Rabbit anti-Smad2/3 | Sigma-Aldrich | 07-408 |
| Rabbit anti-phospho-Smad2/3 | Sigma-Aldrich | SAB4504208 |
| FITC mouse anti-Cytokeratin19 | Thermo Fisher Scientific | MA5-28646 |
| Mouse anti-Cytokeratin 12 | Santa Cruz Biotechnology | sc-515882 |
| Rabbit anti-ABCG2 | Abcam | ab229193 |
| Goat anti-mouse IgG HRP | Abcam | ab6789 |
| Goat anti-rabbit IgG HRP | Abcam | ab6721 |
| Goat anti-mouse IgG Alexa Fluor 568 | Thermo Fisher Scientific | A-11031 |
| Goat anti-rabbit IgG FITC | Thermo Fisher Scientific | F2765 |

**Table 3.2** Primers used for qPCR.

| Gene | Primer sequence (5' – 3') | Product length (bp) |
|---|---|---|
| hCTNNB1 | F: CTGAGGACAAGCCACAAGATTACA | 121 |
| | R: TGGGCACCAATATCAAGTCCAA | |
| hABCG2 | F: GTGCACATGCTTGGTGGTCTTGTT | 159 |
| | R: ACCTCGGTCTTAACCAAAGGCTCA | |
| hTP63 | F: GCTCTGAAATCTTCCCATGCAT | 106 |
| | R: ACATTACCTTTTAGAGCCACGC | |
| hKRT3 | F: CTCCAGATAAAGAGCACGCATC | 203 |
| | R: CGGAGAGAAGAGCCTGAAATTC | |
| hKRT12 | F: TATTCTCTCGGGCAATGATGGA | 201 |
| | R: TTGCTGTAATCGCTCTGTGAAG | |
| hKRT15 | F: GGAGGTGGAAGCCGAAGTAT | 194 |
| | R: GAGAGGAGACCACCATCGCC | |
| hKRT19 | F: CTGCGGGACAAGATTCTTGGT | 73 |
| | R: CCAGACGGGCATTGTCGAT | |
| hPAX6 | F: TCTTTGCTTGGGAAATCCG | 167 |
| | R: CTGCCCGTTCAACATCCTTAG | |
| hGAPDH | F: TGCACCACCACCTGCTTAGC | 87 |
| | R: GGCATGGACTGTGGTCATGAG | |

## 3.4 Results

### 3.4.1 Human WJ-MSCs characterization

Primary human WJ-MSCs were successfully isolated by explant culture. Cells were plastic-adherent and showed fibroblast-like morphology (Figure 3.2 A). Flow cytometry results indicated that > 95% cell population expressed standard markers of

MSCs (positive rates of CD90, CD73 and CD105 were 99.78%, 99.54%, and 99.03%, respectively, Figure 2 B) and < 2% cell population expressed hematopoietic markers (positive rates of CD34 and CD45 were 0.12% and 0.55%, respectively, Figure 3.2 B). Multipotency was determined by trilineage differentiation protocols. After adipogenic differentiation, cells produced lipid droplets that stained with Oil Red O (Figure 3.2 C, left). Calcified matrix deposition was confirmed with Alizarin Red staining (Figure 3.2 C, middle) after osteogenic differentiation. The glycosaminoglycans was stained with Alcian blue (Figure 3.2 C, right) after treatment with chondrogenic medium. Self-renewal capacity of human WJ-MSCs was demonstrated by PDT analysis. PDT of the cells at passage 3 (P3) was similar with the cells at P4 (27.22 ± 0.82 h vs 28.88 ± 0.60 h; $p > 0.05$), but lower than the cells at P5 to P10 ($p < 0.05$) (Figure 3.2 D). PDTs of cells at P5 to P10 were not significantly different (average 37.37 h; $p > 0.05$).

3.4.2 Cytotoxicity

Cytotoxicity effects of RA, SB505124, and DMSO on the viability of human WJ-MSCs were shown in Figure 3.3. DMSO treatment was used as vehicle control. DMSO caused concentration-dependent decrease in cell viability. DMSO at dose 0.1% did not significantly reduce cell viability ($p > 0.05$). However, DMSO at concentration 0.25%, 0.5% and 1% significantly decreased cell viability compared with control without DMSO (92.31 ± 1.43%, 87.53 ± 1.51% and 85.02 ± 2.08% vs 100.00 ± 1.69%, respectively; $p < 0.001$). RA also showed cytotoxicity with WJ-MSCs. The survival rates of WJ-MSCs following treatment with RA 2.5, 5, 10, 20 μM were significantly lower than control (77.83 ± 4.38%, 84.45 ± 2.03%, 81.43 ± 2.08% and 80.03 ± 1.69% vs 100 ± 1.69%; $p < 0.05$). Unlike RA and DMSO, SB505124 was not cytotoxic. Treatment with SB505124 showed a trend increased in the viability of WJ-MSC but was not significant compared to control.

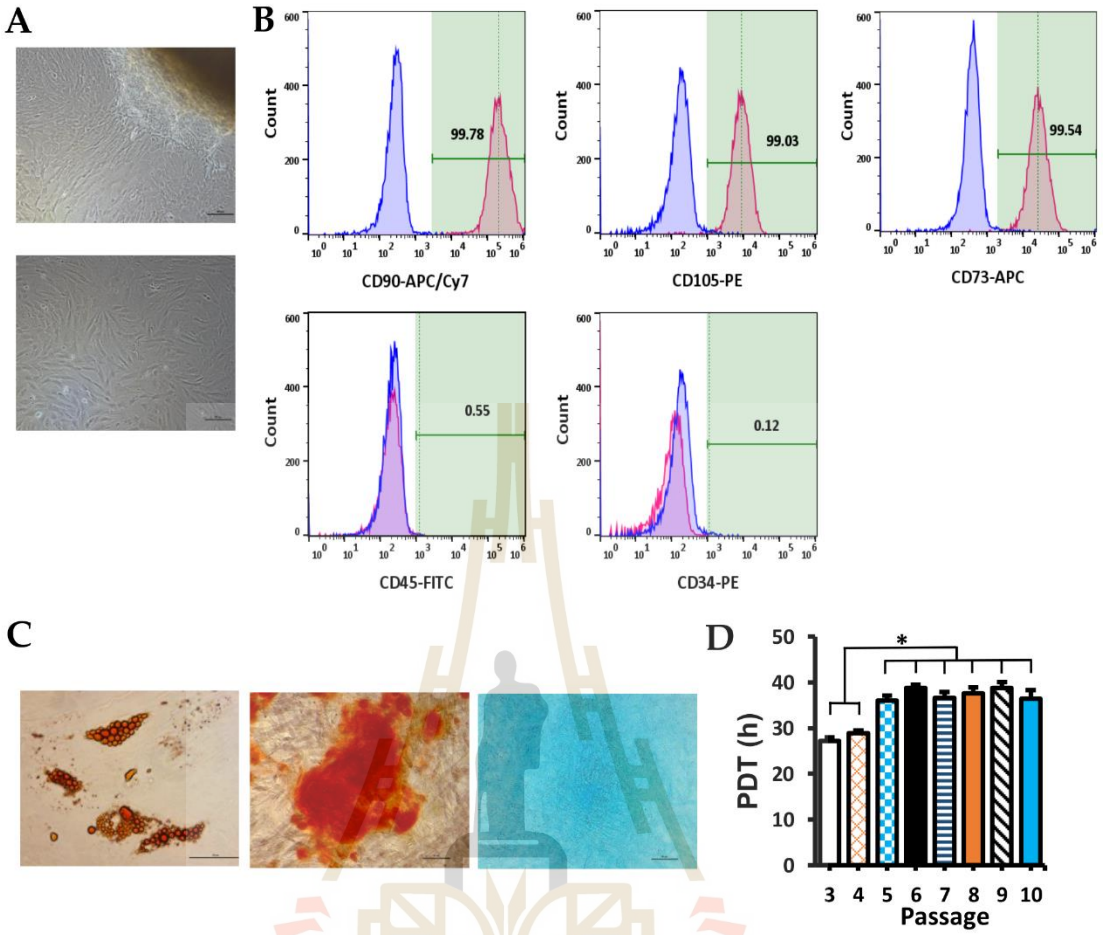


**Figure 3.2** Characterization of human WJ-MSCs. (A) Figure of explant culture of WJ tissue at day 8 (upper) and WJ-MSCs of P1 day 3 (lower); scale bar, 100 μm. (B) Flow cytometry results with MSC markers (CD90, CD73, CD105) and hematopoietic markers (CD34, CD45). (C) Trilineage differentiated cells with Oil Red O staining (left), Alizarin Red staining (middle), and Alcian Blue staining (right); scale bar, 50 μm. (D) PDT at different passages (from 3 to 10). Data are presented as mean + SEM. * $p < 0.05$.

3.4.3 Effect of RA on localization and expression of β-catenin

Human WJ-MSCs remained fibroblast-like morphology in control while RA treatment caused the cells to become more flatten and shorter in length (Figure 3.4). RA treatment had no effect on total β-catenin protein expression (Figure 3.5 C, D) and

mRNA expression (Figure 3.5 E). However, ratio of mean fluorescence intensity of β-catenin in the nucleus to the cytoplasm was significantly suppressed in both RA groups (5 μM and 10 μM) compared with the control group (0.88, 0.97 vs 1.15; $p < 0.05$) (Figure 3.5 B). RA 5 μM and 10 μM inhibited β-catenin translocated from the cytoplasm into nucleus. RA treatment did not affect mRNA and protein expression of β-catenin but both concentrations of RA (5 and 10 μM) could suppress Wnt/β-catenin signaling pathway via reducing translocation of β-catenin from cytoplasm into nucleus.

3.4.4 Effect of SB505124 on inhibition of p-Smad2/3

Western Blot results of SB505124 treatment were shown in Figure 3.6 A. Ratio of p-Smad2/Smad2 protein intensity was significantly reduced after treatment with all concentrations of SB505124 (Figure 3.6 C, left). Phosphorylation of Smad3 tended to decrease after treatment with SB505124 (Figure 3.6 C, right). However, only 20 μM SB505124 was significantly suppressed on phosphorylation of Smad3.

3.4.5 Effect of BMP4 for increasing p-Smad1/5/8

Western Blot results of SB505124 treatment were shown in Figure 3.6 B. Treatment with BMP4 for 1 h did not affect phosphorylation of Smad1/5/8 (Figure 3.6 D). The ratio of p-Smad1/5/8/Smad1/5/8/9 was not different after 2 h of 50 ng/ml BMP4 treatment. Treatment with 25 ng/ml BMP4 for both 1 h and 2 h did not increase phosphorylation of Smad1/5/8. Both concentrations of BMP4 had no significant effect on the phosphorylation of Smad1/5/8 proteins, indicating no activation of the BMP signaling pathway.

3.4.6 Characterization of human CECs

Isolated human CECs showed characteristics of normal CECs such as corneal specific marker (CK12) and other markers of CECs (E-cadherin, ZO-1, Involucrin). Human CEC morphology were shown in Figure 3.7 A. Cells looked like cobblestone, varying in size and shape. Cells at P1 stained positive with CK12 and E-cadherin. ZO-1 and Involucrin stained in the large CECs.

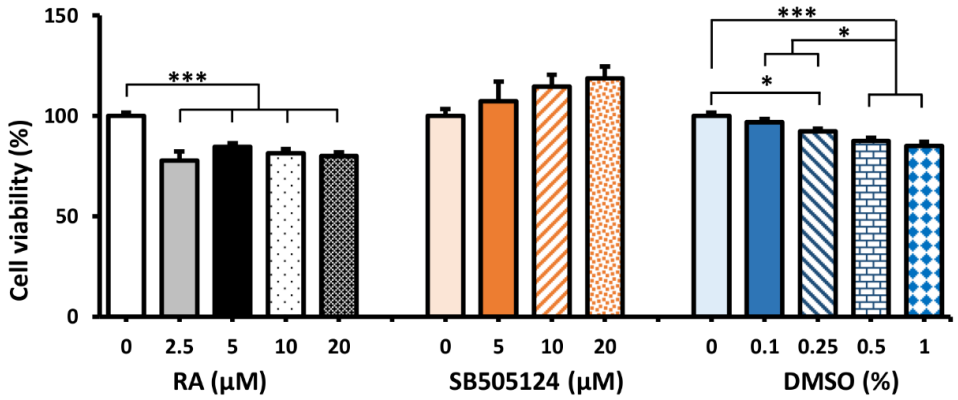


**Figure 3.3** Cytotoxicity of treatment factors (RA, SB505124, and DMSO) on WJ-MSCs. Data are presented as mean + SEM. * $p < 0.05$, *** $p < 0.001$.

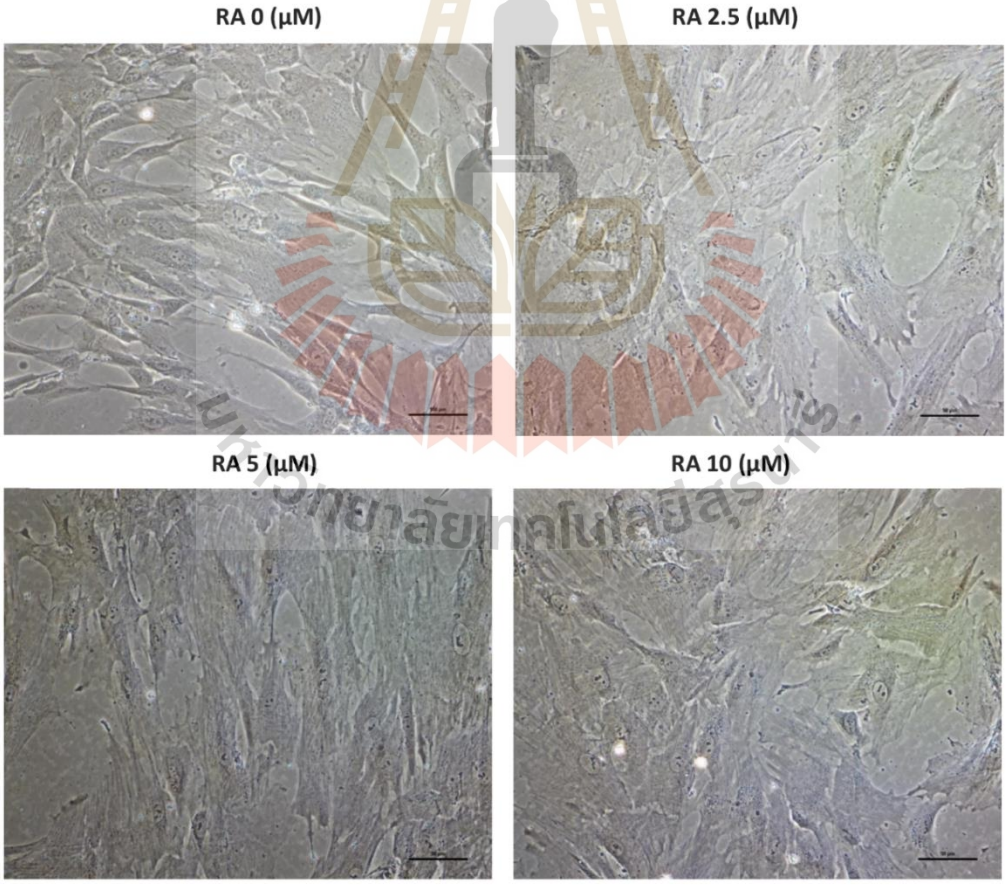


**Figure 3.4** Effect of RA treatment on cell morphology. Scale bar, 50µm.

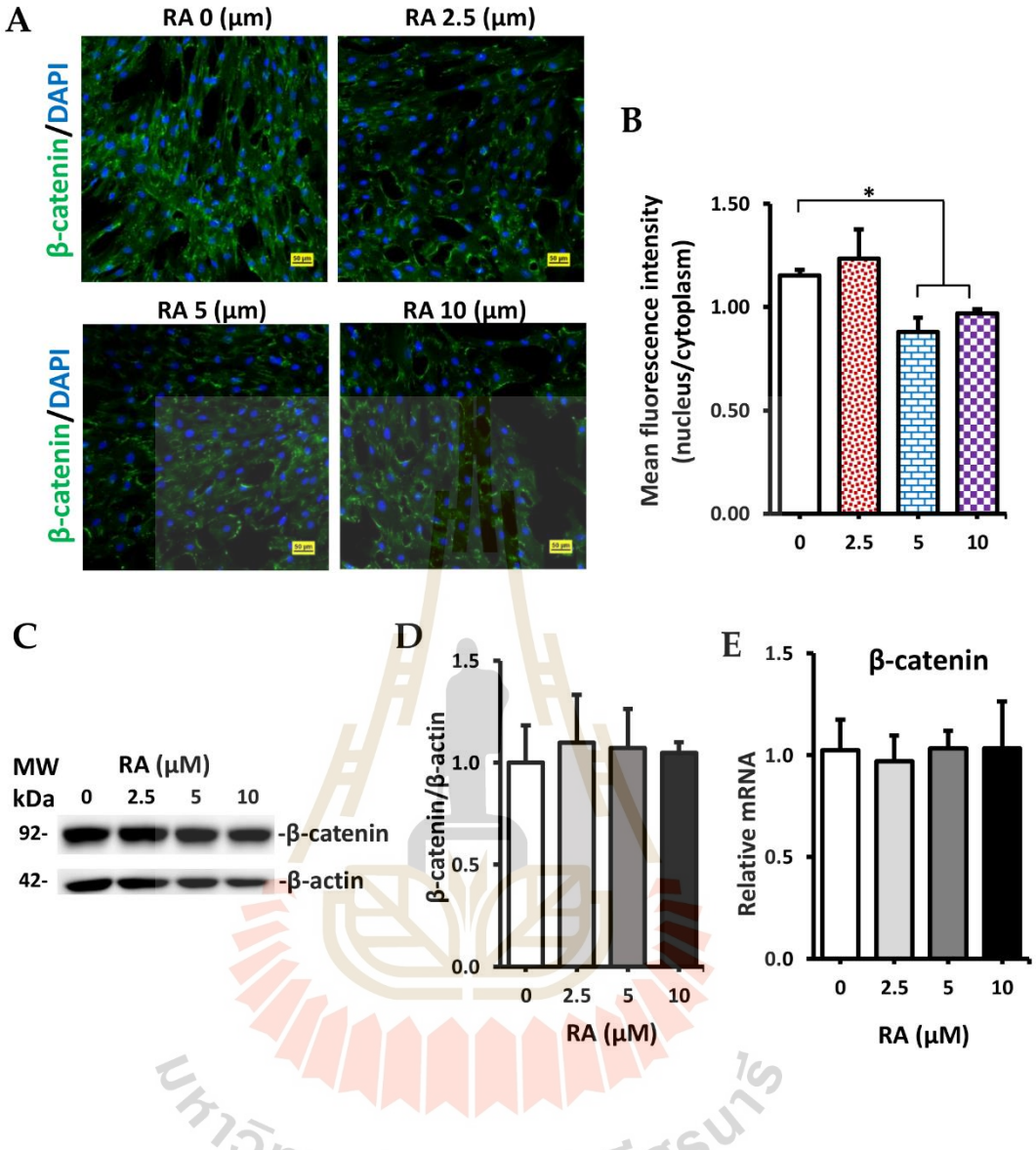


**Figure 3.5** Effect of RA on β-catenin expression. (A) Immunostaining of WJ-MSCs with β-catenin (green) after treatment with RA. Scale bar, 50μm. (B) Ratio of mean fluorescence intensity of β-catenin in the nucleus to cytoplasm was analyzed by confocal microscopy. (C) Western blot images of β-catenin, β-actin expression. (D) Quantification of western blot results. (E) The relative mRNA expression of β-catenin. Data are presented as mean + SEM. * $p <$ 0.05.

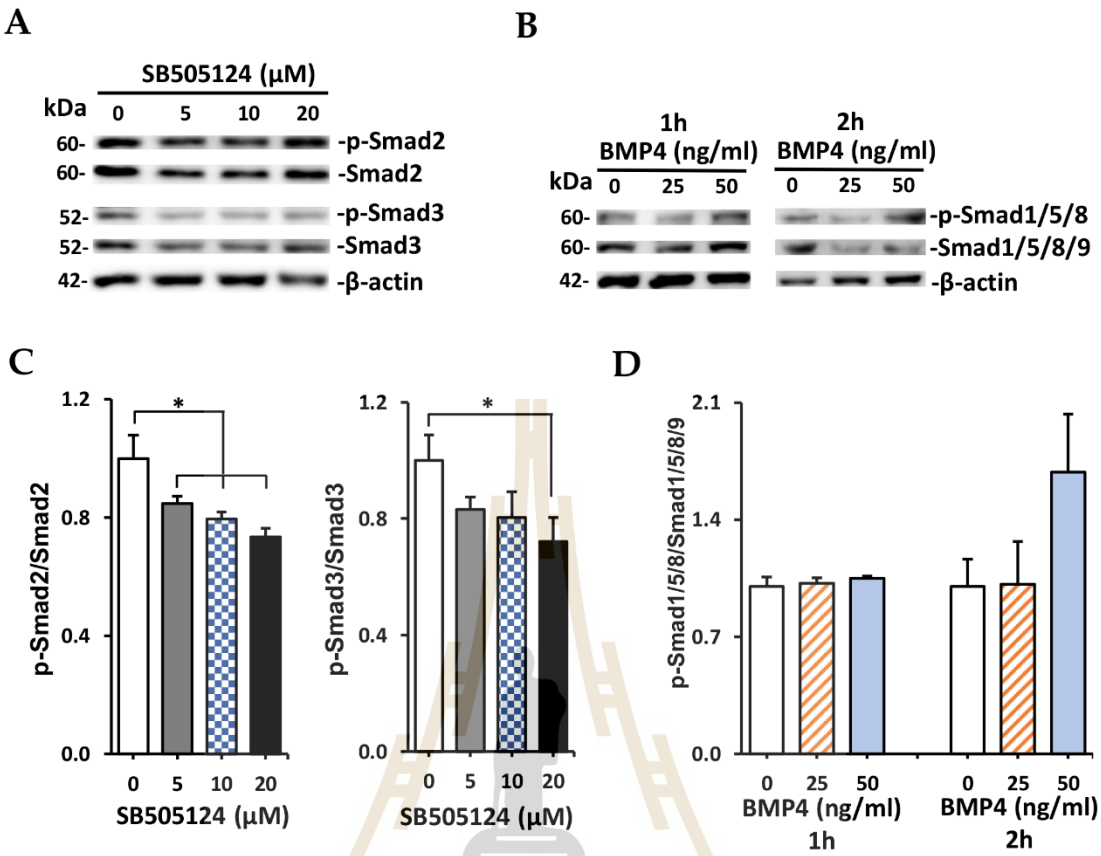


**Figure 3.6** Effect of SB505124, BMP4 on phosphorylation of Smad2/3, Smad1/5/8 (respectively). (A) Western blot images of p-Smad2/3, Smad2/3, β-actin expression. (B) Western blot images of p-Smad1/5/8, Smad1/5/8/9, β-actin expression. (C) Quantification of western blot results of p-Smad2 (left), and p-Smad3 (right). (D) Quantification of western blot results of p-Smad1/5/8. Data are presented as mean + SEM. * $p < 0.05$.

3.4.7 Differentiation of human WJ-MSCs into CECs

During differentiation, the morphology of cells was changed in all groups (Figure 3.7 B). After 9 days, cells became larger and flatter. Especially the morphology of differentiated cells in group G2 at day 9 and group G1, G2, G3 at day 12 looked similar with epithelial-like cells. CK12 protein (specific marker of corneal epithelial

cells) expression was shown in Figure 3.8 A. In BM group, there were rarely cells stained with CK12. However, in group G1, G2, and G3, the positive CK12 cell number were increase from day 3 to day 9 then reduced at day 12. CK12 expressed highest in group G2 at day 9 after differentiation. Although, levels of both CK12 and CK3 (specific CEC markers) mRNA expression in G2 at day 9 were lower than in cornea, they were significantly higher than that in control ($p < 0.05$; Figure 3.7 B). ATP-binding cassette transporter (ABCG2, a marker of putative LESCs) protein expression was shown in Figure 3.9 A. Almost cells in control and treatment groups showed expression of ABCG2. However, the expression of ABCG2 in control groups was very low. After treatment, ABCG2 expression was higher in all groups than control groups. ABCG2 expression in day 12 was lower than day 3 and day 6 in all groups. Level of ABCG2 mRNA expression tended to increase in all treatment groups compared with control group but there was no significant difference between them (Figure 3.8 B, left). Moreover, other corneal epithelial progenitor markers (CK15 and p63) were significantly increased mRNA expression in group G2 at day 9 compared with control group ($p < 0.05$; Figure 3.9 B, 3.10 B, right). Additionally, Paired Box 6 (PAX6, an essential transcription factor for development and function of the cornea) was also upregulated in group G2 at day 9 compared with control groups (Figure 3.11). CK19 (a marker of conjunctival epithelial marker) staining was shown in Figure 3.10 A. Subpopulation of cells in control group stained strong positively with CK19. After treatment, the intensity of CK19 was reduced in all treatment groups. Besides, level of CK19 mRNA showed decrease in all treatment groups compared with control group. Level of CK19 mRNA in cornea was lower than control WJ-MSCs but higher than all treatment groups ($p < 0.001$). All results indicated that treatment condition of group G2 using combination of RA, SB505124, BMP4, EGF in the first step could generate corneal epithelial cells from human WJ-MSCs with highest efficiency after 9 days.

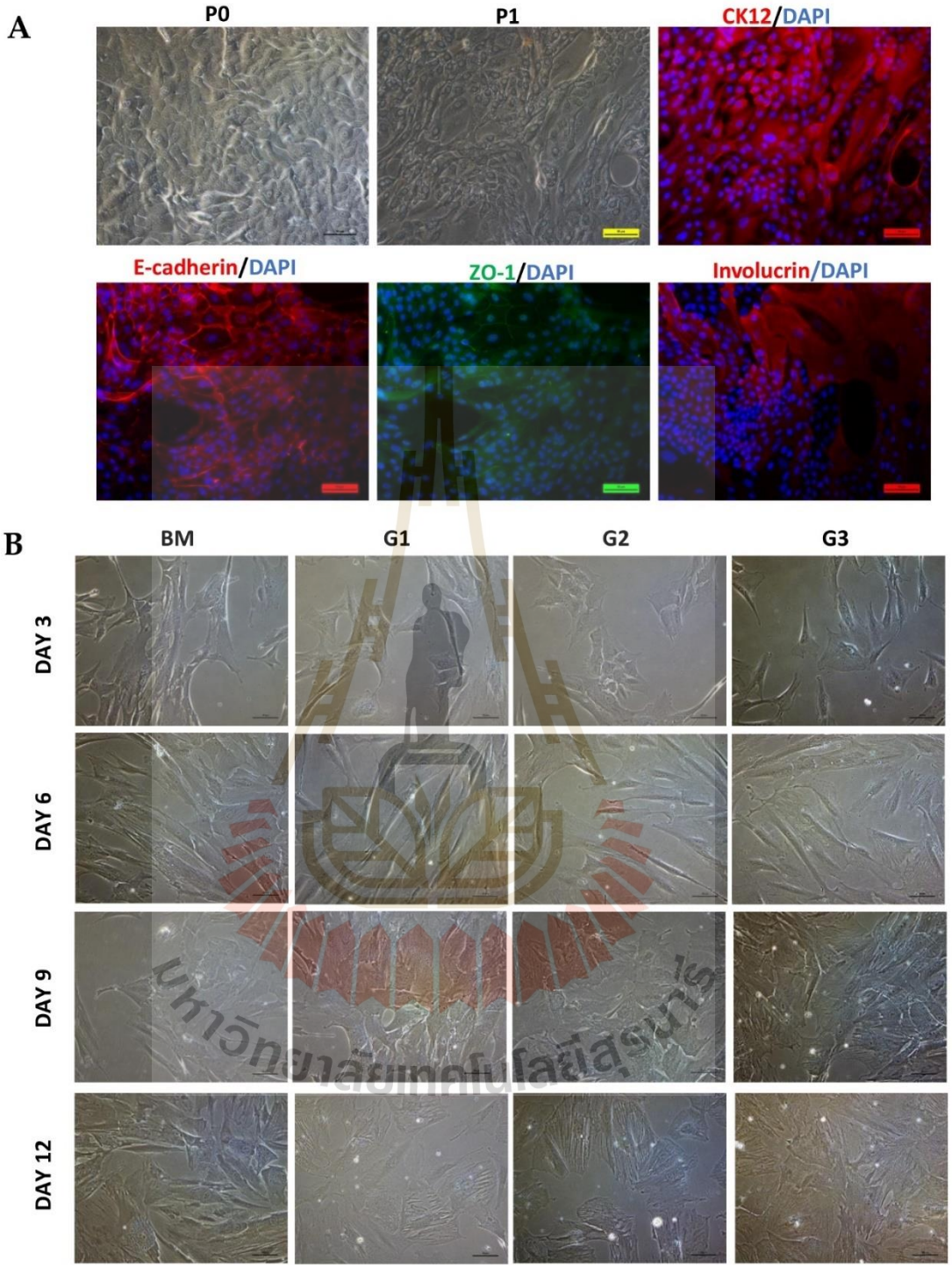


**Figure 3.7** Morphology of CECs and WJ-MSCs during differentiation. (A) Morphology of CECs at P0, P1 (bright field) and IF with of CK12, Ecadherin, ZO-1, involucrin. (B) Morphology changed during differentiation into CECs from WJ-MSCs. (A) and (B), scale bar, 50μm.

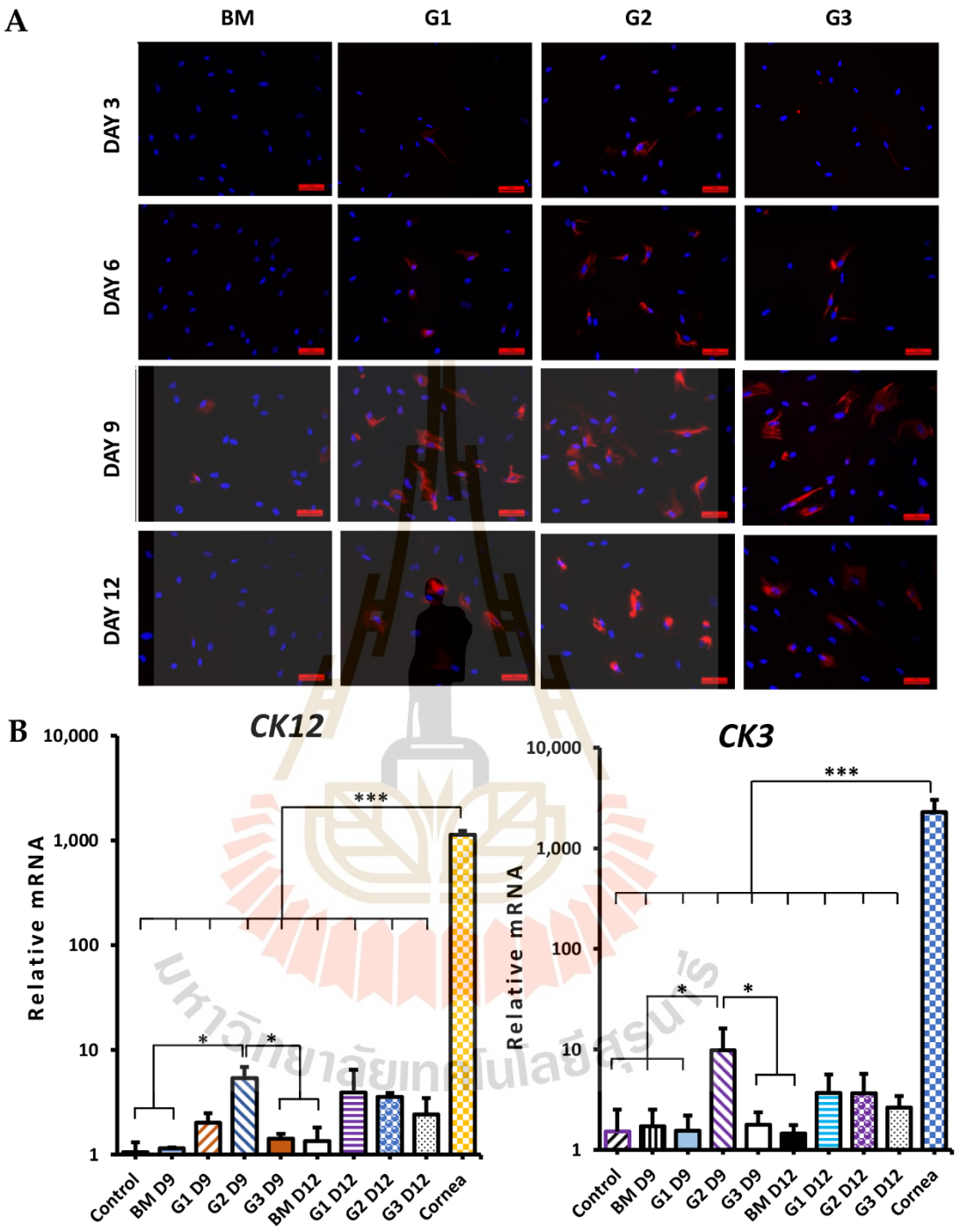


**Figure 3.8** CK12, CK3 expression during CEC differentiation from WJ-MSCs. (A) IF with CK12 (red color), blue color (nucleus). Scale bar, 50μm. (B) The relative mRNA expression of CK12 (left) and CK3 (right). Data are presented as mean + SEM. * $p < 0.05$, *** $p < 0.001$.

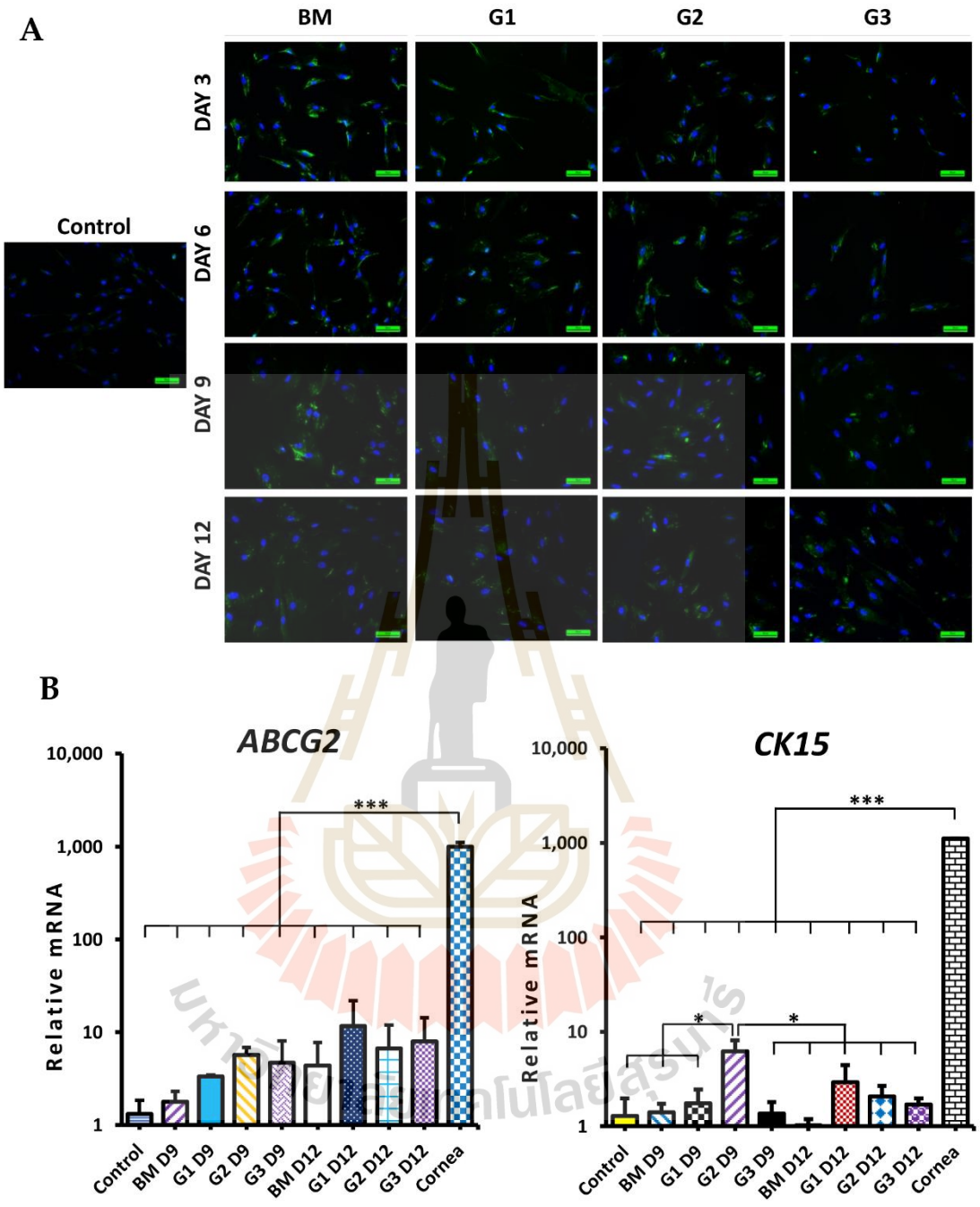


**Figure 3.9** ABCG2, CK15 expression during CEC differentiation from WJ-MSCs. (A) IF with ABCG2 (green color), blue color (nucleus). Scale bar, 50μm. (B) The relative mRNA expression of ABCG2 (left) CK15 (right). Data are presented as mean + SEM. * $p < 0.05$, *** $p < 0.001$.

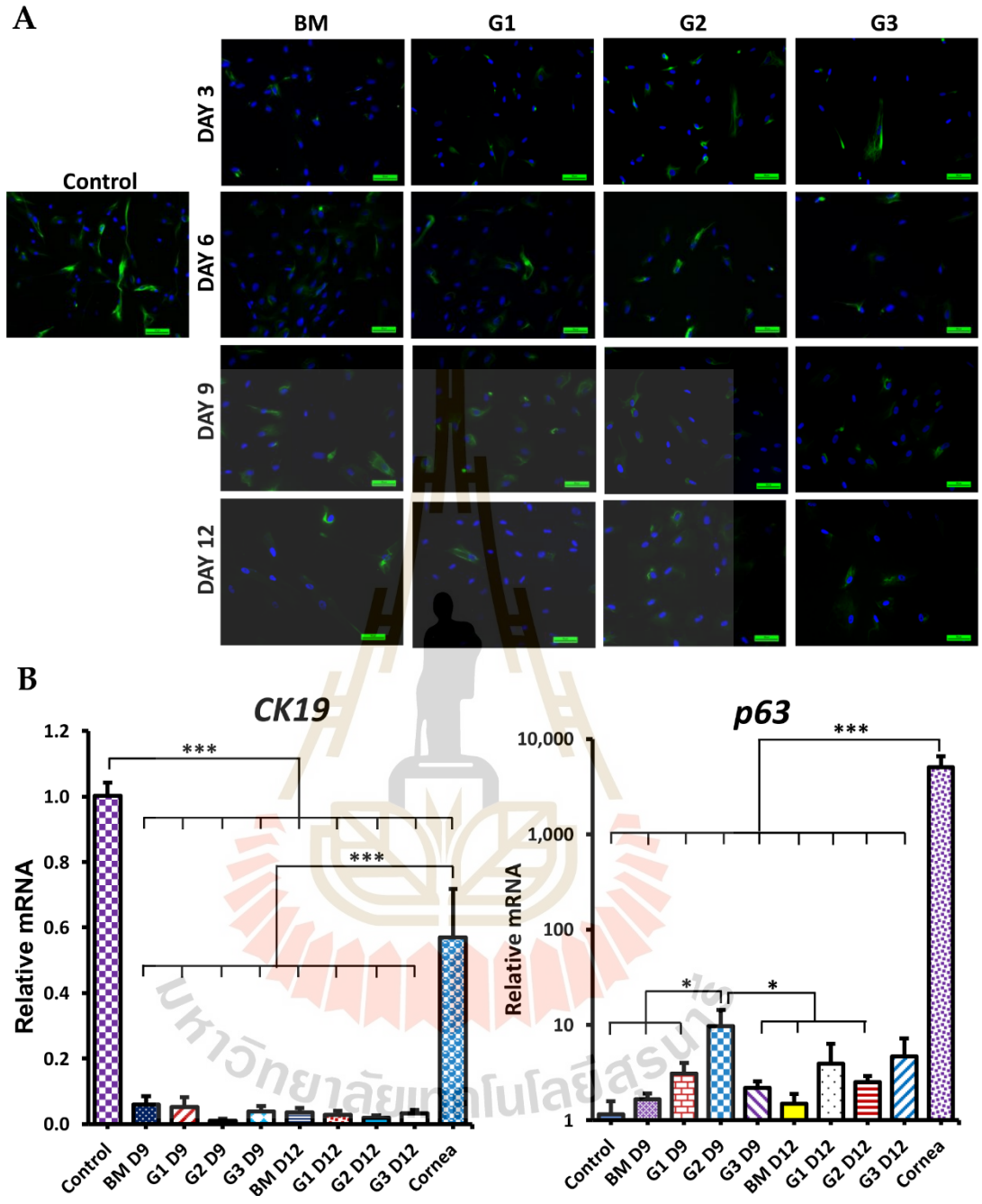


**Figure 3.10** CK19, p63 expression during CEC differentiation from WJ-MSCs. (A) IF with CK19 (green color); blue color (nucleus). Scale bar, 50μm. (B) The relative mRNA expression of CK19 (left) and p63 (right). ). Data are presented as mean + SEM. * $p < 0.05$, *** $p < 0.001$.

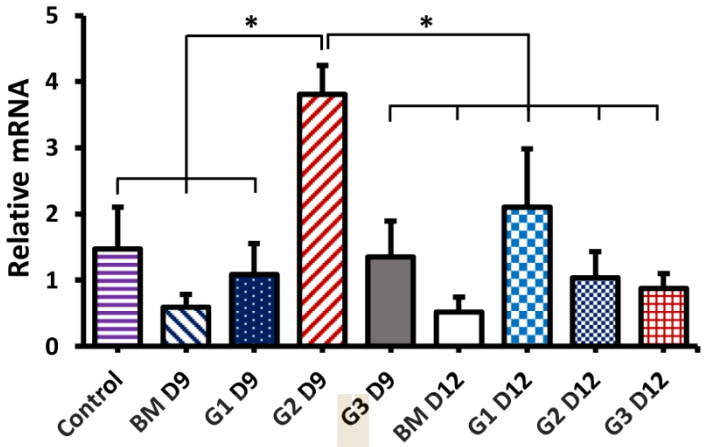


**Figure 3.11** PAX6 mRNA expression during CEC differentiation from WJ-MSCs. Data are presented as mean + SEM. * $p < 0.05$.

## 3.5 Discussion

MSCs are one of the most common cell types that are used for regenerative medicine (Hmadcha et al., 2020). Especially, WJ-MSCs are good candidates for cellular therapies in allogenic transplantation due to their immune suppression and immune avoidance capacity (Li et al., 2014; Marino et al., 2019). Moreover, WJ-MSCs are easier isolated and have higher proliferation potential compared with MSCs from adipose tissue, cord blood, placenta, and bone marrow (Li et al., 2014). In this study, successfully isolated and expanded human WJ-MSCs qualified the minimal criteria characterizing human MSCs (Dominici et al., 2006) such as *i)* plastic-adherent; *ii)* express CD105, CD73, CD90 and lack expression of CD34, CD45; *iii)* can differentiate to osteoblasts, adipocytes, and chondroblasts. Moreover, like the reported WJ-MSCs (Kim et al., 2011; Li et al., 2014), isolated WJ-MSCs in this study were also fibroblast-like cells and showed high potency of self-renewal capacity. Cell at passage 3 and 4 had higher self-renewal capacity than cells in passage 5-10.

Although transplantation of MSCs successfully reconstructed the damaged corneal surfaces of rats (Ma et al., 2006), mice (Lin et al., 2013), and rabbits (Monteiro et al., 2009), the therapeutic effectiveness of MSC transplantation may be caused by their

suppression of inflammation and angiogenesis rather than the epithelial transdifferentiation (Galindo et al., 2017; Ma et al., 2006). Rat cornea transplanted with MSCs did not express CK3, CK12 (Bandeira et al., 2020; Ma et al., 2006). These results indicated that the transdifferentiation potential of transplanted MSCs *in vivo* model was uncertain. Other studies focused on finding methods of generating CECs from MSCs *in vitro*. These methods were based on co-culture with LESCs (Sikora et al., 2019), CECs (Soleimanifar et al., 2018; Tsai et al., 2015); or conditioned medium from limbal explant (Venugopal et al., 2020). These methods are needed to culture signal providing cells which had risks of contamination or disease transmission. The medium compositions used in these methods were undefined and uncontrollable. Moreover, co-culture system required expensive equipment. Other researches used defined media to induce CECs derived from conjunctiva-MSCs, BM-MSCs (Katikireddy et al., 2014; Nieto-Nicolau et al., 2020; Soleimanifar et al., 2018; Soleimanifar et al., 2017). This study focused on finding an optimal method to differentiate WJ-MSCs into CECs *in vitro* by comparing three combinations in the first step and differentiation duration (9 or 12 days). This study found that the combination (RA, SB505124, BMP4, EGF) is the best, and differentiation time is 9 days. After differentiation, cells were positively stained with specific marker of CECs (CK12) and mRNA expressions of both CK3 and CK12 were upregulated.

Wnt/β-catenin signaling pathway plays a vital role during proliferation of LESCs (Nakatsu et al., 2011). During normal homeostasis of the corneal epithelium, Wnt/β-catenin signaling may be relatively inactive and β-catenin is mainly membrane bound in normal intact corneal epithelium (Nakatsu et al., 2011). Inhibiting Wnt signaling results in differentiation into corneal epithelial cells (Lian et al., 2013; Mikhailova et al., 2014). In this study, RA (5μM and 10μM) treatment could suppress Wnt/beta-signaling pathway via inhibiting translocation of β-catenin from cell cytoplasm into nucleus. Lower concentration of RA (1 μM) induced membrane localization of β-catenin and downregulated expression of β-catenin in nucleus of human ESCs (Lian et al., 2013). However, 1 μM RA did not only suppress the canonical Wnt signaling pathway but also activate the noncanonical Wnt signaling pathway in murine ESCs (Osei-Sarfo and Gudas, 2014). Therefore, in this study, 10

μM RA was used for inducing WJ-MSCs differentiation into CECs. Furthermore, TGF-β signaling pathway also regulates epithelial differentiation in eye development (Kahata et al., 2018). Suppression of TGF-β signaling is necessary for generating CECs from human iPSCs (Mikhailova et al., 2014). SB505124 is one of the selective inhibitors of activin and TGF-β signaling pathway (Byfield et al., 2004). In this study, SB505124 treatment inhibited phosphorylation of cytoplasmic signal transducer (Smad2) of TGF-β signaling pathway, so SB505124 could inhibit this signaling pathway. In previous studies, BMP4 combined with suppressing Wnt/β-catenin signaling together with/without inhibiting TGF-β signaling had effect on CEC differentiation from human iPSCs (Mikhailova et al., 2014), and BM-MSCs (Katikireddy et al., 2014). In this study, BMP4 (25 or 50 ng/mL) supplementation did not significantly improve phosphorylation of transducer (Smad1/5/8). Other signaling pathway, bFGF, was necessary for generating CECs from human iPSCs (Mikhailova et al., 2014; Yang et al., 2018). However, supplementation of bFGF did not improve CEC differentiation from human WJ-MSCs in this study. This result may be caused by the presence of BMP4 in the treatment groups. Like bFGF, BMP4 (10 ng/mL) upregulated phosphorylation of extracellular signal-related kinases (ERK1/2) in human CECs (Zhang et al., 2015). In this study, the combination of Wnt and TGF-β signaling inhibitors together with BMP4 and EGF supplementation could generate corneal epithelial cells from human WJ-MSCs with the highest efficiency compared to other treatment combinations. After 9 days of differentiation, induced cells expressed specific protein of CECs (CK12) and mRNA expression of specific markers (CK12, CK3) was upregulated. Increasing expression of both CK3 and CK12 was also reported in CEC derived human iPSCs (Kamarudin et al., 2018; Mikhailova et al., 2014), conjunctiva-MSCs (Soleimanifar et al., 2018; Soleimanifar et al., 2017), BM-MSCs (Nieto-Nicolau et al., 2020).

ATP-binding cassette transporter (ABCG2), breast cancer resistance protein 1 (BCRP1), is considered as a marker for many stem cell lines (Zhou et al., 2001). ABCG2 was identified as a marker of putative LESCs (de Paiva et al., 2005; Gouveia et al., 2019; Schlötzer-Schrehardt and Kruse, 2005). ABCG2 was also shown positive with human umbilical cord matrix stem cells (hUCMS) (Weiss et al., 2006), human dental pulp-MSC (Monteiro et al., 2009), and rat BM-MSCs

(Poleshko and Volotovski, 2016). In this study, human WJ-MSCs showed low expression of ABCG2 but the expression of ABCG2 was upregulated after differentiation. Increasing ABCG2 gene expression was also indicated in corneal epithelial-like cells derived from human iPSCs (Kamarudin et al., 2018). Together with ABCG2, CK15 and p63 are also putative markers of LESCs (Gouveia et al., 2019; Guo et al., 2020; Schlötzer-Schrehardt and Kruse, 2005). Upregulation of CK15 and p63 genes of induced cells in this study was similar with previous CECs derived human iPSCs (Mikhailova et al., 2014). Moreover, increasing gene expression of PAX6, a coactivator of CK12 gene (Liu et al., 1999), in this study was similar with the previous study (Kamarudin et al., 2018). Another marker of LESCs, CK19, was shown in conjunctival epithelial cells and peripheral corneal basal cells (Kivelä and Uusitalo, 1998). CK19 expression was shown in the subpopulation of chorionic-plate-MSCs, chorionic villi-MSCs and WJ-MSCs (Kim et al., 2011). In this study, some human WJ-MSCs also stained positive for CK19. However, CK19 gene expression was downregulated after differentiation in this study. Reduced expression of CK19 also was observed in CECs derived from BM-MSCs (Nieto-Nicolau et al., 2020).

## 3.6 Conclusions

In summary, this study describes the effects of treatment factors (RA, SB505124, and BMP4) on the involved signaling pathways in human WJ-MSCs, then compares several combinations of these treatment factors on the differentiation of these cells into CECs. RA inhibits Wnt signaling via reducing translocation of β-catenin while SB505124 supresses TGF-β signaling by decreasing phosphorylation of Smad2. This study indicates a feeder-free, non-conditioned medium 2-step method to generate CECs from WJ-MSCs within 9 days. This differentiation method consists of two steps: first step using combination of RA, SB505124, BMP4 and EGF and the second step using SHEM medium. Induced CECs derived WJ-MSCs are valuable for research studies on LSCD treatment *in vivo* model.

## 3.7 References

Ahmad, S. (2012). Concise review: Limbal stem cell deficiency, dysfunction, and distress. **Stem Cells Transl. Med.** 1(2): 110-115.

Bandeira, F., Goh, T.-W., Setiawan, M., Yam, G. H.-F., and Mehta, J. S. (2020). Cellular therapy of corneal epithelial defect by adipose mesenchymal stem cell-derived epithelial progenitors. **Stem Cell Res. Ther.** 11(1): 14.

Baylis, O., Figueiredo, F., Henein, C., Lako, M., and Ahmad, S. (2011). 13 years of cultured limbal epithelial cell therapy: A review of the outcomes. **J. Cell Biochem.** 112(4): 993: 1002.

Byfield, S. D., Major, C., Laping, N. J., and Roberts, A. B. (2004). SB-505124 is a selective inhibitor of transforming growth factor-beta type I receptors ALK4, ALK5, and ALK7. **Mol. Pharmacol.** 65(3), 744-752.

Chen, Z., de Paiva, C. S., Luo, L., Kretzer, F. L., Pflugfelder, S. C., and Li, D. Q. (2004). Characterization of putative stem cell phenotype in human limbal epithelia. **Stem Cells** 22(3): 355-366.

de Paiva, C. S., Chen, Z., Corrales, R. M., Pflugfelder, S. C., and Li, D.-Q. (2005). ABCG2 transporter identifies a population of clonogenic human limbal epithelial cells. **Stem Cells** 23(1): 63-73.

Dominici, M., Le Blanc, K., Mueller, I., Slaper-Cortenbach, I., Marini, F., Krause, D., Deans, R., Keating, A., Prockop, D., and Horwitz, E. (2006). Minimal criteria for defining multipotent mesenchymal stromal cells. The International Society for Cellular Therapy position statement. **Cytotherapy** 8(4): 315-317.

Dua, H. S., Saini, J. S., Azuara-Blanco, A., and Gupta, P. (2000). Limbal stem cell deficiency: Concept, aetiology, clinical presentation, diagnosis and management. **Indian J. Ophthalmol.** 48(2): 83-92.

Galindo, S., Herreras, J. M., López-Paniagua, M., Rey, E., de la Mata, A., Plata-Cordero, M., Calonge, M., Nieto-Miguel, T. (2017). Therapeutic effect of human adipose tissue-derived mesenchymal stem cells in experimental corneal failure due to limbal stem cell niche damage. **Stem Cells** 35(10): 2160-2174.

Gouveia, R. M., Lepert, G., Gupta, S., Mohan, R. R., Paterson, C., and Connon, C. J. (2019). Assessment of corneal substrate biomechanics and its effect on epithelial stem cell maintenance and differentiation. **Nat. Commun.** 10(1): 1496.

Guo, Z. H., Zeng, Y. M., and Lin, J. S. (2020). Dynamic spatiotemporal expression pattern of limbal stem cell putative biomarkers during mouse development. **Exp. Eye Res.** 192: 107915.

Hmadcha, A., Martin-Montalvo, A., Gauthier, B. R., Soria, B., and Capilla-Gonzalez, V. (2020). Therapeutic potential of mesenchymal stem cells for cancer therapy. **Front. bioeng. biotechnol.** 8: 43.

Kahata, K., Dadras, M. S., and Moustakas, A. (2018). TGF-beta family signaling in epithelial differentiation and epithelial-mesenchymal transition. **Cold Spring Harb. Perspect. Biol.** 10(1).

Kamarudin, T. A., Bojic, S., Collin, J., Yu, M., Alharthi, S., Buck, H., Shortt, A., Armstrong, L., Figueiredo, F. C., and Lako, M. (2018). Differences in the activity of endogenous bone morphogenetic protein signaling impact on the ability of induced pluripotent stem cells to differentiate to corneal epithelial-like cells. **Stem Cells** 36(3): 337-348.

Katikireddy, K. R., Dana, R., and Jurkunas, U. V. (2014). Differentiation potential of limbal fibroblasts and bone marrow mesenchymal stem cells to corneal epithelial cells. **Stem Cells** 32(3): 717-729.

Kim, M. J., Shin, K. S., Jeon, J. H., Lee, D. R., Shim, S. H., Kim, J. K., Cha, D.-H; Yoon, T. K., and Kim, G. J. (2011). Human chorionic-plate-derived mesenchymal stem cells and Wharton's jelly-derived mesenchymal stem cells: A comparative analysis of their potential as placenta-derived stem cells. **Cell Tissue Res.** 346(1): 53.

Kivelä, T., and Uusitalo, M. (1998). Structure, development and function of cytoskeletal elements in non-neuronal cells of the human eye. **Prog. Retin. Eye Res.** 17(3): 385-428.

Li, X., Bai, J., Ji, X., Li, R., Xuan, Y., and Wang, Y. (2014). Comprehensive characterization of four different populations of human mesenchymal stem cells as regards their immune properties, proliferation and differentiation. **Int. J. Mol. Med.** 34(3): 695-704.

Lian, X., Selekman, J., Bao, X., Hsiao, C., Zhu, K., and Palecek, S. P. (2013). A small molecule inhibitor of Src family kinases promotes simple epithelial differentiation of human pluripotent stem cells. **PLoS One** 8(3): e60016.

Lin, K.-J., Loi, M.-X., Lien, G.-S., Cheng, C.-F., Pao, H.-Y., Chang, Y.-C., Ji, A. T.-Q., and Ho, J. H.-C. (2013). Topical administration of orbital fat-derived stem cells promotes corneal tissue regeneration. **Stem Cell Res. Ther.** 4(3): 72.

Liu, C.-Y., and Kao, W. W.-Y. (2015). Chapter five - Corneal epithelial wound healing. In J. F. Hejtmancik and J. M. Nickerson (Eds.), **Progress in Molecular Biology and Translational Science** 134: 61-71.

Liu, J. J., Kao, W. W., and Wilson, S. E. (1999). Corneal epithelium-specific mouse keratin K12 promoter. **Exp. Eye Res.** 68(3): 295-301.

Livak, K. J., and Schmittgen, T. D. (2001). Analysis of relative gene expression data using real-time quantitative PCR and the 2(-Delta Delta C(T)) Method. **Methods** 25(4): 402-408.

Lo, B., and Parham, L. (2009). Ethical issues in stem cell research. **Endocrine reviews** 30(3): 204-213.

Ma, Y., Xu, Y., Xiao, Z., Yang, W., Zhang, C., Song, E., Du, Y., and Li, L. (2006). Reconstruction of chemically burned rat corneal surface by bone marrow–derived human mesenchymal stem cells. **Stem Cells** 24(2): 315-321.

Marino, L., Castaldi, M. A., Rosamilio, R., Ragni, E., Vitolo, R., Fulgione, C., Castaldi, S. G., Serio, B., Bianco, R., Guida, M., and Selleri, C. (2019). Mesenchymal stem cells from the Wharton's jelly of the human umbilical cord: Biological properties and therapeutic potential. **Int. J. Stem Cells**, 12(2): 218-226.

Mikhailova, A., Ilmarinen, T., Uusitalo, H., and Skottman, H. (2014). Small-molecule induction promotes corneal epithelial cell differentiation from human induced pluripotent stem cells. **Stem Cell Rep.** 2(2): 219-231.

Monteiro, B. G., Serafim, R. C., Melo, G. B., Silva, M. C. P., Lizier, N. F., Maranduba, C. M. C., Smith, R. L., Kerkis, A., Cerruti, H., Gomes, J. A. P., and Kerkis, I. (2009). Human immature dental pulp stem cells share key characteristic features with limbal stem cells. **Cell Prolif.** 42(5): 587-594.

Nakamura, T., Endo, K., Cooper, L. J., Fullwood, N. J., Tanifuji, N., Tsuzuki, M., Koizumi, N., Inatomi, T., Sano, Y., and Kinoshita, S. (2003). The successful culture and autologous transplantation of rabbit oral mucosal epithelial cells on amniotic membrane. **Invest. Ophthalmol. Vis. Sci.** 44(1): 106-116.

Nakatsu, M. N., Ding, Z., Ng, M. Y., Truong, T. T., Yu, F., and Deng, S. X. (2011). Wnt/beta-catenin signaling regulates proliferation of human cornea epithelial stem/progenitor cells. **Invest. Ophthalmol. Vis. Sci.** 52(7): 4734-4741.

Nieto-Nicolau, N., Martín-Antonio, B., Müller-Sánchez, C., and Casaroli-Marano, R. P. (2020). *In vitro* potential of human mesenchymal stem cells for corneal epithelial regeneration. **Regen. Med.** 15(3): 1409-1426.

Notara, M., Alatza, A., Gilfillan, J., Harris, A. R., Levis, H. J., Schrader, S., .Vernon, A., and Daniels, J. T. (2010). In sickness and in health: Corneal epithelial stem cell biology, pathology and therapy. **Exp. Eye Res.** 90(2): 188-195.

Notara, M., Lentzsch, A., Coroneo, M., and Cursiefen, C. (2018). The role of limbal epithelial stem cells in regulating corneal (lymph)angiogenic privilege and the micromilieu of the limbal niche following UV exposure. **Stem Cells Int.** 2018: 8620172-8620172.

Osei-Sarfo, K., and Gudas, L. J. (2014). Retinoic acid suppresses the canonical Wnt signaling pathway in embryonic stem cells and activates the noncanonical Wnt signaling pathway. **Stem Cells** 32(8): 2061-2071.

Petsa, A., Gargani, S., Felesakis, A., Grigoriadis, N., and Grigoriadis, I. (2009). Effectiveness of protocol for the isolation of Wharton's jelly stem cells in large-scale applications. **In Vitro Cell. Dev. Biol. Animal** 45(10): 573.

Poleshko, A. G., and Volotovski, I. D. (2016). The role of ABCG2 in maintaining the viability and proliferative activity of bone marrow mesenchymal stem cells in hypoxia. **Biophysics** 61(2): 271-276.

Puangsricharern, V., and Tseng, S. C. G. (1995). Cytologlogic evidence of corneal diseases with limbal stem cell deficiency. **Ophthalmology** 102(10): 1476-1485.

Redaelli, S., Bentivegna, A., Foudah, D., Miloso, M., Redondo, J., Riva, G., Baronchelli, S., Dalprà, L., and Tredici, G. (2012). From cytogenomic to epigenomic profiles: monitoring the biologic behavior of *in vitro* cultured human bone marrow mesenchymal stem cells. **Stem Cell Res. Ther.** 3(6): 47-47.

Riggs, J. W., Barrilleaux, B. L., Varlakhanova, N., Bush, K. M., Chan, V., and Knoepfler, P. S. (2013). Induced pluripotency and oncogenic transformation are related processes. **Stem Cells Dev.** 22(1): 37-50.

Satake, Y., Higa, K., Tsubota, K., and Shimazaki, J. (2011). Long-term outcome of cultivated oral mucosal epithelial sheet transplantation in treatment of total limbal stem cell deficiency. **Ophthalmology** 118(8): 1524-1530.

Schlötzer-Schrehardt, U., and Kruse, F. E. (2005). Identification and characterization of limbal stem cells. **Exp. Eye Res.** 81(3): 247-264.

Sikora, B., Skubis-Sikora, A., Kimsa-Furdzik, M., Ciszek, W., Kostrzewski, M., Stojko, J., Mazurek, U., and Gola, J. (2019). Adipose-derived stem cells undergo differentiation after co-culture with porcine limbal epithelial stem cells. **Stem Cell Res.** 41: 101609.

Soleimanifar, F., Mortazavi, Y., Nadri, S., Islami, M., and Vakilian, S. (2018). Coculture of conjunctiva derived mesenchymal stem cells (CJMSCs) and corneal epithelial cells to reconstruct the corneal epithelium. **Biologicals** 54: 39-43.

Soleimanifar, F., Mortazavi, Y., Nadri, S., & Soleimani, M. (2017). Conjunctiva derived mesenchymal stem cell (CJMSCs) as a potential platform for differentiation into corneal epithelial cells on bioengineered electrospun scaffolds. **J. Biomed. Mater. Res. A** 105(10): 2703-2711.

Sotozono, C., Inatomi, T., Nakamura, T., Koizumi, N., Yokoi, N., Ueta, M., Matsuyama, K., Miyakoda, K., Kaneda, H., Fukushima, M., and Kinoshita, S. (2013). Visual improvement after cultivated oral mucosal epithelial transplantation. **Ophthalmology** 120(1): 193-200.

Tanthaisong, P., Imsoonthornruksa, S., Ngernsoungnern, A., Ngernsoungnern, P., Ketudat-Cairns, M., and Parnpai, R. (2017). Enhanced chondrogenic differentiation of human umbilical cord Wharton's jelly derived mesenchymal stem cells by GSK-3 inhibitors. **PLoS One** 12(1): e0168059.

Tsai, C. L., Chuang, P. C., Kuo, H. K., Chen, Y. H., Su, W. H., and Wu, P. C. (2015). Differentiation of stem cells from human exfoliated deciduous teeth toward a phenotype of corneal epithelium *in vitro*. **Cornea** 34(11): 1471-1477.

Utheim, T. P., Utheim, Ø. A., Khan, Q.-E. S., and Sehic, A. (2016). Culture of oral mucosal epithelial cells for the purpose of treating limbal stem cell deficiency. **J. Funct. Biomater.** 7(1): 5.

Venugopal, B., Shenoy, S. J., Mohan, S., Anil Kumar, P. R., and Kumary, T. V. (2020). Bioengineered corneal epithelial cell sheet from mesenchymal stem cells-A functional alternative to limbal stem cells for ocular surface reconstruction. J. Biomed. **Mater. Res. Part B Appl. Biomater.** 108(3): 1033-1045.

Weiss, M. L., Medicetty, S., Bledsoe, A. R., Rachakatla, R. S., Choi, M., Merchav, S., Luo, Y., Rao, M. S., Velagaleti, G., and Troyer, D. (2006). Human umbilical cord matrix stem cells: Preliminary characterization and effect of transplantation in a rodent model of Parkinson's disease. **Stem Cells** 24(3): 781-792.

Yang, J., Park, J. W., Zheng, D., and Xu, R.-H. (2018). Universal corneal epithelial-like cells derived from human embryonic stem cells for cellularization of a corneal scaffold. **Transl. Vis. Sci. Technol.** 7(5): 23-23.

Yoon, J. J., Ismail, S., and Sherwin, T. (2014). Limbal stem cells: Central concepts of corneal epithelial homeostasis. **World J. Stem Cells** 6(4): 391-403.

Zhang, Y., Yeh, L.-K., Zhang, S., Call, M., Yuan, Y., Yasunaga, M., Kao, W. W. Y., and Liu, C.-Y. (2015). Wnt/β-catenin signaling modulates corneal epithelium stratification via inhibition of Bmp4 during mouse development. **Development** 142(19): 3383-3393.

Zhou, S., Schuetz, J. D., Bunting, K. D., Colapietro, A.-M., Sampath, J., Morris, J. J., Lagutina, I., Grosveld, G. C., Osawa, M., Nakauchi, H., and Sorrentino, B. P. (2001). The ABC transporter Bcrp1/ABCG2 is expressed in a wide variety of stem cells and is a molecular determinant of the side-population phenotype. **Nat. Med.** 7(9): 1028-1034.

# CHAPTER 4
# TRANSPLANTATION OF INDUCED CEC SHEET INTO THE LSCD RABBIT MODEL

## 4.1 Abstract

LSCD is an eye disease which is the main cause of corneal blindness. Cell sheet transplantation is promise therapy for treatment LSCD. This study aimed to generate cell sheet from induced CECs derived from human WJ-MSCs and evaluate efficiency of CEC sheet transplantation on recovery of LSCD in rabbit model. Induced CECs derived from human WJ-MSCs were seeded onto dhAM to generate cell sheet. This induced CEC sheet consisted of 1- to 4-layers of cells and these cells remained expression of CK12. LSCD rabbit model was created in 9 right eyes of rabbits by treatment with 1N NaOH on corneal and limbal epithelium for 30s. After 28 days, rabbit right eyes showed mild (1 rabbit) and moderate stage (8 rabbits) of LSCD by fluorescein staining, neovascularization, nearly total corneal opaque were observed in these eyes. These 9 rabbits were divided into 3 groups: G1 (no transplantation), G2 (dhAM transplantation) and G3 (induced CEC sheet transplantation). 30 after transplantation, rabbits were sacrificed, and their eyes were collected for examination. In G1, CK12 was observed in limbus and peripheral cornea, goblet cells and blood vessels only invaded into peripheral cornea, opacity was increased. In G2, there was no human cells were detected in rabbit cornea, CK3 and CK12 were not expressed, goblet cells and blood vessels grew inward to central cornea, opacity was increased. However, in G3, human cells were confirmed in corneal epithelium of rabbit cornea, CK3 and CK12 were shown in cornea, not in limbus, opacity was reduced. These results indicated that only alkali burn treatment could not destroy all LESCs so the remained LESCs could regenerate CECs in the peripheral cornea and inhibit growth of conjunctiva and blood vessels into the central cornea in no transplantation group. However, alkali burn, and surgery process

removed all LESCs that functioned both barrier and generation CECs, so conjunctiva and blood vessels grew faster, and CECs were not observed in dhAM transplantation group. Induced CECs could survive, grow in rabbit cornea, support recovery of cornea epithelium, and reduce cornea opacity in CEC sheet transplantation group. This study reveals that transplantation of induced CECs derived from WJ-MSCs improves recovery of LSCD in rabbit model.

## 4.2 Introduction

LSCD is an eye disease that causes loss of corneal integrity and function, resulting in corneal blindness (Ahmad, 2012). Cultivated limbal epithelial transplantation (CLET) and cultivated oral mucosal epithelial transplantation (COMET) are two common therapeutic treatments of LSCD. However, both techniques give variation in success rate, use animal-derived material, and cause peripheral corneal neovascularization (Chen et al., 2004; Satake et al., 2011; Sotozono et al., 2013). Therefore, researchers are focusing on finding better cell sources for treatment LSCD. WJ-MSCs might be good candidate because they are safe and have capacity for immune suppression and immune avoidance (Marino et al., 2019) that are necessary for allogenic transplantation. Human WJ-MSCs was reported that they could differentiate into CECs in a three-dimensional (3D) model *in vitro* (Garzón et al., 2014). However, CK3/12 expression in the 3D model was unclear because CK3/12 were expressed in cell nucleus in the epithelial layer and in corneal keratocyte layer.

Corneal epithelium is the outmost layer of cornea that is directly contact with outside environment, so cell carriers are generally used for cell transplantation in treatment LSCD. Among these cell carriers, hAM is widely used for ocular surface therapy because it is transparent, anti-inflammatory, anti-angiogenic, poorly immunogenic, contains important growth factor, supports wound healing ophthalmology (Malhotra and Jain, 20142014; Ramuta and Kreft, 2018). Although both hAM and dhAM support the growth of LESCs and retain the expression of putative LESC

markers, dhAM promotes to better migration of LESCs than hAM (Shortt et al., 2009). Several methods such as treatment with trypsin-EDTA, EDTA, thermolysin, Dispase, urea, etc. are studied for de-epithelialization of hAM but these treatments take long time, fail to remove all epithelial cells, and damage the hAM (Zhang et al., 2013; Hopkinson et al., 2008). Recently, a simple method using sodium hydroxide for decellularization of hAM was fast and efficient in de-epithelialization of hAM (Saghizadeh et al., 2013).

This study aimed to generate induced CEC sheet by seeding human induced CECs derived from human WJ-MSCs on dhAM. Induction of human WJ-MSCs into CECs was performed using the optimal method in Chapter 3 of this thesis. Afterwards, this study investigated effect of induced CEC sheet transplantation on LSCD eyes of rabbit model.

## 4.3 Materials and Methods

### 4.3.1 Ethics Statement

Ethical approval for this study was obtained from the Animal Ethics Committee of Suranaree University of Technology, Thailand (Approval Number: U1-03131-2559).

### 4.3.2 Establishment of LSCD eyes in rabbit model

The rabbits were obtained from National Laboratory Animal Center (Mahidol University, Nakhon Pathom, Thailand). A total of 15 male New Zealand white rabbits aged 2-9 months were used for the experiment. The rabbits were fed according to the Laboratory Animals Ethics and Welfare (Suranaree University of Technology, Thailand), and allowed free access to food and water. All rabbits were anesthetized by using isoflurane (Aerrane isoflurane, Baxter Healthcare Corporation, USA) at concentration of 4-5% for induction and 2% for maintenance. The right eye of each rabbit was subjected to limbal, and corneal damage as previously described (Tananuvat et al., 2017) with some modification. Briefly, the right eyes were local anesthetized with a drop of 0.5%

tetracaine hydrochloride (Alcon-Couvreur, Belgium) before treatment with Whatman filter paper discs (15-16 mm diameter) soaked with 1N NaOH for 30sec and then washed with normal saline solution. Diclofenac sodium 1 mg/ml (Volta Oph, Seng Thai, Thailand), 0.5% Levofloxaxin (Cravit, Santen Pharmaceutical, Japan), 0.18% sodium hyaluronate (Vislube, HOLOPACK Verpackungstechnik GmbH, Belgium) were applied to the wounded eye twice a day for 5 days. Corneal epithelial loss was confirmed by fluorescein staining. The morphology of treated eyes was observed and took photos every 7 days. The degree of LSCD was evaluated after 28 days.

4.3.3 De-epithelialization of hAM

Cryopreserved hAM was ordered from H.R.H. Maha Chakri Sirindhorn Medical Center (Nakhon Nayok, Thailand) and de-epithelialized according to previously study (Saghizadeh et al., 2013) with some modification. Briefly, thawed hAM was placed on PVDF membrane in 60 mm petri dish with epithelial side facing up. Afterwards, hAM was treated with 0.5M NaOH for 30s, then wash 3 times in PBS for 5 min each. Then the epithelium layer of hAM was removed by rubbing with cotton-tipped applicator under stereo microscope. Finally, the dhAM was washed with PBS. De-epitheliazation of hAM was confirmed by staining with heamatoxylin and eosin (H&E), and DAPI.

4.3.4 Generation and characterization of human induced CEC derived WJ-MSC sheet on dhAM

Human WJ-MSCs at passage 4 were seeded at a density of $10^3$ cells/$cm^2$ and cultured in the culture medium (αMEM supplemented with 10% fetal bovine serum (FBS), 100 U/ml penicillin, 100 µg/ml streptomycin) for 2 days. Then these cells were treated with combinations of 10 µM RA, 10 µM SB505124, 25 ng/ml BMP4, 10 ng/ml EGF in basic medium (BM: DMEM low glucose supplemented with 2% FBS, 1% NEAA, 100 U/ml penicillin, 100 µg/ml streptomycin) for 3 days. After that, these cells were cultured in supplemented hormonal epidermal medium (SHEM: containing mixture of DMEM low glucose and DMEM/F12 medium (1:1 v/v) supplemented with 5% FBS, 10 ng/mL EGF, 1% of insulin-transferrin-sodium selenite (ITS-H), 0.5 µg/ml hydrocortisone, 0.05% DMSO, 200

nM adenine, 100 U/ml penicillin, 100 µg/ml streptomycin) for additional 6 days. To generate cell sheet, the induced CECs were seeded at a density of $3x10^5$ cells/well on dhAM in insert well with medium that contained mixture of DMEM low glucose and DMEM/F12 medium (1:1 v/v), 5% FBS, 10 ng/ml EGF, 1% ITS-H, 0.5 µg/ml hydrocortisone, 0.5% DMSO, 200 nM adenine, 100 U/ml penicillin, 100 µg/ml streptomycin. The medium was supplemented in the top and bottom well for 3 days. Afterwards, the medium on the top of insert well were reduced to create an air-liquid interface for 6 days and the medium were changed daily. The harvested CEC sheets were used for transplantation or characterization with H&E staining and IF staining with CK12. Summary procedure of induced CEC sheet generation and characterization is shown in Figure 4.1.

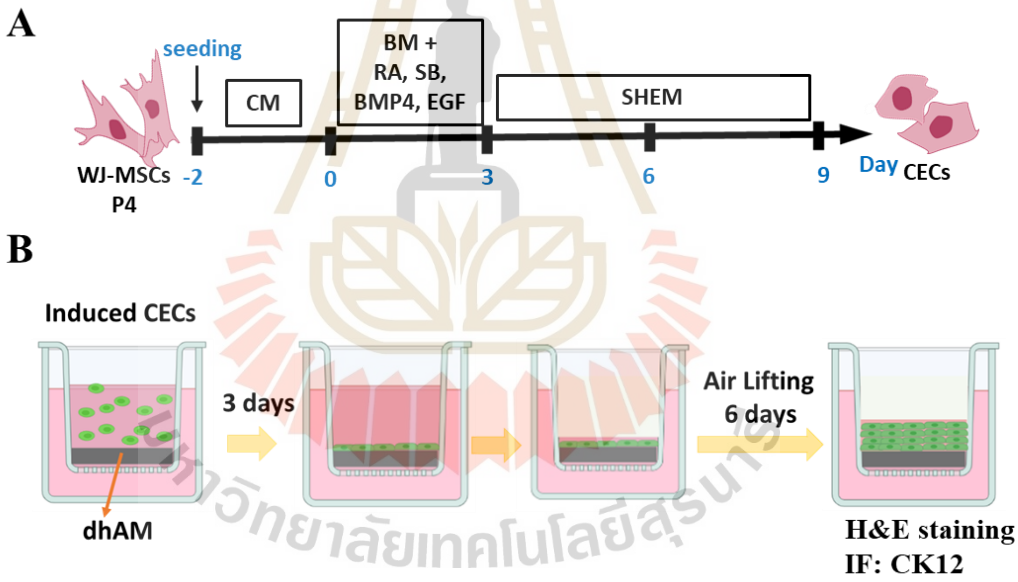


**Figure 4.1** Generation and characterization of human induced CEC sheet. (A) Differentiation of human WJ-MSCs into CECs. (B) Induced CECs were seeded onto dhAM to generate induced CEC sheet.

4.3.5 Transplantation CEC sheet into LSCD eyes

Four weeks after alkali burn treatment, the right LSCD rabbit eyes were divided into 3 groups (3 rabbits/each group): G1 (no transplantation), G2 (dhAM transplantation), and G3 (induced CEC sheet transplantation). The left non-treated rabbit eyes were used as control. Grouping model is shown in Figure 4.2.

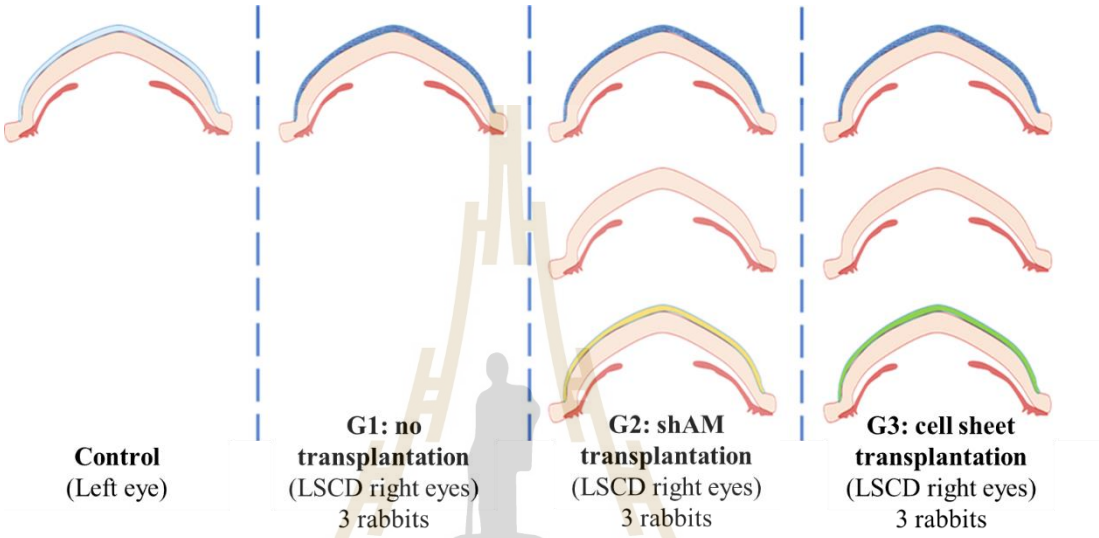


**Figure 4.2** Grouping of LSCD treatment. Control: normal eye, G1: LSCD eye without surgery and transplantation. G2: LSCD eye with dhAM transplantation. G3: LSCD eye with induced CEC sheet transplantation. Light blue layer: transparent corneal epithelium of normal cornea, dark blue layer: white conjunctival epithelium of LSCD cornea, yellow layer: dhAM, green layer: induced CEC sheet.

Firstly, the LSCD rabbits of G2 and G3 were anesthetized as previous procedure. The surgery procedure was performed by a veterinary ophthalmologist. The LSCD eyes were subjected to drop 1% atropine sulfate (1% ISOPTO* ATROPINE, Alcon-Couvreur, Puurs-Sint-Amands, Belgium). The conjunctival and subconjunctival scar tissue from the cornea and limbus were removed to expose corneal stroma by Crescent knife (Mani Inc., Honshu, Japan). Then the dhAM or CEC sheet were placed on the doughnut round shape PVDF membrane

(inner diameter: 12 mm, outer diameter: 15 mm) and immediately washed by PBS and placed on the surgical site. Afterwards, the PVDF membrane was remove and the implant was secured by absorbable suture 8-0 (KRUUSE Sacryl, Korea) in four corners and equably in another 8 positions. All operated eyes were treated with be treated with 0.5% moxifloxacin hydrochloride (Vigamox, Alcon Laboratories, USA) and 0.18% sodium hyaluronate (Vislube, Holopack Verpackungstechnik Gmbh, Germany). The rabbits were also injected subcutaneous with 10 mg/kg enrofloxacin (5% Enfloxacin, General Drugs House Co. Ltd, Bangkok, Thailand), 4 mg/kg carprofen (Rimadyl, Zoetis, New Jersey, USA). The eyes were observed every week. Rabbits were sacrificed after 30 days post transplantation and the eyes were harvested for H&E staining, Periodic acid-Schiff (PAS) staining and IF (CK12, CK3, human nuclei (mouse anti-nuclei antibody, ab254080, Abcam)).

4.3.6 Fixation, paraffin embedding, and section samples

The rabbit eye, hAM, dhAM, and induced CEC sheet was fixed in 10% neutral-buffered formalin at 4°C overnight, then washed with cold PBS 4x10 min each. Then the samples were dehydrated in 70% ethanol for 1 h, 90% ethanol for 1 h, 95% ethanol 2x1 h, and 100% ethanol 3x30 min. The rabbit eyes were cut into equal halves. All samples were immersed in xylene 2x1 h at room temperature (RT) before embedding in paraffin at 60°C. They were placed in xylene: paraffin (2:1 for 1 h, 2:1 for 1 h, 1:2 for 1 h), melted paraffin for 2 h, and embedded in paraffin. Embedded samples were kept at 4°C until tissue section. The embedded samples were cut into 10 µm-thick cross-sections by using a rotary microtome (HM 340E Electronic Rotary Microtome, Thermo Fisher Scientific). Sections were floated in a 60°C deionized water bath before mounting onto gelatin-coated or silane coated histological slides. The slides were dried overnight by heating at 40°C and then stored at RT in slide storage boxes until H&E staining or IF staining with CK12 and CK3.

4.3.7 H&E staining

Sections were deparaffinized by immersing in xylene 3x5 min. Then sections were rehydrated by placing in 100% ethanol for 2x5 min, 95% ethanol 2x5 min, and

70% ethanol for 5 min. Afterwards, sections were rinsed with deionized water. Sections were first stained nuclei with Mayer's Hematoxylin for 30 sec. Then sections were rinsed with running tap water for 10 min. Then sections were stained with Eosin Y for 10 sec. Afterward, sections were washed with tap water and dehydrated with 95% ethanol 2x3 min, 100% ethanol 2x3 min and put in xylene 2x3 min. Finally, sections were mounted with Fast drying mounting medium HI-MO (05-HM500, Bio-Optica Milano Spa, Milano, Italy) and covered with cover slip.

4.3.8 PAS staining

PAS staining was performed to determine location of the goblet cells. The rabbit eye tissue sections were deparaffinized, rehydrated, rinsed in distilled water. Afterwards, sections were treated with 0.5% periodic acid for 5 min and then rinsed in distilled water for 5 min. Sections were placed in Schiff reagent (1% basic fuchsin, 1.9% sodium metabisulfite in for 0.03N HCl) for 15 min and then washed in tap water for 10 min. Afterwards, sections were counterstained with Mayer's Hematoxylin for 30 sec, washed in tap water for 10 min. Finally, sections were dehydrated and placed in xylene twice before applying with the mounting medium and covering with cover slip.

4.3.9 Immunofluorescent staining

Section were deparaffinized, rehydrated, rinsed in deionized water, and washed with PBS. Sections were treated with antigen retrieval solutions (Tris/EDTA for CK3 and human nuclei staining or citrate buffer for CK12 staining) for 10 min in microwave, then permeabilized with 0.2% TritonX-100 in PBS for 20 min before blocking in 1% BSA in PBS for 1h to block antigen. Tissue sections were incubated with primary antibodies (CK3, CK12, human nuclei), secondary antibody (goat anti-mouse IgG Alexa Fluor 568) and counterstained with DAPI. Finally, tissue sections were mounted and covered with cover slip, then slides were kept at 4°C until analysis.

## 4.4 Results

4.4.1 De-epithelialization of hAM

The histology of hAM was shown in Figure 4.3 (A-D). The hAM consisted of a monolayer of amniotic epithelial cells (top layer), basal lamina (under the top layer), and avascular stroma (under basal lamina). Human amniotic epithelial cells (Figure 4.3 B, D, red arrows) were connected. Basal lamina could be seen clearly in dhAM (Figure 4.3 F, blue arrowhead). Avascular stroma contained the compact collagen layer (connects with basal lamina), amniotic mesenchymal stromal cells, and spongy layer (Figure 4.3 B). Unlike amniotic epithelial cells, amniotic mesenchymal stromal cells (Figure 4.3 B, D, black arrows) were separated and lower density. Besides, the thickness of hAM ranged from 0.05 to 0.2 mm.

De-epithelialization of hAM was successful performed by treatment with 0.5M NaOH for 30s and then rubbing with cotton tip. As shown in Figure 4.3 (E-H), dhAM contained none of human amniotic epithelial cells while amniotic mesenchymal stromal cells were retained. Moreover, the integrity of amniotic basement membrane was retained.

4.4.2 Generation and characterization of CEC derived hWJ-MSC sheet on dhAM

After seeding human induced CEC derived from WJ-MSCs onto dhAM and airlift culture, there were 1-4 cell layers that attached on the membrane (Figure 4.4 A, B). The thickness of the dhAM was variable due to the wide range of hAM membrane source. Induced CECs derived from WJ-MSCs remained expression of specific marker of CECs (CK12) (Figure 4.4 E, F).

4.4.3 Establishment of LSCD eyes in rabbit model

The eye morphology was changed after treatment with 1N NaOH for 30s (Figure 4.5). Before treatment, the eye did not stain with fluorescein (FL) staining and the eye cornea was clear, transparent, pupil was clear visible (Figure 4.5 A). After alkaline burnt, the cornea become white or opacity, and pupil could not be seen (Figure 4.5 B) and the cornea stained with FL staining (green color under cobalt blue light) that confirmed epithelium loss (Figure 4.5 C). Afterwards, the dead CECs were sloughed off into the tears, the cornea became light opacity, and the pupil was unclear. Then, opacity was developed, and pupil was rarely seen. Besides, the neovascularization appeared from

day 7-14 (Figure 4.6 B, C, yellow arrows), and the blood vessel grew from limbal area to cornea area (Figure 4.6 D). After 28 days, the eyes were subjected to grade LSCD stage, the details were shown in Figure 4.6 and 4.7. Eight treatment rabbit eyes were classified as several stage of LSCD (8-10 points) and one rabbit eye was classified as moderate stage of LSCD (7 points). Nine LSCD eyes were divided in 3 groups (G1, G2, G3) for transplantation experiment.

4.4.4 Effect of transplantation on treatment LSCD

Transplantation procedure is showed in Figure 4.8. dhAM or induced CEC sheets were harvested using PVDF supporter and transplanted onto LSCD eyes of rabbits at day 28 after alkali burn.

As shown in Figure 4.10, morphology of LSCD eyes in G1 (no transplantation) showed the persistent of neovascularization in the cornea, especially in G2 (dhAM transplantation), many blood vessels invaded into center of cornea. However, in G3 (induced CEC sheet transplantation), blood vessels showed only small area of peripheral cornea. Although there was no significant difference between three groups, both opacity of center and periphery of cornea were reduced in G3 while opacity of central cornea was remained, and opacity of peripheral cornea was increased in G1 and G2 (Figure 4.9).

Control cornea surface was smooth, the epithelium was integral, and the thickness of cornea was quite similar between central and peripheral cornea (Figure 4.11 A). Besides, there was no blood cell in both stroma and epithelium of control cornea. In G1, corneal stroma became thicker in the peripheral part but thinner in the center cornea. Furthermore, the epithelium of LSCD eye was defected in periphery and center of cornea, and specially disappeared in small part of center cornea (Figure 4.11 B). Blood cells appeared in corneal stroma and some part of corneal epithelium in G1. The deficiency of epithelium was even worst in G2 than G1 (Figure 4.11 C). Blood cells were also observed in stroma and some part of epithelium in G2. The deficiency of corneal epithelium was improved, and blood cells existed in stroma, but they appeared very rarely in epithelium in G3 (Figure 4.11 D).

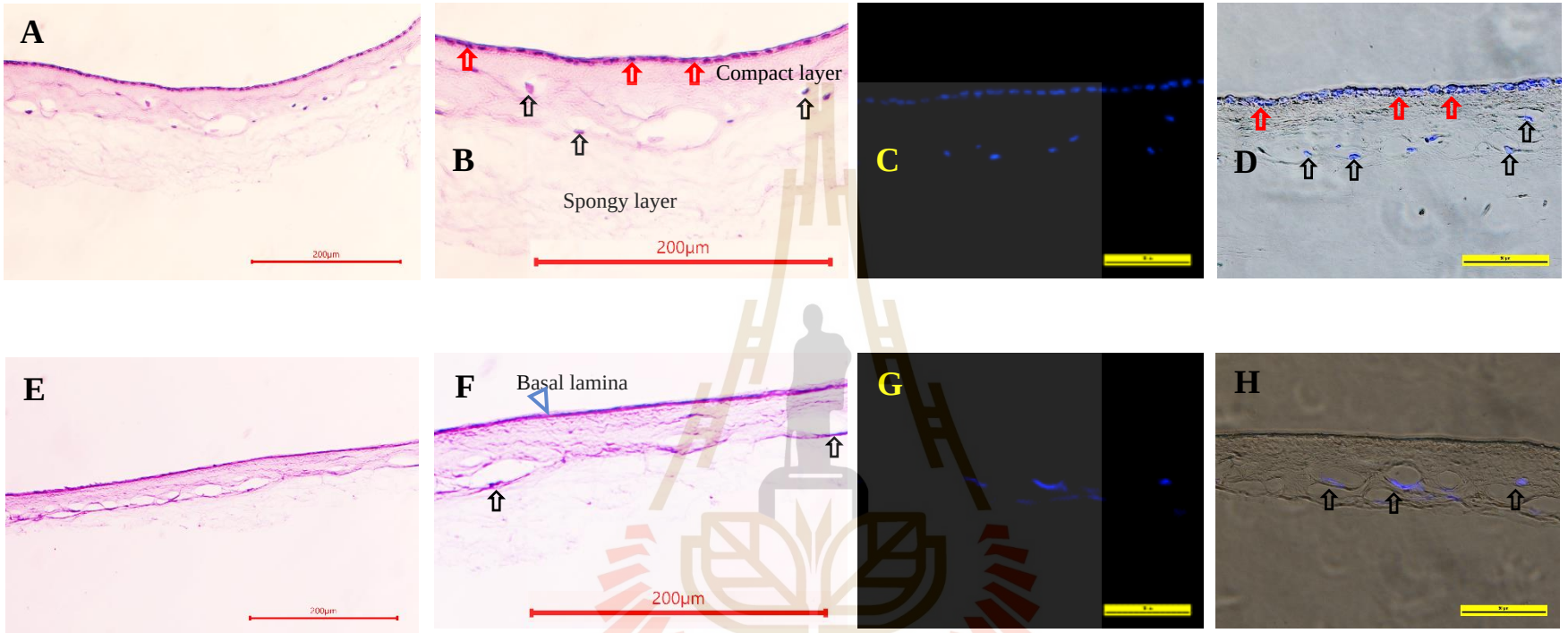


**Figure 4.3** hAM and dhAM staining with H&E and DAPI staining. (A, B) H&E staining of hAM, (C, D) DAPI staining of hAM with nuclei stained blue, (E, F) H&E staining of human dhAM, (G, H) DAPI staining of human dhAM with nuclei stained blue. Red arrows: human amniotic epithelial cells; black arrows: human amniotic mesenchymal stromal cells; and blue arrowhead: basal lamina. Red scale bar: 200 µm; and yellow scale bar: 50 µm.

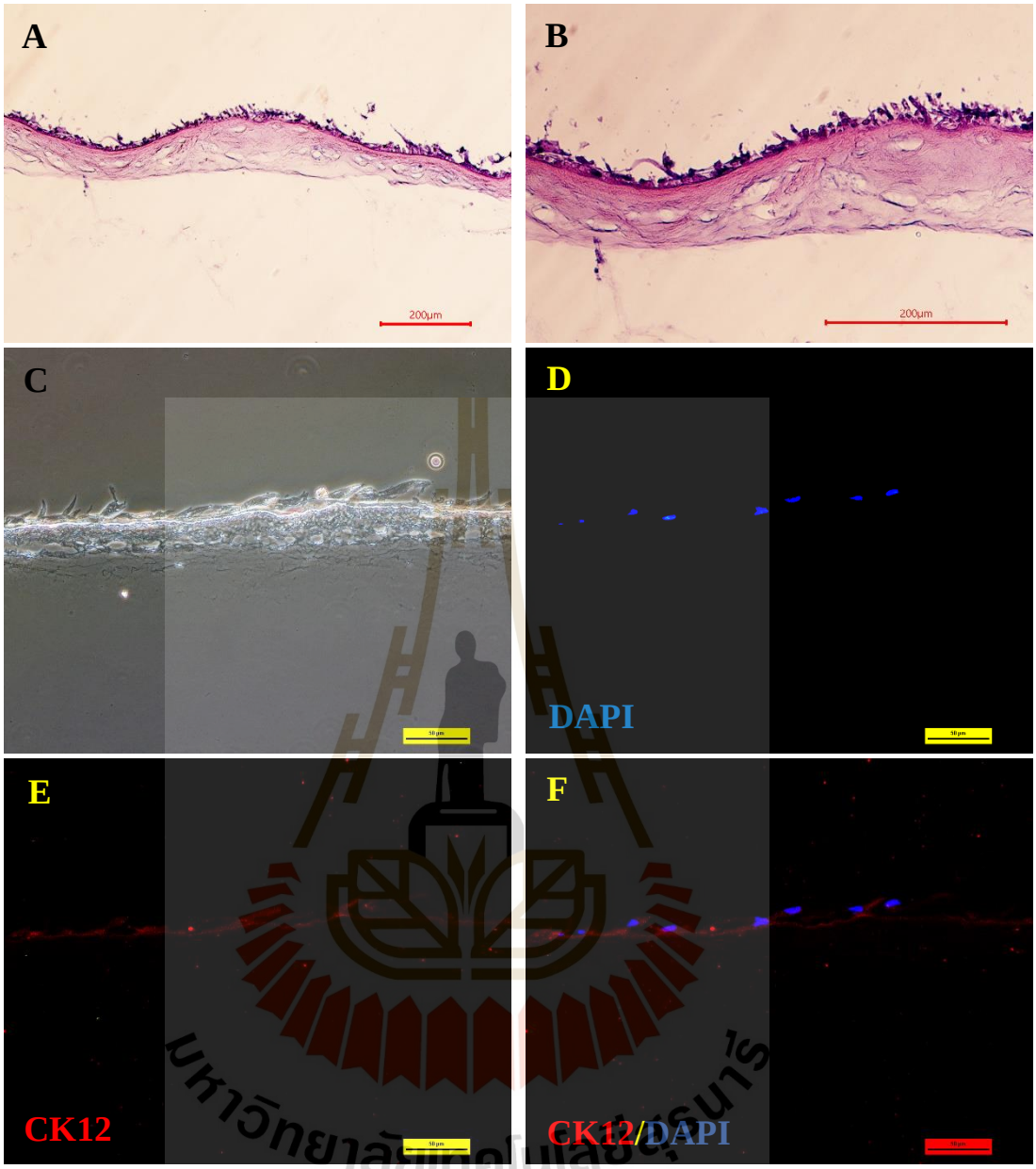


**Figure 4.4** Induced CEC derived hWJ-MSC sheet staining with H&E and IF. (A, B) H&E staining at magnification 10x, and 20x, scale bar: 200 μm (C-F) IF with CK12. Bright field (C), (D-F) Red: CK12, blue: DAPI. Scale bar: 50 μm.

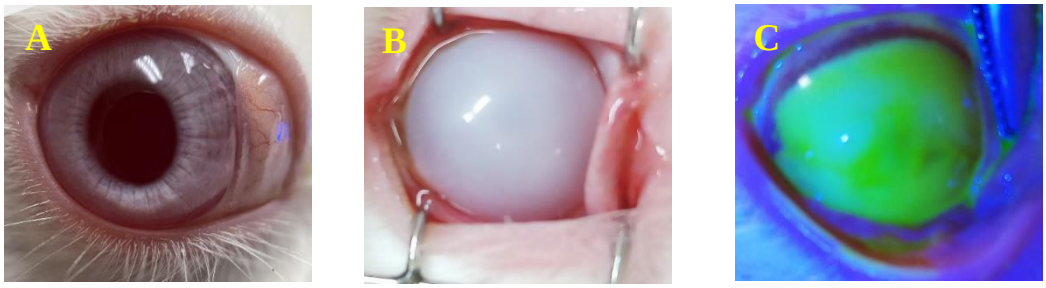


**Figure 4.5** Rabbit eye before and after treatment with NaOH (day 0). (A) Right eye before NaOH treatment. (B) Right eye after NaOH treatment. (C) Right eye stained with fluorescein after NaOH treatment.

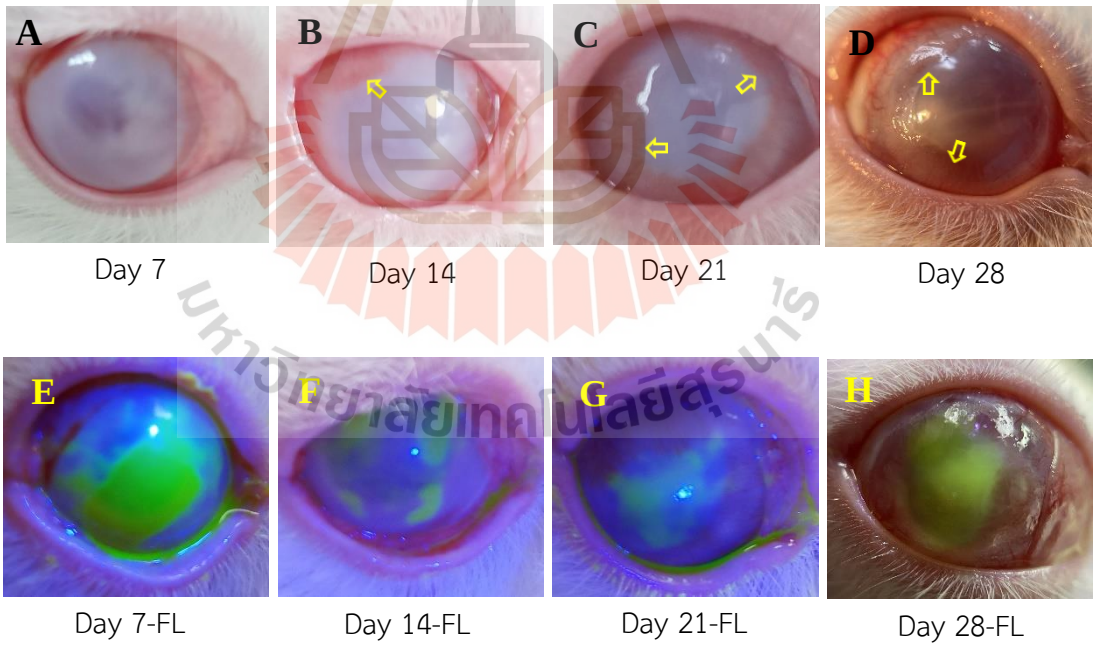


**Figure 4.6** Rabbit eye after treatment with NaOH from day 7-28. (A-D) Rabbit eyes without fluorescein staining (FL) under white light (E-H). Rabbit eyes with FL under cobalt blue light. Arrows indicate blood vessels.

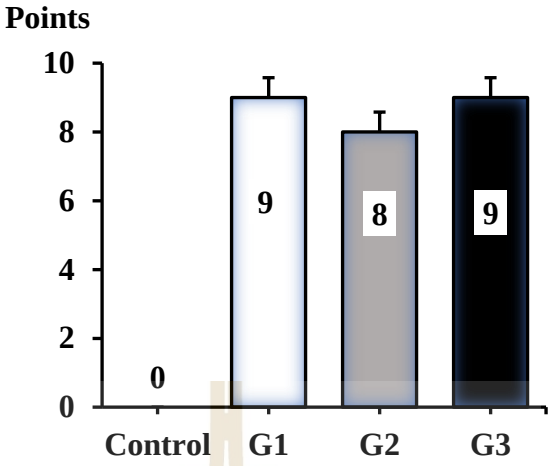


**Figure 4.7** LSCD grading of alkaline burn rabbit eyes at day 28 followed previous method (Aravena et al., 2019). Control: normal eye, G1: no transplantation, G2: dhAM transplantation, G3: cell sheet transplantation.

PAS staining results were shown in Figure 4.11 (E-H) and Table 4.1. In normal eyes (control), goblet cells were only present in conjunctiva and absent in both limbus and cornea (Figure 4.11 E). However, goblet cells were detected in limbus and peripheral corneal of all treatment groups (G1-G3). Moreover, in G2 goblet cells invaded into central cornea of 2 rabbit eyes. This result indicated the growing inward of conjunctival epithelium.

CK12 was expressed throughout the cornea epithelial surface in control eyes (Figure 4.12 A). All layers of corneal epithelium showed strongly positive with CK12 staining. In limbus, cells in the basal layer were negative with CK12 while cells in upper layers were positive with CK12 (Figure 4.12 E). In G1, CK12 expression was observed in upper layers of limbus and peripheral cornea (Figure 4.12 B, F). In G2, CK12 was negative in both limbus and cornea (Figure 4.12 C, G). In G3, CK12 was negative in limbus but it was positive in cornea (Figure 4.12 D, H). This result indicated that treatment with NaOH did not destroy all population of rabbit LESCs in G1. Therefore, remained LESCs could

develop and differentiate to be corneal epithelial cells that expressed CK12. However, after surgery, remained LESCs were removed, so there are no CECs in cornea of G2. After CEC sheet transplantation in G3, induced CECs could survive and develop in cornea.

CK3 was strongly positive in the superficial layer of corneal epithelium of control cornea but weakly expressed in supra-basal and basal layer of corneal epithelium (Figure 4.13 A). However, CK3 was not observed in cornea in both G1 and G2 (Figure 4.13 B, C). In G3, CK3 was expressed in the supra-basal and superficial layer of cornea (Figure 4.13 D).

Nucleus of human WJ-MSCs were positive with anti-human nuclei antibody while nucleus of rabbit CECs were negative with this antibody (Figure 4.14 A, B). This result confirmed this antibody stained with human cells, but it did not stain with rabbit cells. Anti-human nuclei antibody was negative in control, G1 and G2 (Figure 4.14 C-E). However, it was positive in G3 (Figrue 4.14 F). Most human cell population located in the superficial layer and basal layer of corneal epithelium, only few migrated into corneal stroma. This result indicated of survival and development of induced CECs derived human WJ-MSCs in rabbit cornea after transplantation.

**Table 4.1** Summary results of PAS staining.

| Group | Conjunctiva | Limbus | Peripheral Cornea | Centre Cornea |
|---|---|---|---|---|
| **Control** | 3/3 | 0/3 | 0/3 | 0/3 |
| **G1** | 3/3 | 2/3 | 2/3 | 0/3 |
| **G2** | 3/3 | 3/3 | 3/3 | 2/3 |
| **G3** | 3/3 | 3/3 | 2/3 | 0/3 |

Control: normal eye, G1: no transplantation, G2: dhAM transplantation, G3: cell sheet transplantation. Data present as Number of eyes that have goblet cells/Total eyes.

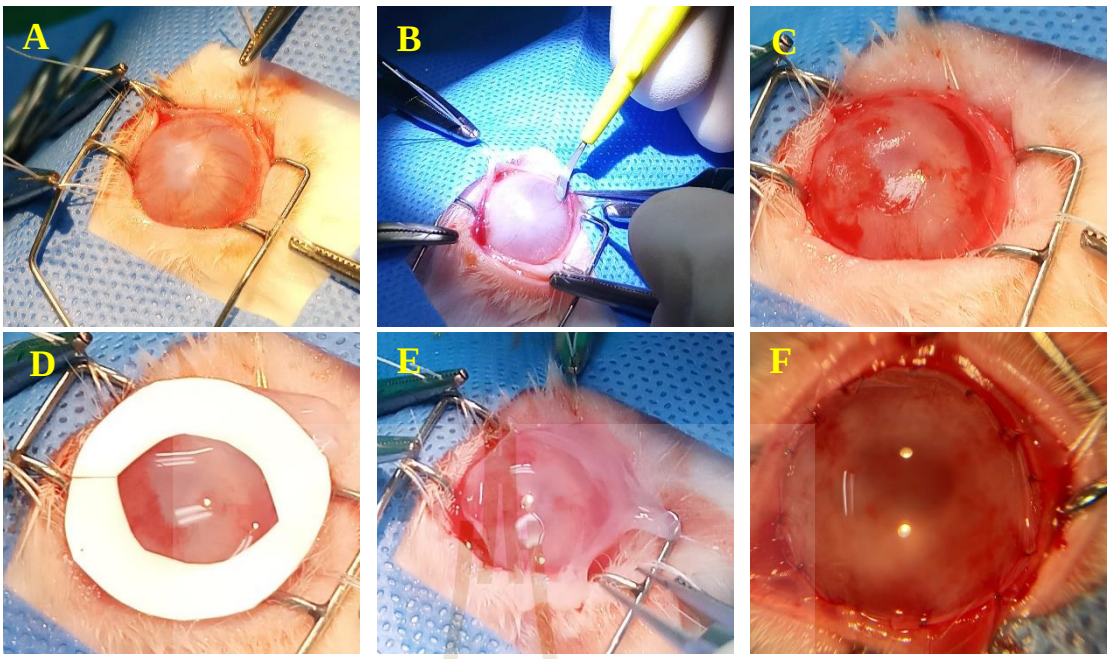


**Figure 4.8** Transplantation process of induced CEC sheet or dhAM onto LSCD rabbit cornea. A) Rabbit eye before transplantation, B) Remove corneal conjunction by crescent knife, C) Rabbit eye after removing corneal conjunction, D) dhAM harvested using doughnut-shape PVDF supporter (white color) was placed onto stroma bed of cornea, E) Removing PVDF supporter then fix and make membrane fit to cornea, suture F) rabbit eye after transplantation.

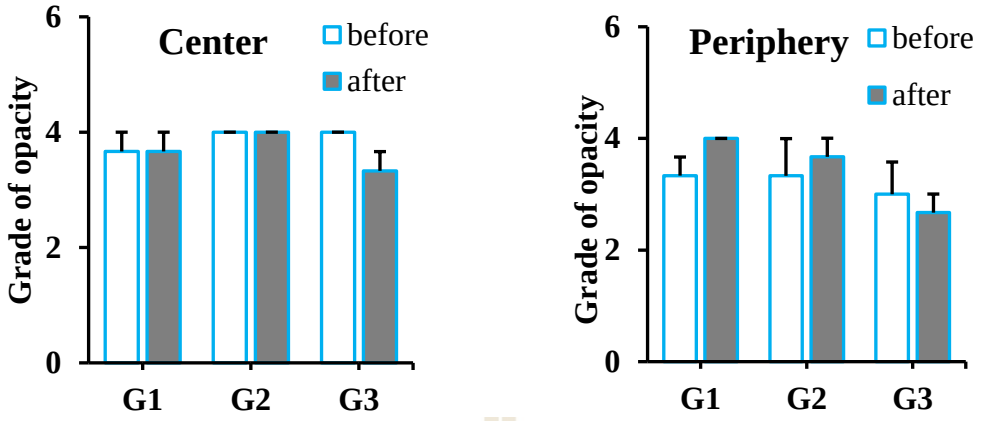


**Figure 4.9** Grade of corneal opacity before and after transplantation 30 days in center (left) and periphery (right).

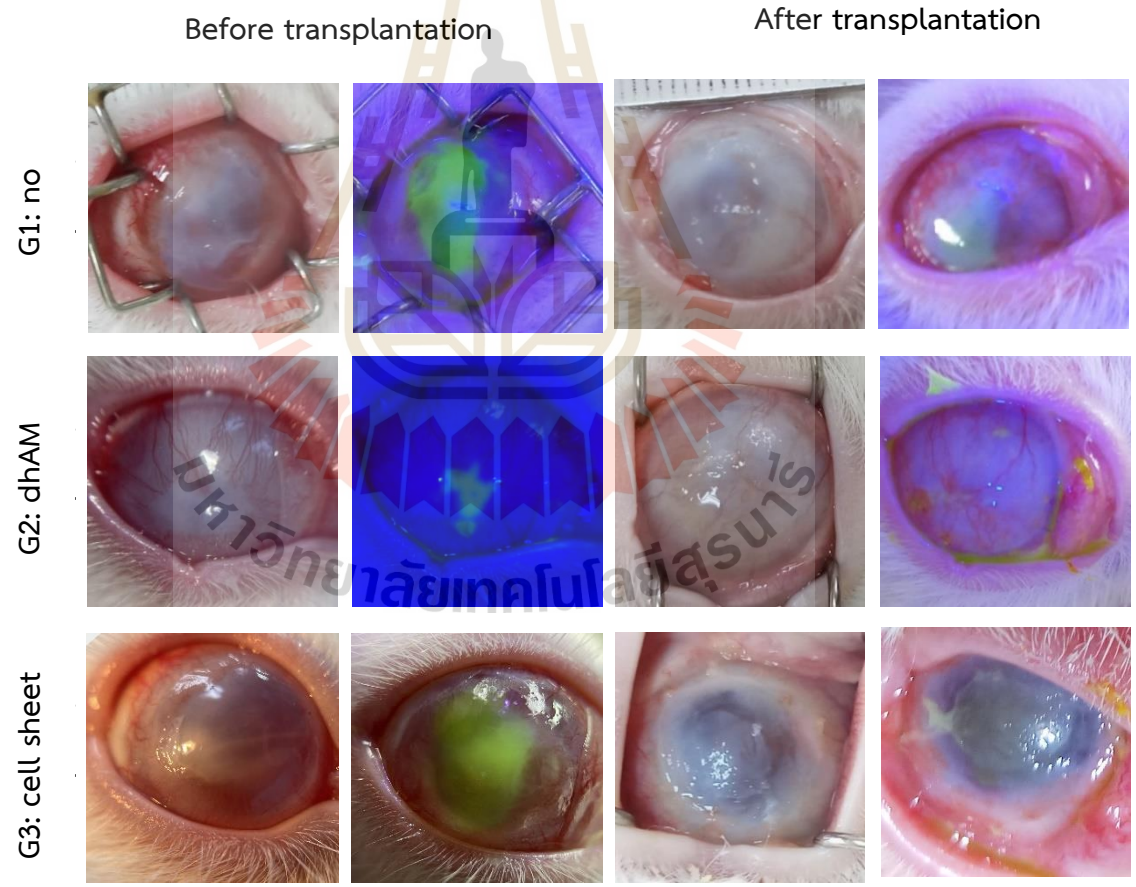


**Figure 4.10** Rabbit eyes of three groups before and after transplantation (30 days) with and without FL staining.

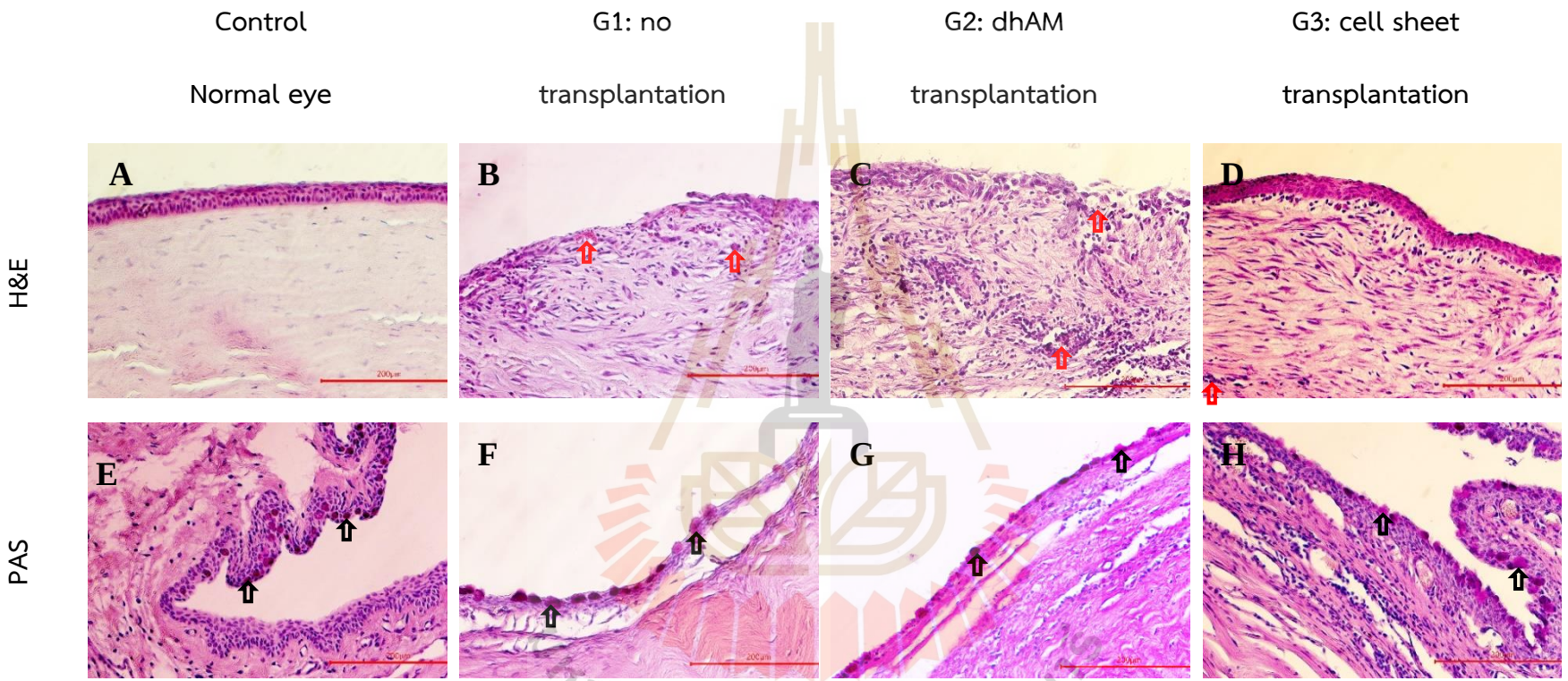


**Figure 4.11** H&E and PAS staining in rabbit eyes. (A-D) H&E staining in cornea. (E-H) PAS staining with in conjunctiva-corneal periphery. Red arrows: blood cells, Black arrows: goblet cells. Scale bar 200 μm.

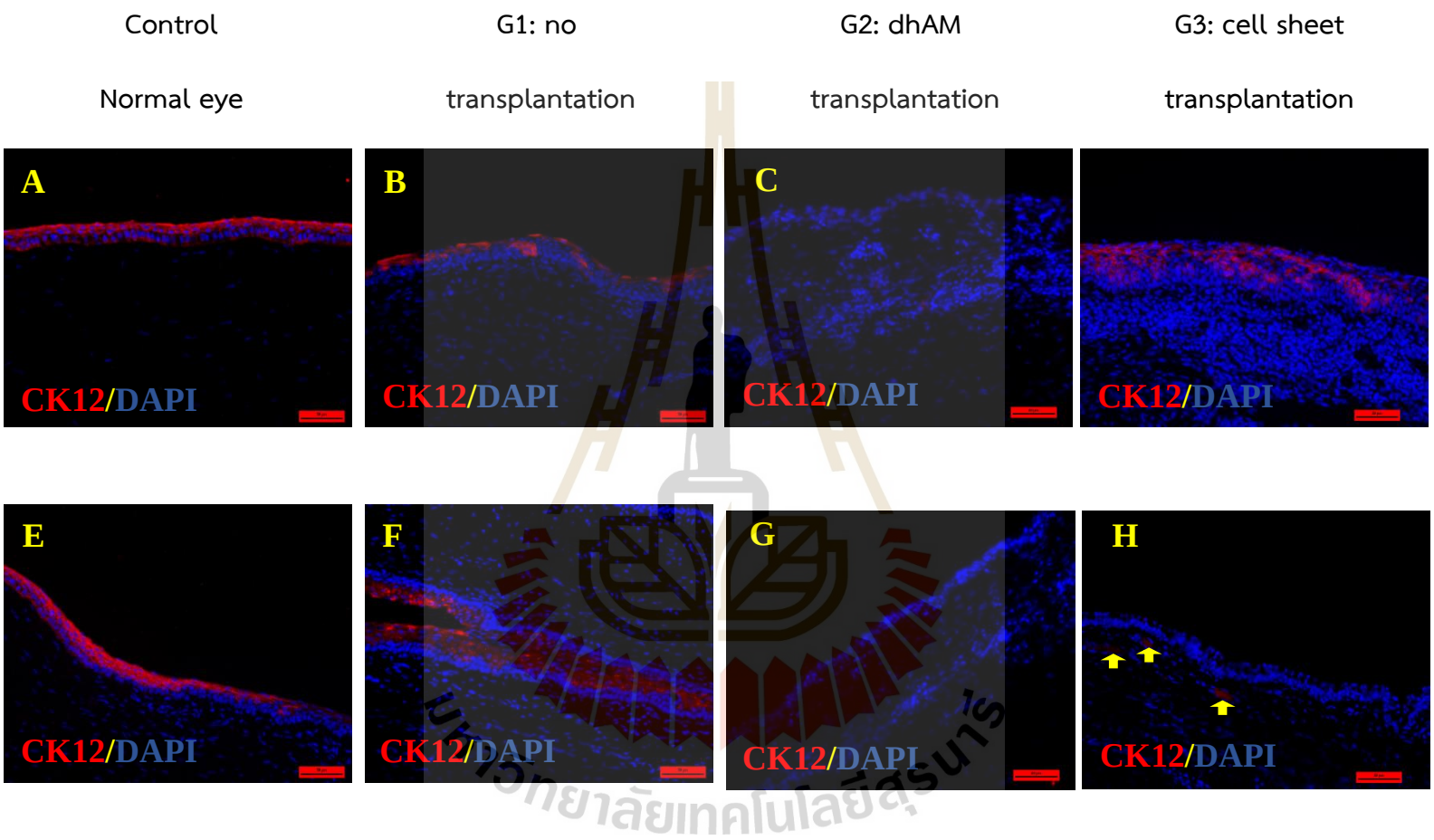


**Figure 4.12** IF staining with CK12 and DAPI. (A-D) stain in cornea, (E-H) stain in limbus and peripheral cornea. Yellow arrows: blood cells in stroma. Scale bar 50 μm.

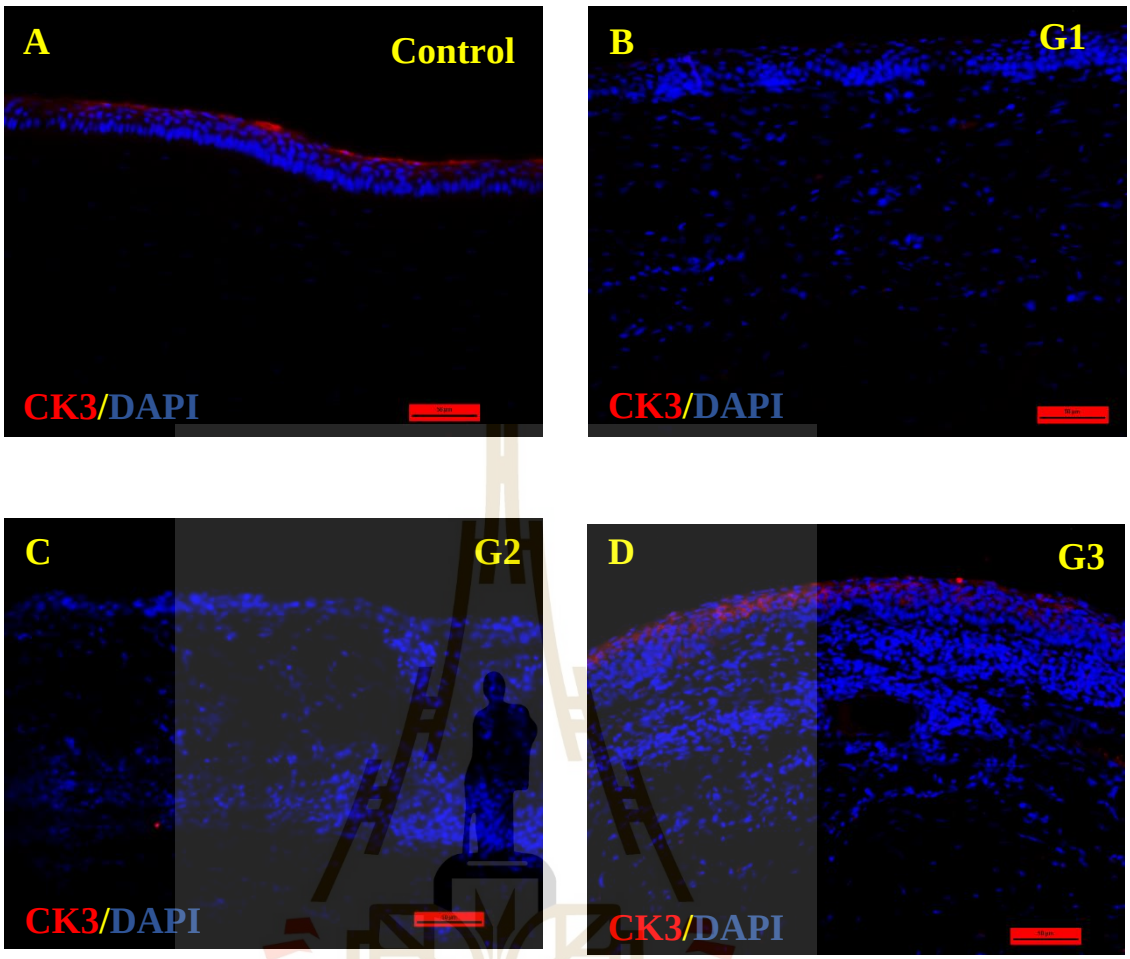


**Figure 4.13** IF staining in the cornea with CK3 and DAPI. (A) in normal left eye. (B) in LSCD eye without transplantation. (C) in dhAM transplanted eye. (D) in induced CEC sheet transplanted eye. Scale bar 50 μm.

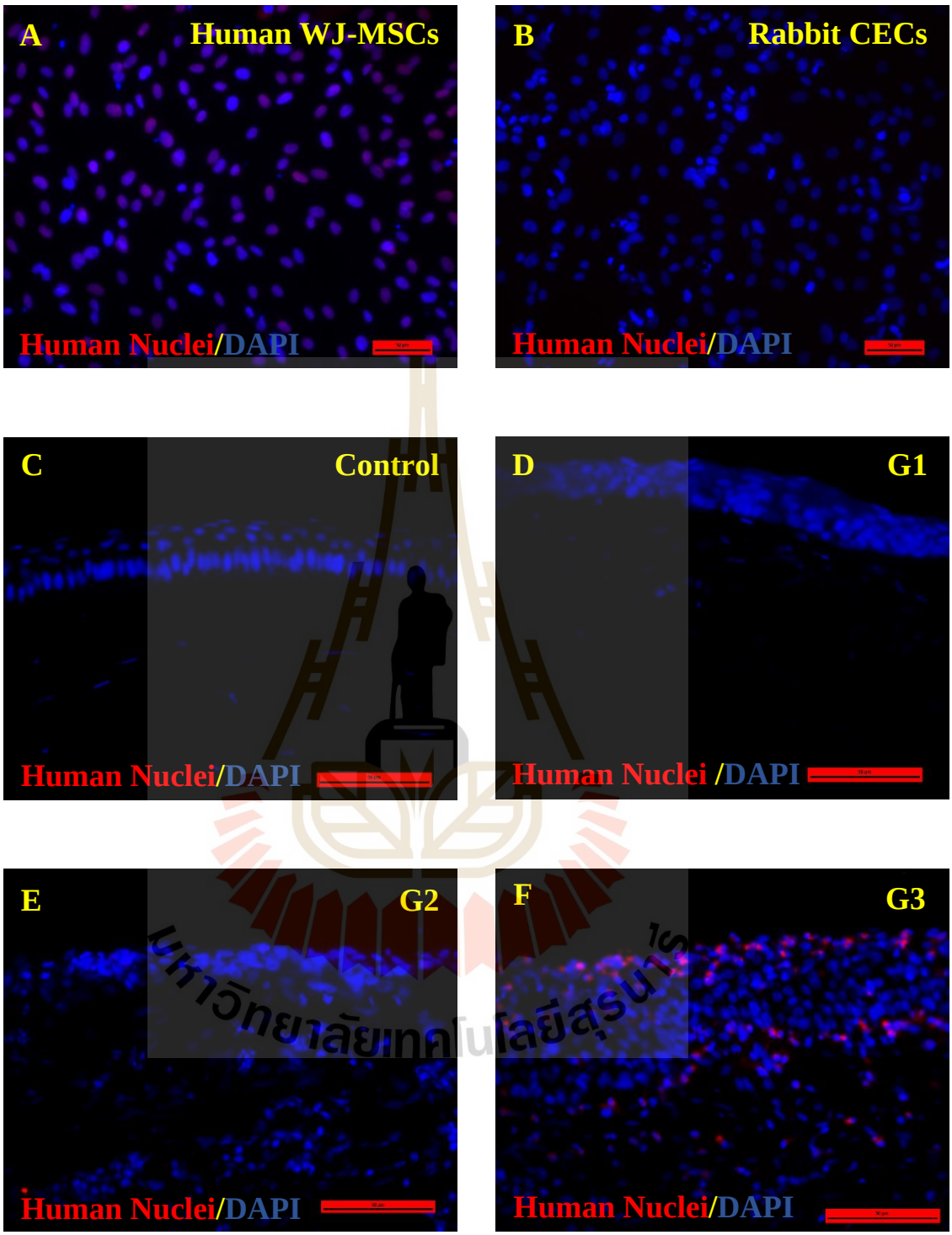


**Figure 4.14** IF staining with human nuclei and DAPI. (A, B) cells culture *in vitro*. (C-F) rabbit cornea. Scale bar 50 μm.

## 4.5 Discussion

hdAM is general used as scaffold for generation cell sheet from limbal and mucosal epithelial cells (Tananuvat et al., 2017), adipose derived MSCs (Galindo et al., 2017), tissue-engineered human CECs (Xu et al., 2012), corneal epithelium derived from clinical-grade human ESCs (He et al., 2020). There are several methods for de-epithelialization of AM, but these methods take a long time, fail to remove all epithelial cells, and damage hAM (Zhang et al., 2013; Hopkinson et al., 2008). Recently, a simple method using sodium hydroxide for de-epithelialization of hAM was fast and efficient in de-epithelialization of AM (Saghizadeh et al., 2013). This study modified method of Saghizadeh et al. (2013) by treatment with 0.5N NaOH for 30s then rubbing with cotton-tipped applicator under stereo microscope and succussed to remove all epithelial cells of hAM without damage to its integrity.

Generation of LSCD model in animal by alkaline burn was used in several studies (Bandeira et al., 2020; Gomes et al., 2010; Ma et al., 2006; Tananuvat et al., 2017). By treatment with 1N NaOH for 30s, this study developed mild and moderate stage LSCD in rabbit model. The treated eyes were opacity, pupils were rarely seen, and blood vessels invaded into cornea after 28 days. This result was similar with previous study (Kethiri et al., 2021). Moreover, defected corneal epithelium was detected by positive FL staining. 30 days later, opacity of both central and peripheral cornea in CEC sheet transplantation group was reduced while it was remained in center or increased in periphery in untreated and dhAM transplantation group. Besides, neovascularization and goblet cells grew inward to central cornea in dhAM transplantation. These results confirmed that dhAM transplantation did not improved recovery of cornea, but CEC sheet transplantation supported corneal recovery after alkali burn.

Survival of human induced CEC after transplantation were confirmed by positive staining with human nuclei that was negative with rabbit cells. Transplanted cells almost located in the superficial and basal layer of corneal epithelium, only few

migrated into corneal stroma. The induced CECs derived from human ESCs also almost located in corneal epithelium after transplantation (He et al., 2020). However, human adipose tissue derived MSCs migrated to limbal stroma and did not locate in corneal epithelium after transplantation (Galindo et al., 2017). This different result may cause by MSCs did not differentiate into CECs *in vivo*, so they remained good migration capacity. In group of dhAM transplantation, cells were negative with human nuclei could be cause by degradation of mesenchymal stromal cells in rabbit eyes after transplantation. That was similar with previous studies (Galindo et al., 2017; He et al., 2020).

CK12 were observed in limbus and peripheral cornea of LSCD eye without transplantation (no transplantation group). This result indicated some LESCs still remained after alkali burn, so they could grow and differentiate to CECs, but these CECs were not enough mature to express CK3 so CK3 was negative in this group. However, both CK12 and CK3 expression were not expressed in limbus and cornea in dhAM transplantation group. In previous study (He et al., 2020), CK3/12 was negative in limbus but it was discontinuously expressed in very thin corneal epithelium in dhAM transplantation group. The expression of CK12 in cornea in He et al. (2020) might be cause by some rabbit CECs remained after corneal epithelial scraping. This result indicated that after alkali burn and surgery for removing conjunctiva cover limbus and cornea stroma, all LESCs were removed. In CEC sheet transplantation, CK3 and CK12 was negative in limbus but positive in corneal epithelium. This indicated surgery process almost removed remaining LESCs and human induced CECs could survive and grow on rabbit corneal epithelium. This result similar with previous study (He et al., 2020). Transplantation of adipose MSC cell sheet was fail to reconstruction of rabbit cornea epithelium with total LSCD case (Bandeira et al., 2020; Galindo et al., 2017). However, transplantation of induced CECs derived from WJ-MSCs improves recovery of LSCD in rabbit model.

Many studies used CK3 as marker for CECs *in vivo* (Zhao et al., 2018; Galindo et al., 2017; Monteiro et al., 2009; Xu et al., 2012) but these results suggested that CK12 was better marker for analysis of CECs due to uniform strong expression in CECs while CK3 showed lower and different expression with CECs.

## 4.6 Conclusions

In summary, this study showed easy and efficiency method to denude AM by treatment with 0.5N NaOH for 30s then rubbing with cotton-tipped applicator under stereo microscope. Besides, treatment with NaOH could not generate total LSCD in rabbit model so remained LESCs regenerated CECs in peripheral cornea and inhibited growing into central cornea of conjunctiva and blood vessels. However, alkali burn, and surgery procedure removed all LESCs that were functioned in both barrier and generation CECs, so conjunctiva and blood vessels grew faster, and CECs were not observed. Moreover, this study showed the method to generate cell sheet from induced CECs derived human WJ-MSCs and then induced CECs could survive, grow in rabbit cornea and they could support recovery of cornea epithelium, improve cornea opacity. This study reveals that transplantation of induced CECs derived from WJ-MSCs improved recovery of LSCD in rabbit model.

## 4.7 References

Ahmad, S. (2012). Concise review: Limbal stem cell deficiency, dysfunction, and distress. **Stem Cells Transl. Med.** 1(2): 110-115.

Aravena, C., Bozkurt, K., Chuephanich, P., Supiyaphun, C., Yu, F., and Deng, S. X. (2019). Classification of limbal stem cell deficiency using clinical and confocal grading. **Cornea** 38(1): 1-7.

Bandeira, F., Goh, T.-W., Setiawan, M., Yam, G. H.-F., and Mehta, J. S. (2020). Cellular therapy of corneal epithelial defect by adipose mesenchymal stem cell-derived epithelial progenitors. **Stem Cell Res. Ther.** 11(1): 14.

Chen, Z., de Paiva, C. S., Luo, L., Kretzer, F. L., Pflugfelder, S. C., and Li, D.-Q. (2004). Characterization of putative stem cell phenotype in human limbal epithelia. **Stem Cells** 22(3): 355-366.

Galindo, S., Herreras, J. M., López-Paniagua, M., Rey, E., de la Mata, A., Plata-Cordero, M., Calonge, M., Nieto-Miguel, T. (2017). Therapeutic effect of human adipose tissue-derived mesenchymal stem cells in experimental corneal failure due to limbal stem cell niche damage. **Stem Cells** 35(10): 2160-2174.

Garzón, I., Martín-Piedra, M. A., Alfonso-Rodríguez, C., González-Andrades, M., Carriel, V., Martínez-Gómez, C., Campos, A., and Alaminos, M. (2014). Generation of a biomimetic human artificial cornea model using Wharton's jelly mesenchymal stem cells. **Invest. Ophthalmol. Vis. Sci.** 55(7), 4073-4083.

Gomes, J. A., Geraldes Monteiro, B., Melo, G. B., Smith, R. L., Cavenaghi Pereira da Silva, M., Lizier, N. F., Kerkis, A., Cerruti, H., and Kerkis, I. (2010). Corneal reconstruction with tissue-engineered cell sheets composed of human immature dental pulp stem cells. **Invest. Ophthalmol. Vis. Sci.** 51(3): 1408-1414.

He, J., Ou, S., Ren, J., Sun, H., He, X., Zhao, Z., Wu, H., Qu, Y., Liu, T., Jeyalatha, V., Zhang, L., Li, Q., Reinach, P. S., Quantock, A., Hao, J., Liu, Z., and Li, W. (2020). Tissue engineered corneal epithelium derived from clinical-grade human embryonic stem cells. **Ocul. Surf.** 18(4): 672-680.

Hopkinson, A., Shanmuganathan, V. A., Gray, T., Yeung, A. M., Lowe, J., James, D. K., and Dua, H. S. (2008). Optimization of amniotic membrane (AM) denuding for tissue engineering. **Tissue Eng. Part C Methods** 14(4): 371-381.

Kethiri, A. R., Singh, V. K., Damala, M., Basu, S., Rao, C. M., Bokara, K. K., and Singh, V. (2021). Long term observation of ocular surface alkali burn in rabbit models: Quantitative analysis of corneal haze, vascularity and self-recovery. **Exp. Eye Res**. 205:108526.

Ma, Y., Xu, Y., Xiao, Z., Yang, W., Zhang, C., Song, E., Du, Y., and Li, L. (2006). Reconstruction of chemically burned rat corneal surface by bone marrow–derived human mesenchymal stem cells. **Stem Cells** 24(2): 315-321.

Malhotra, C., and Jain, A. K. (2014). Human amniotic membrane transplantation: Different modalities of its use in ophthalmology. **World J. Transplant.** 4(2): 111-121.

Marino, L., Castaldi, M. A., Rosamilio, R., Ragni, E., Vitolo, R., Fulgione, C., Castaldi, S. G., Serio, B., Bianco, R., Guida, M., and Selleri, C. (2019). Mesenchymal stem cells from the Wharton's jelly of the human umbilical cord: Biological properties and therapeutic potential. **Int. J. Stem Cells**, 12(2): 218-226.

Monteiro, B. G., Serafim, R. C., Melo, G. B., Silva, M. C. P., Lizier, N. F., Maranduba, C. M. C., Smith, R. L., Kerkis, A., Cerruti, H., Gomes, J. A. P., and Kerkis, I. (2009). Human immature dental pulp stem cells share key characteristic features with limbal stem cells. **Cell Prolif.** 42(5): 587-594.

Ramuta, T. Ž., and Kreft, M. E. (2018). Human amniotic membrane and amniotic membrane-derived cells: How far are we from their use in regenerative and reconstructive urology? **Cell Transplant.** 27(1): 77-92.

Saghizadeh, M., Winkler, M. A., Kramerov, A. A., Hemmati, D. M., Ghiam, C. A., Dimitrijevich, S. D., Sareen, D., Ornelas, L., Ghiasi, H., Brunken, W. J., Maguen, E., Rabinowitz, Y. S., Svendsen, C. N., Jirsova, K., and Ljubimov, A. V. (2013). A simple alkaline method for decellularizing human amniotic membrane for cell culture. **PLoS One** 8(11): e79632.

Satake, Y., Higa, K., Tsubota, K., and Shimazaki, J. (2011). Long-term outcome of cultivated oral mucosal epithelial sheet transplantation in treatment of total limbal stem cell deficiency. **Ophthalmology** 118(8): 1524-1530.

Shortt, A. J., Secker, G. A., Lomas, R. J., Wilshaw, S. P., Kearney, J. N., Tuft, S. J., and Daniels, J. T. (2009). The effect of amniotic membrane preparation method

on its ability to serve as a substrate for the *ex-vivo* expansion of limbal epithelial cells. **Biomaterials** 30(6): 1056-1065.

Sotozono, C., Inatomi, T., Nakamura, T., Koizumi, N., Yokoi, N., Ueta, M., Matsuyama, K., Miyakoda, K., Kaneda, H., Fukushima, M., and Kinoshita, S. (2013). Visual improvement after cultivated oral mucosal epithelial transplantation. **Ophthalmology** 120(1): 193-200.

Tananuvat, N., Bumroongkit, K., Tocharusa, C., Mevatee, U., Kongkaew, A., and Ausayakhun, S. (2017). Limbal stem cell and oral mucosal epithelial transplantation from *ex vivo* cultivation in LSCD-induced rabbits: Histology and immunologic study of the transplant epithelial sheet. **Int. Ophthalmol.** 37(6): 1289-1298.

Xu, B., Fan, T.-J., Zhao, J., Sun, A., Wang, R.-X., Hu, X.-Z., Yu, H.-Z., Fan, X.-Y., and Xu, X.-H. (2012). Transplantation of tissue-engineered human corneal epithelium in limbal stem cell deficiency rabbit models. **Int. J. Ophthalmol.** 5(4): 424-429.

Zhang, T., Yam, G. H., Riau, A. K., Poh, R., Allen, J. C., Peh, G. S., Beuerman, R. W., Tan, D. T., and Mehta, J. S. (2013). The effect of amniotic membrane de-epithelialization method on its biological properties and ability to promote limbal epithelial cell culture. **Invest. Ophthalmol. Vis. Sci.** 54(4): 3072-3081.

Zhao, X.-Y., Xie, H.-T., Duan, C.-Y., Li, J., and Zhang, M.-C. (2018). Rat limbal niche cells can induce transdifferentiation of oral mucosal epithelial cells into corneal epithelial-like cells *in vitro*. **Stem Cell Res. Ther.** 9(1): 256.

# CHAPTER 5
# OVERALL CONCLUSION

Human WJ-MSCs are good candidate for allogenic transplantation therapies. Finding optimal method to generate CECs from human WJ-MSCs will provide a chance for recovery ocular surface from LSCD. This study described the effects of treatment factors (RA, SB505124 and BMP4) on the involved signaling pathways, that related differentiation into CECs, in human WJ-MSCs, then compares three combinations of these treatment factors on the differentiation of these cells into CECs. RA inhibited Wnt signaling via reducing translocation of β-catenin while SB505124 suppressed TGF-β signaling by decreasing phosphorylation of Smad2. This study indicated a feeder-free, non-conditioned medium 2-step method to generate CECs from human WJ-MSCs within 9 days. This differentiation method consisted of two steps: first step using combination of RA, SB505124, BMP4 and EGF and the second step using SHEM medium. Induced CECs derived WJ-MSCs are valuable for research studies on LSCD treatment *in vivo* model.

Furthermore, this study showed easy and efficiency method to de-epithelialization of hAM by treatment with 0.5N NaOH for 30s then rubbing with cotton-tipped applicator under stereo microscope. Treatment by NaOH could not generate total LSCD in rabbit model so remained LESCs regenerated CECs in peripheral cornea and inhibited growing into central cornea of conjunctiva and blood vessels. However, alkali burn, and surgery procedure removed all LESCs that were functioned in both barrier and generation CECs, so conjunctiva and blood vessels grew faster, and CECs were not observed. Moreover, this study showed the method to generate cell sheet from induced CECs derived human WJ-MSCs and then induced CECs could survive, grow in rabbit cornea and they could support recovery of cornea epithelium, improve cornea opacity. This study revealed that transplantation of induced CECs derived from WJ-MSCs improved recovery of LSCD in rabbit model. Further study should consider the efficiency of transplantation for longer period to examine stability and development of human cells in rabbit model.

# VITAE

Ms. Nguyen Thi Hong was born in Hanoi, Vietnam on November 21st, 1987. She finished a Bachelor Degree in Veterinary Husbandry in Vietnam National University of Agriculture (VNUA), Hanoi, Vietnam in 2009. After that, she has worked in Laboratory of Embryo Technology, Institute of Biotechnology, Hanoi, Vietnam. In 2013, she obtained a Master Degree (MS) in Animal Science in VNUA. In same year, she recieved the short term fellowship in Faculty of Veterinary Science, Chulalongkorn University. Next year, she got another short term scholarship in Department of Animal Science, Chungbuk National University, South Korea. In 2016, she attended Japan International Cooperation Agency (JICA) counter part training program in National Institute of Agrobiological Sciences, Japan. In 2019, she received the Suranaree University of Technology's Graduate research fellowship. The research topic is "Induction and transplantation of corneal epithelial cells derived from human Wharton's jelly mesenchymal stem cells into the rabbit model". She published two papers: one review paper (Theerakittayakorn et al., 2020) and one research article (Nguyen et al., 2022). The chapter 3 in this thesis was published as the research article. The two papers are as follows:



Theerakittayakorn, K., Thi Nguyen, H., Musika, J., Kunkanjanawan, H., Imsoonthornruksa, S., Somredngan, S., Ketudat-Cairns, M., and Parnpai, R. (2020). Differentiation induction of human stem cells for corneal epithelial regeneration. **Int. J. Mol. Sci.** 21(21): 7834.

Nguyen, H. T., Theerakittayakorn, K., Somredngan, S., Ngernsoungnern, A., Ngernsoungnern, P., Sritangos, P., Ketudat-Cairns, M., Imsoonthornruksa, S., Assawachananont, J., Keeratibharat, N., Wongsan, R., Rungsiwiwut, R., Laowtammathron, C., Bui, N. X., Parnpai, R. (2022). Signaling Pathways Impact on Induction of Corneal Epithelial-like Cells Derived from Human Wharton's Jelly Mesenchymal Stem Cells. **Int. J. Mol. Sci.**, 3078.